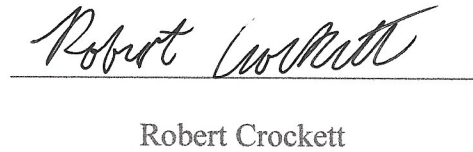**Design and Analysis of CubeSats in Low Earth Orbit**

A Major Qualifying Project Report
Submitted to the Faculty of the
WORCESTER POLYTECHNIC INSTITUTE
In Partial Fulfillment of the Requirements for the
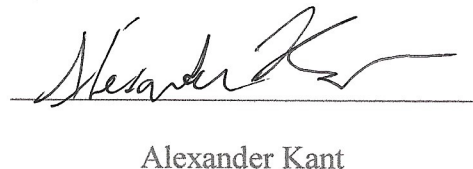Degree of Bachelor of Science
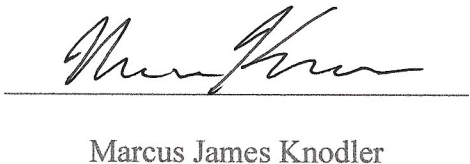In Aerospace Engineering

by

_____   _____
Matias Campos Abad   Robert Crockett

_____   _____
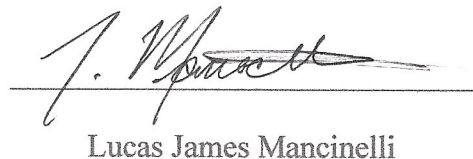Matthew Escalante-Hurtado   Alexander Kant
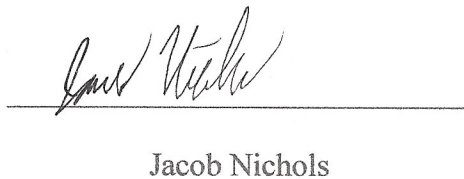

_____   _____
Marcus James Knodler   Lucas James Mancinelli

_____
Jacob Nichols

March 2, 2018

Approved by: _____
Professor John J. Blandino, Advisor
Aerospace Engineering Program
WPI

Abstract

This work evaluated the power, propulsion, and telecommunications subsystems for CubeSats to support two missions in low earth orbit; a Rendezvous (formation flying) mission and a mission to explore extreme low earth orbit. After selecting a baseline set of hardware for each spacecraft, trade studies were performed to evaluate options. Chemical and electric propulsion options for both primary and attitude control were considered. Thrusters for attitude control were compared with reaction wheels and performance compared for both required maneuvers and disturbance torque compensation. Power subsystem trades considered different solar arrays and battery options. Telecommunication subsystem trades compared data link budgets for different orbit inclinations and receiving station networks.

Acknowledgements

We would like to thank the following individuals and groups for their help and support throughout the entirety of this project.

Table of Authorship

Section	Author
1 Introduction	
1.1	All
1.2.1	MFCA
1.2.1.1	JJN
1.2.1.2	MEH
1.2.1.3	MFCA
1.2.2	LJM, MJK
1.2.2.1	LJM
1.2.2.2	ABK
1.2.2.3	MJK
1.3	All
1.3.1	MFCA
1.3.2	MFCA
1.4	MFCA
2 Background	
2.1.1	JJN, LJM
2.1.2	MEH, ABK, RCC
2.1.3	MJK, MFCA
2.2	JJN, LJM
2.3.1	ABK
2.3.2	ABK, RCC
2.3.3	MEH
2.4.1	MJK
2.4.2	MFCA
3 Methodology	
3.1.1	JJN
3.1.2	LJM
3.2.1.1	MEH, AK
3.2.1.2	ABK
3.2.2.1	ABK, RCC

3.2.2.2	RCC
3.2.2.3	MEH
3.3.1	MFCA
3.3.2	MJK
4 Results	
4.1.1	JJN
4.1.2	LJM
4.2.1	RCC
4.2.2	MEH
4.2.3	ABK
4.3	MFCA, MJK
4.3.1	MFCA
4.3.2	MJK
5 Conclusions and Recommendations	
5.1.1	JJN
5.1.2	LJM
5.2.1	MEH
5.2.2	ABK, RCC
5.3.1	MFCA
5.3.2	MJK
Appendix A	MEH, ABK, RCC
Appendix B	MFCA
Appendix C	MFCA, MJK
Appendix D	JJN
Appendix E	LJM
Appendix F	MEH
Appendix G	RCC, ABK

Table of Contents

List of Figures

List of Tables

Executive Summary

The 2017 CubeSat MQP consisted of the design of two sets of spacecraft subsystems to support two different missions; the extreme low Earth orbit mission (eLEO) and the Rendezvous mission. Each mission had specific requirements that needed to be met. Three different MQP teams worked on different subsystems. This report presents the results of the power, propulsion, and telecommunication subsystem teams for each of the two missions. These teams focused on performing research and trade studies for their respective subsystems and mission. Using MATLAB and Systems Tool Kit (STK), these teams were able to complete various trade studies, having collected valuable data pertaining to which components should be implemented on a future CubeSat mission. The power teams communicated with all subsystems that used power to create a power budget. This provided information required to select a battery and solar power system that would meet the mission requirements. The propulsion teams looked into primary and attitude control systems to maintain the CubeSat orbit and attitude. To choose propulsion components, the teams analyzed disturbance torques, detumble maneuvers, and 180-degree slew maneuvers. The Telecommunication subsystem team developed an uplink and downlink budget to determine when the CubeSat could receive and transmit information, as well as how much information each mission could transmit per orbit. In conclusion, the new baseline design presented in this report, alongside the work of the other two MQP teams, is a viable solution for an eLEO and a Rendezvous mission.

eLEO

The eLEO mission is characterized by the high atmospheric drag present at the 210 km orbit. Historically, there have been few missions at this altitude as the drag limits the lifespan of the spacecraft. This lower range of LEO remains widely unexplored and of high commercial,

military, and scientific interest. The team's main objective was to design a CubeSat that would be able to fly a customer's payload in an eLEO orbit for as long as possible. The team's main focus was on the Power, Propulsion and Telecommunication Subsystems. Propulsion was the most important, as it had to maintain the attitude and overcome the drag forces that would force the spacecraft to deorbit prematurely. Electric options for main propulsion and a comparison between reaction wheels and thrusters for attitude control were contemplated as trade studies. An electric primary thruster and PPTs for ACS were selected to extend mission lifespan to approximately 31 days, with the limiting factor being the amount of fuel that can be carried. The power subsystem team selected the power production and storage technology in order to keep the propulsion system operational when in the umbra and penumbra regions of the orbit. The power subsystem was also responsible for providing power to the other CubeSat subsystems. Performance of solar arrays and batteries were studied. Body mounted solar arrays and a 40 W-hr battery were selected to supply the required power and keep a steady charge and discharge battery cycle. Finally, the telecommunications subsystem team was tasked with maximizing the data and telemetry transmission to a selected Ground Station Network. Transmission capabilities to different GSN as well as different onboard components were studied. The NASA Space Network and a compatible onboard telecommunication architecture were selected due to the fast transmission rates and constant availability. Important mission information is always being transferred to Earth with no limitations, allowing for as much data transfer as possible, even in case of an unexpected deorbit.

Rendezvous

The Rendezvous mission consists of flight in low earth orbit (LEO) at an altitude of 300 km. This mission involves two CubeSats in flying in a formation, where one of the CubeSats, the "leader," is considered to have a virtual nanosat controlling the Rendezvous maneuver in order to

maintain a 100 km arc distance between the two satellites. The team's main objective was to design a CubeSat that would be able to meet the mission requirements in LEO, with a focus on propulsive control to maintain the 100 km arc distance between the two CubeSat's flying in formation. The team's main focus was on the Power, Propulsion and Telecommunication Subsystems. Propulsion was the most important, as it had to maintain the arc distance between the two CubeSat's flying in formation and have the ability to vary the thrust in order to compensate for disturbances that would cause the arc distance to change. The propulsion subsystem team determined the appropriate main thruster and secondary thrusters in order to maintain the specificity of the Rendezvous mission. The team identified various options with different benefits to the mission. The study involved finding times to complete certain maneuvers, power required to achieve or counteract certain angular momentums, disturbance torque compensation, and the size of each actuator with respect to the CubeSat to optimize available space utilization. The components that were studied were the μPPT from Busek, the PPTCUP from Mars Space Ltd., the RW-100 reaction wheel from Blue Canyon Tech, and the Hybrid ADN/RCS thruster from VACCO. The reaction wheels proved to be ineffective as they would require a second system to move the spacecraft while they were desaturating. While taking a long time to complete maneuvers, the PPTCUP and the μPPTs both performed well with high Isp's and decent power draws and were small enough to not create a volume issue in the CubeSat. The larger Hybrid ADN/RCS thruster was much more powerful and could complete maneuvers quickly and without a larger power loss. Its greatest downside is its size as it is almost the size of half a U. The power subsystem selected components to maintain the power consumption and generation on the satellite. It was determined that, in order to maintain the mission requirements, a 20 U CubeSat would be needed in order to generate enough power to recharge the battery after it drained in shadow. The components selected for use on the CubeSat

were a 40 W-hr battery and FlexU EPS board from Clyde Space and custom solar panels from Innovative Solutions in Space (ISIS). The power subsystem team also created a power budget that identified all of the components that consume power on the CubeSat and balance these power requirements with the generation the solar arrays produced in sunlight. The Telecommunication subsystem team created an uplink and downlink budget that provided the Rendezvous CubeSat with adequate uplink and downlink data transmission through use of the NASA Near Earth Network ground stations. The Telecommunication team selected an ISIS Full Duplex Transceiver and Hybrid Antenna System as the hardware components for the uplink and downlink requirements of the mission.

1   Introduction

1.1 Overall Project Description

This year, the 2018 CubeSat Major Qualifying Project (MQP) team investigating Power, Propulsion, and Telecommunications subsystem consisted of seven students and one advisor. The overall group was split into two teams, each working on separate missions. The two teams were tasked with analyzing the Power, Propulsion, and Telecommunications subsystems of a CubeSat in flight. The first mission had three members assigned to it and involved a CubeSat operating in Extreme Low Earth Orbit (eLEO). The second mission has four members assigned to it and consists of two CubeSats in Low Earth Orbit (LEO) flying in formation with one another. Within these two teams, are subsystem groups, each working on a specific component of the mission. The power subsystem groups were responsible for choosing hardware necessary to generate, condition, store, and distribute electric power to the satellite and were responsible for maintaining a power budget that will supply other subsystems with their power requirements. The Telecommunications (Telecom) subsystem groups were responsible for selecting a candidate ground station network and the appropriate telecom hardware necessary to make an optimal communication architecture that fulfills the data downlink and uplink requirement. The propulsion subsystem was tasked with designating primary and attitude control thrusters for the Rendezvous and eLEO missions in order to maintain the desired orbit and spacecraft orientation.

1.2 Mission Descriptions & Objectives

1.2.1 eLEO

The CubeSat used for the eLEO mission will be composed of 4 units (4Us) whose dimensions for each U are 100 mm-long on each side and have a mass limit of 1.33 kg. In order to

expand the value of missions focused on scientific, commercial, and defense purposes, the eLEO baseline mission consists of a 210 km, circular orbit, an unexplored region where solar wind energy couples to the Earth's upper atmosphere [1].

1.2.1.1 Power

The power subsystem for eLEO is responsible for how much power is generated, stored, and distributed throughout the CubeSat. Many components of the CubeSat will require continuous power draw for the CubeSat to remain functional in orbit. To account for this, a power budget was created considering all the hardware that will be implemented into the design. To ensure proper power delivery, hardware power requirements and their operational priority was taken into consideration. A power budget timeline of hardware was created. The timeline demonstrated what hardware should be turned on and off throughout the mission for each orbit.

1.2.1.2 Propulsion

The propulsion subsystem for this mission has he primary role of providing continuous thrust for adaptive drag compensation (not *cancellation*). According to Figure 1 from Conklin et al. [2], thruster lifetime during drag-free operations for CubeSats orbiting at 210 km last approximately 4 days.
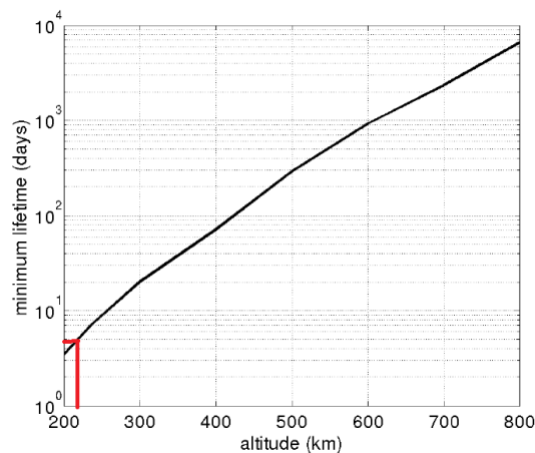
Figure 1: Estimated lifetime of drag-free operation Copyright © 2017 AIAA [2]

As can be seen in Figure 1, atmospheric drag at extremely low altitudes result in a relatively short CubeSat lifetime followed by to reentry or deorbiting. This highlights the importance of having an adequate thruster. Nevertheless, Requirement 3.1.3 for launch from a P-POD precludes the use of solid chemical rocket propulsion systems [3].

An objective of this subsystem was to select which thruster was the best possible option given the mission parameters. Since this project was the first time that a mission in eLEO had been evaluated by an undergraduate student MQP group at WPI, it was necessary to define a subsystem baseline. The steps to choose the appropriate main propulsion system were adapted and reproduced in Table 1 from Chapter 17 of Space Mission Analysis and Design textbook by Larson and Wertz [4]. Another objective was to study how to effectively counteract atmospheric drag to prolong the life of the mission as effectively as possible.

Table 1: Propulsion subsystem selection and sizing process [4]

Step	Description of Process
1	List applicable spacecraft propulsion functions, e.g., orbit insertion, orbit maintenance, attitude control, and controlled de-orbit or reentry
2	Determine ΔV budget and thrust level constraints for orbit insertion and maintenance
3	Determine total impulse for attitude control, thrust levels for control authority, duty cycles (% on/off, total number of cycles) and mission life requirements
4	Determine propulsion system options: • Combined or separate propulsion systems for orbit and attitude control • High vs low thrust Liquid vs solid vs electric propulsion technology
5	Estimate key parameters for each option • Effective I_{sp} for orbit and attitude control • Propellant mass • Propellant and pressurant volume • Configure the subsystem and create equipment list
6	• Estimate total mass and power for each option
7	Establish baseline propulsion subsystem
8	Document results and iterate as required

1.2.1.3 Telecom

Telecommunication subsystem for the eLEO mission has three main objectives. The first is to select the appropriate Telecommunication Hardware to make an optimal communication architecture that would interface with the rest of the spacecraft subsystems to fulfill the subsystem requirements. The second is to establish a reliable, candidate Ground Station Network (GSN) that will allow our spacecraft to fulfill its data transmission requirements. The third is to characterize the uplink and downlink budgets and quantify the daily data budget that CubeSat can support.

1.2.2 Rendezvous

The Rendezvous mission is characterized by two larger nanosats, referred to as a leader and a follower, flying in formation in Low Earth Orbit (LEO). The CubeSat designed for this mission will transfer into LEO orbit (~300 km) after deployment from the International Space Station (ISS) at an altitude ranging between 330 to 435 km. Once the two CubeSats are in LEO, a Rendezvous maneuver is executed in which each spacecraft attempts to Rendezvous with a "virtual" nanosat. The virtual satellite is used to guide a CubeSat along a set path that maintains the desired 100 km arc length between the two nanosats. The objective of the Power, Propulsion and Telecom team is to create a baseline set of components that will be needed to power and maneuver these larger nanosats and communicate the information collected back to the ground stations.

1.2.2.1 Power

The power subsystem team is responsible for identifying how much power can be generated given the size and flight path of the satellite as well as designate when and for what hardware this power will be used. An accurate power budget is required in order to manage the limited electric power available on the CubeSat. The power budget defines how the satellite will

distribute power to the CubeSat subsystem and payload. The identification of hardware components that will be able to interface with the on-board computer is vital for maintaining operation and data collection throughout the mission. The power subsystem must be able to satisfy all the energy requirements of components on the CubeSat, balancing the low rate of power generation with the high-power consumption of the CubeSat subsystem and payload. The final objective for the power subsystem team was to create a timeline of power generation and distribution for the CubeSat over a typical orbit.

1.2.2.2 Propulsion

The Rendezvous propulsion system team was tasked with researching and employing a propulsion system for the Rendezvous CubeSat mission. This propulsion system must be capable of maintaining a low earth orbit that will also be keeping a steady range of distances between the two satellites involved. There are some orbital maneuvers that need to occur throughout the mission, so the propulsion team was responsible for taking these maneuvers into account and making sure the propulsion system would be able to execute these maneuvers. Because the mass of the Rendezvous CubeSat (16U) will be considerably larger than that of a 4U satellite, the power consumption, primarily due to the number of thrusters that will need to be in near–continuous operation, will drive the power system capacity. Throughout the mission, both primary and secondary thrusters will be utilized to maintain its position relative to the target or virtual spacecraft, as well as to maintain the required attitude for science operations.

1.2.2.3 Telecom

A satellite uses the telecommunications subsystem in order to communicate with ground stations on Earth. The telecom subsystem for the Rendezvous mission must be able to send information from the CubeSat to ground stations as well as receive information from the ground

stations in order to perform necessary maneuvers and send sensor data. In order to accomplish this communication, various hardware components need to be defined and be able to effectively work together in the CubeSat. One objective for the telecommunication subsystem is to reevaluate the uplink and downlink budgets based on new parameters for available ground stations. A follow-on objective is to optimize the uplink and downlink so that power is readily available, and the telecom subsystem uses the least amount of power. A third objective is to reevaluate the hardware chosen from the 2017 CubeSat telecom team and investigate new options for further optimization of uplink and downlink of data [5].

1.3 Systems Engineering Group

The Power, Propulsion and Telecommunications teams were part of a larger Systems Engineering Group (SEG). The other spacecraft subsystems that comprised the CubeSat were represented at the SEG meetings and were divided into two additional MQP teams. One focused on thermal data and mechanical design. The other one was in charge of sensors and structural analysis. These two groups worked to develop both the eLEO and the Rendezvous missions.

1.3.1 Thermal, Mechanical Design Team

The Thermal Analysis and Mechanical Design team was responsible for the thermal analysis and defining the mechanical configuration of the spacecraft. The thermal analysis work consisted of evaluating the transient thermal state of the spacecraft and how this might affect the structure, components and other subsystems. The Mechanical Design work focused on generating Computer Aided Design (CAD) solid models that represent the entire CubeSat.

1.3.2 Sensors, Structures Team

The Sensor and Structures team was responsible for the sensor integration and evaluating the structural integrity of the spacecraft. The sensors team concerns picking sensors to gather data

to maintain attitude and control. The structures team evaluates the general stress and fatigue complications that the spacecraft will encounter during the mission.

1.4 Computational Tools

To perform the different trade studies for the Power, Propulsion and Telecom different computational tools were needed. The first, Systems Tool Kit (STK) a physics-based software package developed by Analytical Graphics Inc. [6] STK allows engineers to model and simulate complex ground, sea, air and space systems using a highly graphical and interactive platform. STK will be used to model our satellite with its orbital parameters in a complete mission scenario, from which we will generate a varied set of reports. The second is MATLAB, a numerical computing environment developed by Mathworks [7]. MATLAB allows engineers to analyze mathematical models running numerical simulations. MATLAB will be used by the team to analysis data and perform numerical computations that will later be represented in the form of tables or graphs.

2   Background

2.1 Previous WPI Research

2.1.1 Power Subsystem

The series of WPI CubeSat MQPs began in 2010 in order to begin definition of a spacecraft capable of supporting several candidate CubeSat missions. Prior to the current year, MQP groups identified hardware components for the power subsystem of a 3U CubeSat. In the 2017 CubeSat MQP Report, hardware that has since been discontinued was identified and changed to hardware currently available, namely from Clyde Space. The majority of this hardware is compatible with the 3U eLEO mission, however the Rendezvous mission CubeSat is notably larger and will require further research to size existing power sources capable of providing the needed output.

2.1.2 Propulsion Subsystem

The most recent MQP that investigated propulsion options for a CubeSat was group 2011 JB3-CBS1 [8] that focused on the construction of a lab-model CubeSat to test current technologies and investigate the feasibility of future of CubeSat projects at WPI. The propulsion subsystem group from Ref. 25 considered a cold gas system and concluded that "due to the strict volume constraints in a 10cm x 10cm x 30cm satellite, it appears that the limiting factor for the effectiveness of this propulsion system will be the 1.2 *atm* limit for any pressure vessels on board" [8]. At this storage pressure, the mass of any gaseous propellant will be insufficient to carry on maneuvers such as orbit raising or inclination changes. The 2011 CubeSat Team [8] found that the liquid fueled MiPS was able to store enough propellant to satisfy the mission requirements, as opposed to a cold gas system. This meant potentially increasing the amount of propellant stored, which in turn increased the mission's lifespan. The 2011 CubeSat MQP propulsion team [8]

recommended that future project groups take external disturbance torques into consideration and ensure that these torques were accounted for.

2.1.3 Telecommunication Subsystem

The telecommunication subsystem team for the 2017 CubeSat MQP defined initial hardware for the communication architecture [5]. An STK scenario was created utilizing onboard hardware and ground station network characteristics. This scenario was then utilized to perform several connection and data link reports. These studies demonstrated that the baseline subsystem was insufficient for mission objective of supporting the Sphinx-NG payload data production. Slow data rates of 101 Mb/day and very limited access time were the cause. Recommendations were made for improving the hardware and expanding the limited available ground station network. One recommendation was to build a mobile ground stations and set them up in Worcester as well as in WPI Interactive Qualifying Project sites around the globe. Another recommendation was to investigate other ground stations options as the Global Education Network for Satellite Operators (GENSO) was determined non-operational.

2.2 Power Subsystem

2.2.1 CubeSat Power Budget

Power is an essential resource for any spacecraft as various components require power to function. When constrained to the size of a CubeSat, power capacity must be substituted as well. To properly accommodate for this downsizing, monitoring of the power production and consumption is essential for a functional CubeSat. In the 2017 Design and Analysis of the Sphinx-NG CubeSat MQP [5], the team developed a table for the power budget using a list of components selected for their mission. Table 2 shows the final power budget generated by the 2017 MQP group [5].

Table 2: Final Power Budget of the 2017 CubeSat MQP [5]

Group	Component	Manufacturer	Part No.	Peak Power (W)	Nominal Power (W)	Quiescient Power (W)	Current (mA)	Voltage (V)
C&DH	OBC	Clyde Space	01-02928	1	0.35	0.165	150	Batt
ADC	Coarse Sun Sensor	Space Micro	CSS-01	0	0	0	3.5	-
	Fine Sun Sensor	New Space Systems	NSS-CSS	0.05	0.05	0	10	5
	Gyroscope	Analog Devices	ADXRS453	0.04	0.03	0.03	8	5
	Magnetic Torquer (3)	ZARM Technik AG	MT0.5-1	0.825	0.3	0	165	5
	GPS	Surrey Satellite Technology	SGR-05S	0.8	0.8	0	160	5
	Magnetometer	Honeywell	HMC5883L	<0.01	<0.01	0	0.1	3.3
Payload	Instrument		Sphinx-NG	8	8	1	1600	5
Power	EPS	Clyde Space	CS 25-02452	0.2	0.2	0.2	24	Batt
	Battery	Clyde Space	CS 01-02686	-	-	-	2400	7.6
	Center Solar Panels	Clyde Space	CS 25-02871	-	-	-	-	-
	Side Solar Panels	Clyde Space	CS 01-02882	-	-	-	-	-
Telecomm	Transceiver	ISIS	TRXUV VHF/UHF	4.8	3.3	0.4	600	Batt

2.2.2 Power Subsystem Hardware

The power subsystem is comprised of components needed to manage production, distribution, and storage of power. This becomes an even greater challenge because of the limited volume in a CubeSat. There are four main power sources for spacecraft; photovoltaic (converts incident solar radiation to electric), thermoelectric (thermal to electric), dynamic (heat engine employing piston or turbine system), and fuel cells [4]. Most CubeSats rely on solar cells (photovoltaic), and batteries to provide energy storage. The solar cells are among the most important as they help recharge the batteries before they are completely drained. To ensure efficiency of power distribution and production, with the spacecraft uses an Electrical Power System (EPS) board. Most EPS boards come with Power Conditioning Modules (PCMs) and Power Distribution Modules (PDMs). PCMs handle the conditioning of power into different voltages and currents that get supplied to the various components. PDMs handle which components are supplied power as directed by the On-Board Computer (OBC). With these

modules continuously operating, a CubeSat runs less risk of electrical failures which can damage components.

Solar Panels

Solar panels are the primary producer of power for a CubeSat due to the near limitless solar energy provided by the sun when operating in LEO. Most solar panels are made up of multiple solar cells. Solar cells are usually made from Gallium-Arsenide due to their high efficiency and slow degradation. These cells are then attached to lightweight substrate materials such as fiberglass, aluminum, and carbon fiber [4].

To confirm the amount of power generated by the solar cells, one must take into account the area of the cells, the efficiency of the material used, their operating temperature, and the illumination angle of incidence relative to the panel. In order to determine the area of solar cells required, the amount of power the solar cells must generate during sunlight must be calculated. In addition, the efficiency and operating temperature need to be determined based on duration of time exposed to the sun at a certain angle of incidence. It is important to note that deployable solar arrays tend to be 5 degrees Celsius cooler than non-spinning body-mounted solar arrays, due to the ability to radiate heat more efficiently [4]. Due to the natural degradation of solar cells resulting from radiation for example, the power production of the solar arrays over a given period of time decreases. However due to the assumed short lifespans of our two missions, this calculation is not needed.

The spacecraft will not be exposed to direct sunlight at all times and will be subject to temperature fluctuations. Due to these factors, the amount of power generated will change over time in an orbit. The voltage and current being generated by the solar panel also varies, leading to different amounts of power being produced. This relationship can be represented as a current-

voltage curve, an example of which is shown in Figure 2. The knee in the curve corresponds to the peak, or maximum, power point, which indicates the maximum power that can be generated from the various voltage and current a solar cell generates.
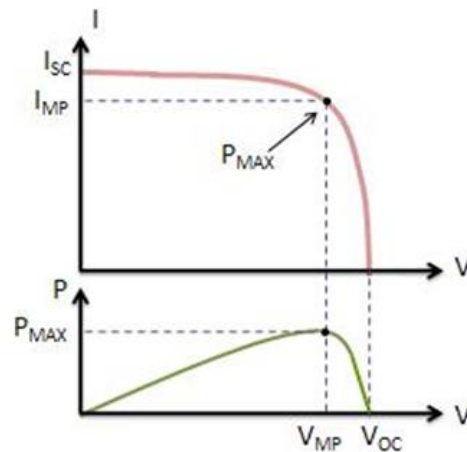
Figure 2: Solar array current vs. voltage Copyright © 2017 National Instruments [9]

The 2017 CubeSat MQP team [5] chose a 3 Unit (3U) solar panel, developed by Clyde Space, that can be mounted on the 3U CubeSat structure directly.

Electrical Power System (EPS) Board

The Electrical Power System (EPS) Board is a single circuit board mounted inside the CubeSat. The EPS board controls and regulates power from its PCM and PDM, mentioned above. The EPS board is directly connected to the solar panels, battery, OBC, and other components that require electrical current. The EPS board monitors their power consumption, generation, and storage to ensure peak performance in all areas while also safeguarding against any dangerous currents. Additionally, the EPS also maintains the peak power point of the solar panels for maximum power generation. The distribution of power by the EPS board is shown in Figure 3.
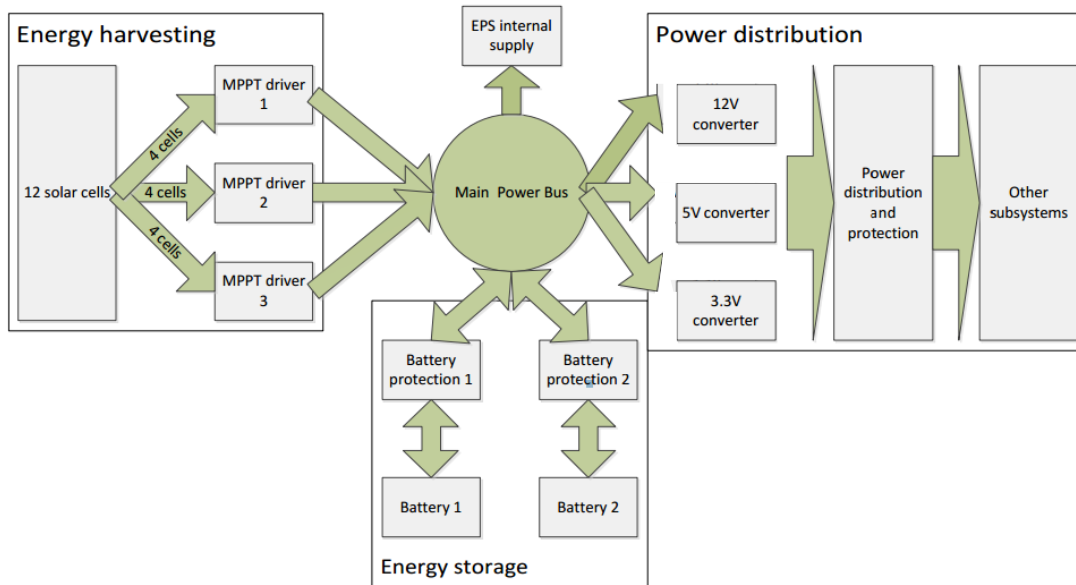
Figure 3: EPS power distribution Copyright © 2017 Jaanus Kalde [10]

The 2017 CubeSat MQP team chose the Clyde Space 3U EPS board which is made specifically for 3U CubeSats [5]. A variety of EPS boards were considered, but the Clyde Space board was adopted as a baseline.

Battery

Batteries are another source of power production and are the main form of power storage on the CubeSat. There are two types of batteries, primary and secondary. In the two missions, secondary batteries will be used, due to their ability to convert chemical energy into electrical energy during discharge, when the satellite is in eclipse, and their ability to convert electrical energy into chemical energy, during solar panel power production. Batteries are vital to photovoltaic satellites in order to store energy from the solar panels when the satellite is in sunlight and to discharge power when the satellite is in eclipse.

The biggest restriction in a small satellite is balancing the available space between additional components, such as sensors, with the required components, such as batteries, needed

13

for flight. Due to this restriction, lithium-ion (Li-ion) and lithium-ion-polymer (Li-Po) cells are the most commonly used cells in CubeSat batteries for their high energy density, 70-110 (W-hr/kg), compared to other secondary batteries [4].

Another important factor that affects the efficiency of secondary batteries is the extreme temperatures a satellite experiences in space. Li-ion and Li-Po batteries operate most efficiently between -20 to 60 degrees Celsius [11]. Aside from the thermal controls on a CubeSat, the battery temperature can be maintained using a heater attached to the battery. The heaters become extremely useful during discharge, as extremely low temperatures, experienced during shadow, can discharge a battery in an extremely short amount of time [12]. During discharge, it is also important to ensure the depth of discharge (DoD), the percentage of battery capacity removed, does not exceed the recommended range when the satellite is in shadow. Satellites in Low Earth Orbit (LEO), on average, have a recommended DoD around 30%, due to the number of charge/discharge cycles experienced in LEO, which is approximately once every 90 minutes [13].

The 2017 CubeSat MQP team chose the Clyde Space 40 Watt-hour battery, compatible with the EPS board above. This battery is compatible with the 3U configuration in the eLEO mission, however it is not large enough to support the Rendezvous mission and a new battery will have to be selected [5].

2.3 Propulsion Subsystem

2.3.1 Propulsion Overview

The driving force of a spacecraft is its propulsion system. There are two sets of thrusters that must be considered when determining a propulsion system for a CubeSat, the primary and secondary, or attitude control thrusters. Primary thrusters are used for translational spacecraft movements and generally are capable of a higher delta-v than the attitude control thrusters. The

secondary, or attitude control thrusters, are used to orient a spacecraft in a desired direction in space. Located strategically around the spacecraft, these thrusters can apply impulses or thrust for extended periods in order to reposition a spacecraft [1]. Reorientation may be required to point the solar arrays toward the sun, pointing in a direction so that the primary thrusters can take over and move the spacecraft, or even to reorient the spacecraft to optimize data collection. There are several types of thrusters that may be considered to complete the maneuvers required for the missions. Types of propulsion can be divided into electric and chemical, depending on the primary energy source used to the accelerate the exhaust gases. There are power constraints that will be different for each type of propulsion.

2.3.2 Types of Propulsion

Ion Engines

Ion engines have a very high efficiency, which is an important factor due to the limited power supply for both the eLEO and Rendezvous missions. Two of the most common types ion engines (based on the discharge) are the DC electron bombardment and the Radio-Frequency ion engines. The DC electron bombardment engine uses a cathode to generate a plasma, which heats a thermionic material so that it emits electrons, which electrons are then extracted. These electrons are accelerated into the discharge chamber and ionize the propellant gas through collisions towards a positively biased, anode surface. The electron trajectories are constrained by a magnetic field to reduce electron loss and increase engine efficiency [1].

Radio-Frequency (RF) ion engines function a little differently. These engines use a discharge process in which a propellant is ionized in a gaseous state by electrons that have been accelerated by RF fields generated by an RF antenna, usually comprised of coils that are wrapped around a dielectric discharge chamber. The ions are then accelerated by an electrostatic field

generated by grids in the same manner as with the DC ion engine. This acceleration of the propellant yields a high exit velocity which in turn produces thrust. The propellant is ionized without electrodes, which helps maximize thruster lifetime. The thruster's longevity is primarily limited by grid erosion due to sputtering [2]. Both RF and DC thrusters require an external cathode to provide electrons to neutralize the positively charged ion beam, avoiding charging of the spacecraft [1].

Busek Co Inc., a leading producer of CubeSat technology located in Natick, Massachusetts, has been developing ion thrusters that can operate with various different propellants. While the thrusters were designed to run on xenon propellant, they have the capability of on other gaseous propellants such as argon, hydrogen, iodine, nitrogen, and helium [3]. Figure 4 from Busek's website illustrating the ion thrusters operating with different propellants.
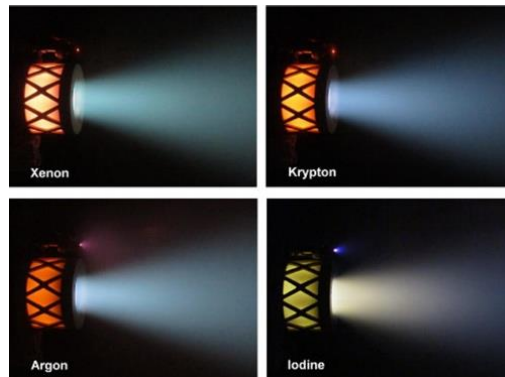
Figure 4: Busek ion thrusters operating with different propellants [3] Copyright © 2017 Busek Ltd.

Much like ion thrusters, the Hall thruster uses ionized propellant, but the ionization process varies slightly. In a Hall thruster, electrons accelerated towards an anode at the end of a ring-shaped, or annular, discharge channel. When passing through the channel they cross a magnetic field that causes the electrons to move circumferentially (i.e. create a "Hall Effect" current) resulting in collisions and ionization of the neutral gas atoms. This collisional region also results

in a potential gradient, or electric field, which then accelerates the ions downstream, producing thrust.

Electrospray Thrusters

Electrospray thrusters use an ionic liquid as a propellant and generate an electrostatic field to accelerate propellant ions from an emitter. The liquid propellant is supplied through a capillary (needle) and the free surface, or meniscus, is distorted by an applied electric field, which is intensified at the tip of the emitter. A proper balance of surface tension, electric field stresses, and flow rate results in the formation of a Taylor Cone at the tip, resulting in an intensified electric field [4]. This process can be seen below in Figure 5.
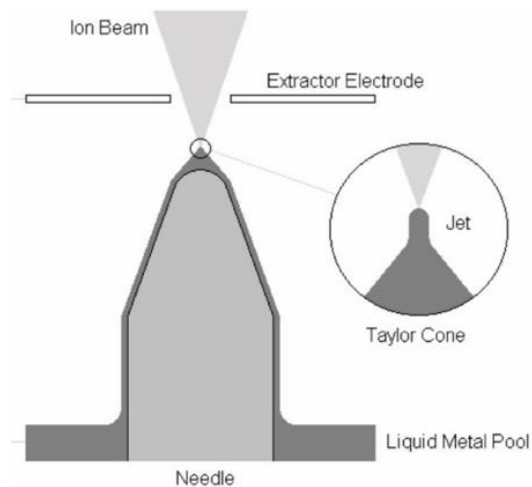
Figure 5: Electrospray thruster showing Taylor Cone Copyright © 2017 Space Propulsion Conference [14]

Hydrazine Propellant

Hydrazine thrusters are commonly used in larger satellites for attitude control and correction maneuvers. In the context of CubeSat and nanosat propulsion, these thrusters can function as primary propulsion thrusters if sufficiently compact. Hydrazine propellant systems are a well-developed technology for space propulsion, offering easier access to custom and off-the-shelf components. Some examples of hydrazine-based thrusters are the line of CHAMPS thrusters. The MPS-120 delivers a thrust of 0.26-2.79 N with a power draw under one watt during operation

and an Isp of 201 sec. The MPS-120 has four thrusters that provide two-axis attitude control as well as a fifth single-axis thruster for main propulsion. The MPS-120 occupies just over 1U on a CubeSat, which along with its low power draw makes it ideal for CubeSat missions with limited space. While the option for multiple cold starts is ideal for missions with short lifespans, the high thrust to power ratio offered by hydrazine is more useful when utilized for larger maneuvers [5].

Non-Toxic "Green" Propellant

A propellant is labelled as non-toxic when it has sufficiently low vapor pressure and the propellant compounds are less toxic than hydrazine [6]. The advantage of a system that uses non-toxic propellants is that the overall cost of the system is reduced because of the less stringent handling and storage requirements. The downside of non-toxic propellants is the need for increased power-draw; non-toxic propellants often have higher combustion temperatures and thus require more power to run the thruster [7]. Despite these limitations, there are many thrusters that are Technology Readiness Level (TRL) 5 and above. For example, the Ecological Advanced Propulsion Systems Inc. (ECAPS) has created the High Performance Green Propulsion (HPGP) system, reaching a TRL of 8. The HPGP comes in 1, 5, and 22 N variants. ECAPS and VACCO also jointly created the Micro Propulsion System (MiPS) that can fit in either 0.5U or 1U and provides attitude control as well as primary propulsion [5].

Cold or Warm Gas Propellant

Cold gas systems produce thrust by storing the propellant gas at high pressures and opening a valve to release them producing thrust. Cold gas thrusters will rely only on the pressure gradient, whereas warm gas systems will heat the gas to get extra expansion and pressures, resulting in higher thrust at the cost of the power for the heater. Cold gas systems are some of the most well-proven propulsion technologies available. The simplicity of their design as well as their robustness

makes them ideal for CubeSat missions where lower total impulses are required. Common propellants for cold and warm gas systems are inert non-toxic gases that are kept in a state of high pressure gas or saturated liquid. Therefore, they incur all the advantages gained from using non-toxic propellant. In addition, cold and warm gas systems are often low weight and occupy a small volume, reducing the weight of missions and increasing available real-estate for other subsystems. These systems produce lower thrust and have lower specific impulse on average than hydrazine thrusters. Take for example Surrey Satellite Technology Ltd.'s Butane propulsion system and Aerojet Rocketdyne's MPS-120; both have similar thrust levels, but the Butane Propulsion System has an Isp of 80 and the MPS-120 an Isp of over 200. Cold gas systems are more effective for attitude control or primary propulsion for missions with small orbital maneuvers. An example of a state-of-the-art cold gas thruster would be NanoSpace's Microelectromechanical systems (MEMS) cold gas propulsion system [7]. The MEMS have four thrusters that operate with butane propellant that can provide up to 2mN of thrust and is fully throttleable with a resolution of 5 μN. The MEMS system was flight-proven on the TW-1 CubeSat launched in September 2015 [7].

Solid Motors

Solid rocket motors use a pyrotechnic solid fuel that, when lit, burns until the fuel is depleted, and cannot be stopped, change thrust level, or reignited. They are most often used for orbital insertion or de-orbit maneuvers. Solid rocket motors offer higher thrust magnitudes in a system compact enough for use in CubeSat designs. There are also hybrid reignitable electronic solid rocket motors that produce millinewtons of thrust. The hybrids are electronic solid rocket motors that use a highly energetic but non-pyrotechnic solid fuel that is kept between two electrodes. When a charge is put through the electrodes the propellant is ignited. This system also has the advantage of requiring no moving parts, reducing the risks of mechanical failure. The

electronic solid rocket motors are ideal as they can be used for attitude maneuvers and do not provide excessive acceleration. When combined with thrust vectoring control systems, solid rocket motors can provide high delta-V that is controllable in a relatively short time. The ISP30s motor developed by Industrial Solid Propulsion is at a TRL of 7 and has a total mass of approximately 1 kg, a specific impulse of 187 seconds, and an average thrust of 37 Newtons. The ISP30s system was used on a series of flight tests to determine the effectiveness of solid rocket motors for attitude control [7].

2.3.3 Propulsion Hardware

Over the years, much progress has been made to CubeSat thrusters. Appendix A shows a compiled list of available CubeSat thrusters on the market.

Chemical Propulsion Hardware

Figure 6: MPS-120 CubeSat High-impulse Adaptable Modular Propulsion System Copyright © 2017 Aerojet Rocketdyne [18]

Table 3: MPS-120 specifications and performance [18]

Name	Type	Thrust Level (mN)	Isp (s)	Power (W)	Wet Mass (kg)	Dimensions (cm)
MPS-120	Chemical	260-2790	206-217	<4 (Startup); <1 (Operation)	1.48	10x10x11.35

An option for *chemical propulsion* systems is Aerojet Rocketdyne's MPS-120 which uses hydrazine as propellant. The 3D printed titanium tank system was selected to undergo extensive testing in late 2014 where one engine successfully performed a hot fire test [15]. The thruster requires an entire 1U of volume but can provide both primary propulsion and 3-axis control

capabilities in a single package which allows for significant ΔV capabilities such as orbit maintenance and attitude control [18].

Figure 7: VACCO Hybrid and Delta-V/RCS System Copyright © 2017 VACCO [19]

Table 4: Delta-V/RCS specifications and performance [17]

Name	Type	Thrust Level (mN)	Impulse Capabilities [Ns]	Power (W)	Wet Mass (kg)	Dimensions (cm)
ADN Delta-V MiPS	Chemical	400	1036	<15(hot-fire); <0.055(Standby)	1.8	4.15x3.54x3.54

The Hybrid ADN/RCS (Ammonium Dinitromide/Reaction Control System) shown in Figure 7 is a good option for a non-toxic propellant thruster which requires less restrictive safety and handling procedures and is capable of delivering higher specific impulse and propellant. A hybrid version is also available which incorporates one 100mN ADN thruster as well as four 10mN cold gas thrusters for attitude control which can provide up to 1036 Ns impulse for ΔV applications and 69Ns for the reaction control system function [17]. Another beneficial characteristic of this thruster is that it is relatively mature, aTRL8 with 900,000 firings during its cycle life having been demonstrated [19].

Electric Propulsion Hardware

Electric propulsion provides high specific impulses with low thrust which translates into long maneuver times. A wide range of propellants have been used successfully, from Iodine, whose

storage density allows the capability for high ΔV maneuvers for transfer trajectories, to polytetrafluoroethylene (PTFE) commonly used in Pulsed Plasma Thrusters for smaller ΔV and attitude control applications [17].
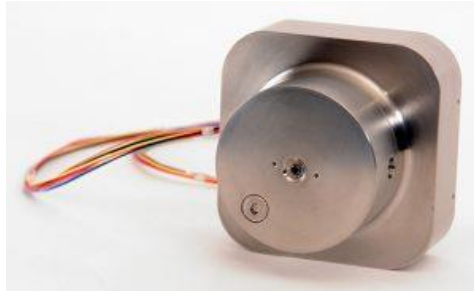
Figure 8: CU Aerospace/VACCO .14U PUC System Copyright © 2017 VACCO [20]

Table 5: PUC specifications and performance [20]

Size	Type	Thrust Level (mN)	Impulse Capabilities [Ns]	Power (W)	Dry Mass (kg)	Dimensions (cm)
.14U	Electric	4.4	213	5.3	.406	9.27x9.73x2.03
.25U	Electric	4.4	317	5.3	.428	9.27x9.73x3.15
0.50U	Electric		551		.477	9.27x9.73x5.65
1U			1016		.575	9.27x9.73x10.65

The Propulsion Unit for CubeSats (PUC), developed by CU Aerospace and VACCO is available in 0.14U, 0.25U, 0.50U, and 1U sizes making it adaptable for various missions. It consumes 5.3W and can reach a thrust level of 4.4mN. The PUC system includes a controller, PPU (Power Processing Unit), valves, sensors and a Micro-Cavity Discharge (MCD) thruster, insuring reliability through simplicity of design, welded titanium construction and frictionless valve technology [20]. VACCO's PUC has been thoroughly tested, successfully completing more than 75,000 firings in a vacuum chamber.
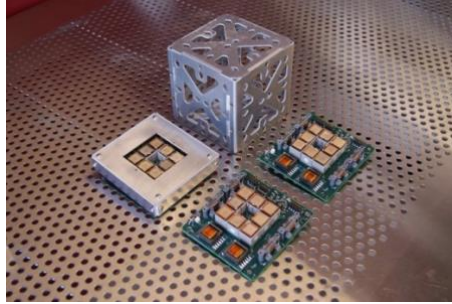
Figure 9: MIT SPL S-iEPS Copyright © 2017 MIT [21]

Table 6: S-iEPS specifications and performance [21]

Name	Type	Thrust Level (mN)	Specific Impulse (s)	Power (W)	Wet Mass (kg)	Dimensions (cm)
S-iEPS	Electric	100	1200	1.5	.1	9x9.6x2.1

The Space Propulsion Laboratory at the Massachusetts Institute of Technology (MIT) developed an electrospray thruster that is the basis for the scalable ion Electrospray Propulsion System (S-iEPS) shown in Figure 9 which features eight thrusters that fire along a single axis [21]. Each thruster consists of thousands of microtips, which is microfabricated allowing ions to shoot out from a packed $8cm^2$ of active emission area featuring non-reactive ionic salt propellants. Without moving parts or pressurization for the propulsion of ions through the microtip emission area, it reduces the risk of any mechanical component faulting [21].

Figure 10: Busek BET-100 Copyright © 2017 Busek [22]

Table 7: BET-100 specifications and performance [22]

Name	Type	Thrust Level (mN)	Impulse Capabilities [Ns]	Power (W)	Wet Mass (kg)	Dimensions (cm)
BET-100	Electric	5-100	175	5.5	.55	9x9x4

Busek's BET-100 uses ionic-liquid, characterized for the European Space Agency Laser Interferometer Space Antenna (ESA LISA) Pathfinder Mission, NASA's contribution to which is known as the ST-7 mission. It provides the convenience of no moving parts, valves nor pressure vessels [22]. Due to its small size, it can be placed in different places within the CubeSat providing throttleable primary propulsion and attitude control.
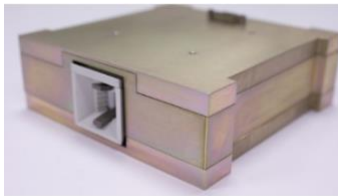
Figure 11: Mars Space Ltd. & Clyde Space Ltd. PPTCUP Copyright © 2017 Clyde Space [23]

Table 8: PPTCUP specifications and performance [23]

Name	Type	Thrust Level (µN)	Impulse Capabilities [Ns]	Power (W)	Wet Mass (kg)	Dimensions (cm)
PPTCUP	PPT	40	48.2	2	0.27	10x10x3.3

The Pulsed Plasma Thruster for CubeSat Propulsion (PPTCUP), is a compact, robust, and scalability thruster with a relatively simple interface. It has demonstrated 200% of the lifetime demonstrating 2,000,000 shots with no performance degradation [23]. Below, Figure 12 shows the thruster the eLEO mission used as the main propulsion system. It comes with the option of a 50 or

100 mL propellant reservoir, the former being the one that was chosen for the mission. Its propellant is ionic liquid which has a density of 1.25 g/cm^3, allowing it to carry 0.06kg of fuel. This would allow the thruster to stay on for 7.8 days with constant thrust and then the ballistic coefficient for a 2kg payload would take over for about 20 days until the CubeSat would deorbit into the atmosphere.

Figure 12: BET-1mN Electrospray Thruster © 2016 Copyright Busek Co. Inc. [22]

Table 9: BET-1mN Electrospray specifications and performance [22]

Name	Type	Thrust Level (mN)	Impulse Capabilities [μNs]	Peak Power (W)	Dry Mass (kg)	Volume
BET-1mN	Electrospray	0.7	605	15	1.15	1U

2.4 Telecommunication Subsystem

2.4.1 Hardware

The combination of receiver, antenna, and ground stations are what compose the communications architecture for a CubeSat. The orbit and altitude of a CubeSat will help determine what telecom hardware is necessary in order to effectively communicate with the ground stations. The orbit itself will determine how much time the satellite has to communicate with the ground station, and the altitude will determine the Earth coverage. The telecom hardware will be

adjusted to fit the orbital and altitude parameters. Data rate and radio frequency will also define parameters used for choosing the proper transceiver and antenna for the mission. A higher data rate will require a more robust transceiver and antenna. Additionally, the frequency chosen will determine the required transceiver power and will need to be approved for use by an agency such as the International Telecommunications Union [4].

Transceiver

The transceiver is a piece of hardware that communicates between the OBC and the antenna of the CubeSat. The transceiver takes data from the OBC and converts it into modulated radio waves that can be sent to a ground station by use of an antenna. Similarly, the transceiver can take modulated radio waves from the antenna and convert them into useable data for the OBC. The latest hardware for CubeSat transceivers includes the ISIS VHF uplink/UHF downlink Full Duplex Transceiver. This transceiver has been flight proven since 2016, uses little power and has low mass, and can easily be configured to a variety of CubeSats involving different data rates and frequencies [24].

Figure 13: ISIS VHF Uplink/UHF Downlink Full Duplex Transceiver Copyright © 2017 Isispace.nl [24]

Antenna

The CubeSat Antenna is used to physically send and receive information for the CubeSat. It works in conjunction with the OBC and the transceiver. During uplink, the antenna will receive commands from the ground stations below and send them to the receiver. During downlink, the antenna will receive commands from the transceiver and send them to the ground stations below. There are many mission-proven antennas available from Isispace Satellite Solutions. Variations of antenna hardware include monopole, dipole, turnstile, and hybrid. While monopole provides the strongest signal, turnstile provides the most coverage. Dipole configuration is the one of the most popular antenna configurations because it balances both coverage and strength of signal. The hybrid antenna design combines both monopole and dipole configurations and can therefore support signal and coverage [25].
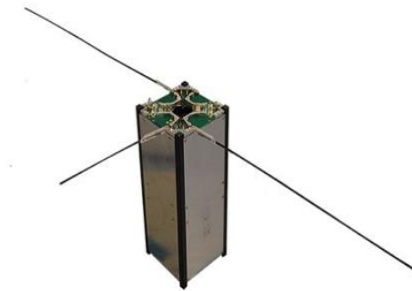
Figure 14: Hybrid Antenna System Copyright © 2017 Isispace.nl [25]

2.4.2 Ground Stations

Ground Stations are a key component of the Telecommunication subsystem of any space mission. They provide the gateway to collecting all the essential data from the spacecraft. The main components of a ground station are the antenna and the transceiver. These are connected to

a computer for data handling. Antenna and transceiver are chosen to match the spacecraft's computing architecture and desired connection frequency. The quality of the components will be driven by the required downlink budget [26]. There are a large number of ground stations available that can be accessed subject to agreements with the ground station's parent institutions.

These stations range from professional to amateur level ground stations. The Near Earth Network (NEN) is a professional ground station network made up of NASA-owned and commercial stations from around the globe. NEN is utilized by both NASA and non-NASA national and international entities [27]. Smaller amateur ground stations exist at several universities around the world, making ground station networks easily available for lower budget missions, particularly those using CubeSat. There is also the possibility of establishing a new ground station by purchasing the required components. These can be assembled into a fully functioning ground station. Another alternative is buying a fully-equipped ground station kit of-the-shelf from vendors. One such example is the Full Ground Station Kit VHF/UHF/S-band by Innovative Solutions in Space (ISIS) [24].

Figure 15: Near Earth Network map, © NASA [27]

3   Methodology

3.1 Power Subsystem

3.1.1 eLEO

3.1.1.1 Power System Evaluation

Determining the CubeSat power requirements is the critical first step in designing the power system. The requirements are determined from an examination of all the power-consuming components for a particular mission. The component active states can vary over time during the course of the mission or even an orbit. Once baseline components are selected, the power required by each was estimated, assuming they were operating continuously (to be conservative). This then needs to be equal to or less than the power generated by the solar panels. The power generated by the solar arrays is calculated by Equation 1:

$$P_{s/a} = \left[\sum_{n=1}^{6} \eta_s \cdot G_s \cdot \left(\hat{\gamma} \cdot \overrightarrow{A_n} \right) \right] \cdot I_{LF} \qquad (1)$$

Where $P_{s/a}$ represents the power of the entire solar array, the sun vector, $\hat{\gamma}$, the area of the solar array, $\overrightarrow{A_n}$, (vector corresponding to the surface normal) per face, the efficiency of the solar cells, η_s, the solar flux constant (1370W/m²), G_s, and the illumination factor of the sun at a given point, I_{LF}. The 2017 MQP team used a similar calculation, however they made different assumptions due to their design and mission [5]. For example, their CubeSat did not require a thruster. This difference removes two areas for solar panels, the front and back faces. The summation in Equation 1 will not include contributions for these faces as they will show zero area of the solar panels. Due to the current CubeSat being unable to face the sun continuously, the calculations had to account for the change in angle of incidence on all the faces.

3.1.1.2 Power Component Selection

The 2017 MQP team [5] chose various Clyde Space components for their mission. These included the battery, EPS board, and solar panels. The present study assumed a similar design from the 2017 MQP team, adopting it as the current baseline, which could be used as a basis for comparison with other components during trade studies. The battery was the Clyde Space 01-02686 40W-hr, which was able to maintain a capacity of 5200mAhr at a nominal voltage of 7.6V [28]. The EPS board was a Clyde Space 25-02452 which this includes a PCM and PDM to safely distribute power to the rest of the components [29]. Finally, they used the Clyde Space 01-02880 and 25-02971 solar panels [30]. The former was a 3U section that was placed on the sides while the latter was placed on the ends of their CubeSat. For the current mission, solar panels on the ends are not an option because of the need to accommodate a thruster on at least one of the two ends. The panels could also be custom made to design specifications. The power system using these components was then evaluated to assess performance and mass.

3.1.1.3 Power Profile Modeling

To evaluate whether the power subsystem was adequate to meet the mission need, components were simulated to compare the power requirements for each component compared with how much the solar panels would generate. MATLAB was used to perform this analysis because it can take data from STK and uses it to calculate the power generated over time. MATLAB was also used to calculate the power consumption over time, which could be adjusted to simulate different mission operational scenarios. Finally, after calculating both production and consumption, this can be used to estimate battery power level at any given time. These simulations helped determine if different components were needed, or changes needed to be made to the power consumption profile by managing the active states of different components.

3.1.2 Rendezvous

3.1.2.1 Power System Evaluation

To perform a power system evaluation, a set of system requirements were needed. This set of system requirements was used to determine the power consumption of the CubeSat in order to obtain an estimate for the total power the solar arrays are required to generate. In addition to determining an operational power budget, the system requirements also defined the location of any hardware on the exterior faces that restricted the solar panel coverage area on each side.

Once this information was determined, the orbital parameters were entered into STK to model the flight of the CubeSat on the Rendezvous mission. The satellite flight is modelled assuming three orbital inclinations: 0°, 45°, and 90°. For each of these three orbits, a body-fixed spacecraft-sun unit vector analysis and report was generated, which modeled the unit vectors of the sun with respect to the satellite reference frame. The satellite was modelled as a point-mass with a body-fixed coordinate system, where the thrust is always aligned with the STK x-direction. Coupled with the spacecraft-sun unit vector report, a solar intensity report was required in order to determine when the satellite is in the sunlight, penumbra, or umbra.

The two reports generated in STK were used to calculate the power output of the chosen solar array configuration using Equation 1. The equation was used in MATLAB to generate a report depicting the amount of power the solar arrays can generate throughout orbit. Prior to running the code, the body-fixed axis system from STK needed to be transformed to ensure that it was identical with the body-fixed axis system defined by the Structures team. For the Rendezvous mission, the z-axis is aligned with the thrust throughout the orbit. The power generation report was run for all three CubeSat size options; 12U, 16U and 20U, to determine what the best size was for a CubeSat with the given payload and mission. Equation 1 in the above approach does not take

into account the inefficiencies that will occur due to the electrical interfaces and the solar arrays temperature.

3.1.2.2 Power Component Selection

The power generation as a function of time for the given orbital parameters defined the power components selected to run models. For the Rendezvous mission, the Clyde Space 3rd Generation FlexU EPS was selected as the EPS board for the CubeSat. Along with performing the main functions of providing protection against analogue circuits and power generation, the FlexU EPS has a built in PDM board with one unregulated battery bus and three regulated output buses of 3.3V, 5V, and 12V. The PDM built within the FlexU EPS also protects the battery from under-voltage and over-current charges [29]. Once the EPS board was selected, a battery was chosen that integrated with the EPS Board. The battery selected for this mission is the Clyde Space 40W-hr CubeSat Battery, as it is designed to interface with the EPS board selected [28]. Although Clyde Space offers "Power Bundles" that include an EPS board and battery, there was no bundle that included the FlexU EPS and a 40W-hr battery.

The final component selected for the power system was the solar arrays. The solar arrays selected are the custom solar panels offered by Innovative Solutions in Space (ISIS). These solar panels were selected as they can be custom made to fit on the size of the CubeSat. The ISIS solar arrays use GaAs triple junction solar cells from AZUR space and have an efficiency of 30%, allowing for enough power to be generated to meet the system requirements for the Rendezvous mission with non-deployable solar panels [31]. The ISIS solar arrays were also selected because they can be integrated with the receiver, selected by the telecommunications team, on the faces where both exist. Clyde Space also offers custom solar panels; however, they operate at a lower efficiency than the ISIS solar arrays used in the models.

3.1.2.3 Power Profile Modeling

In order to meet the system requirements, a computational model of the power subsystem was created using the data available for all the CubeSat subsystems. First, a power budget was created that included all of the components and the power they consume. Second, simulations were produced from data generated from the propagation of orbits in STK, the operational states received from the CDH team, and the MATLAB power generation computations. The simulations were used to create a complete power profile of the satellite through orbit. Using the operational states and the power budget, one of the most useful animations generated displayed a state vector versus time graph that depicted which components were on and which components were off throughout the satellite's orbit.

Using these state vectors, animations were produced to depict the power consumption of the satellite. These animations graph the power being used by each component as a function of time over a period of three orbits. The animations display the solar panel power generation, the satellite power consumption, and the battery discharge and charge level. These profiles are important in determining the feasibility of the selected power components and determine the power available for distribution to other components and the payload. If the profiles are insufficient to meet the mission requirements, then the distribution of power can be altered, or new hardware can be selected.

3.2 Propulsion Subsystem

3.2.1 Propulsion System Evaluation

3.2.1.1 Disturbance Torques and Drag Compensation

Since the propulsion analysis was similar for both missions, the following methodology applies to each. There were four types of disturbance torques to be considered that affected the

angular momentum of the CubeSat while in LEO and eLEO. To determine the sizing of the thrusters, the disturbance torques needed to be considered when doing maneuvers as they would affect the desired motion. These disturbance torques included the torque due to atmospheric drag, solar radiation, gravity gradient, and the Earth's magnetic field. The equations following this section, used to model the disturbance torques are from Wertz and Larsen [4].

Since the CubeSats in both missions operate in eLEO or LEO, they will experience a disturbance torque due to atmospheric drag, which will be especially significant at the eLEO altitude. This torque due to drag must be considered when analyzing these disturbances. Equation 2 is used to calculate the disturbance torque due to atmospheric drag.

$$T_a = \frac{1}{2}\rho A C_D v^2 \left(c_{pa} - c_g\right) \tag{2}$$

In this equation, T_a is the disturbance torque due to aerodynamic drag on the CubeSat, ρ is the atmospheric density at the desired altitude, A is the cross-sectional surface area that is normal to the velocity vector, C_D represents the coefficient of drag for the CubeSat, and v is the speed of the CubeSat. The last two terms, c_{pa} and c_g are the center of aerodynamic pressure and center of mass, respectively. This torque is mainly influenced by the geometry of the spacecraft and the location of its center of gravity relative to the center of pressure.

Solar radiation can play a role in the disturbance torques as the photons from the Sun carry momentum. While the effect is typically small compared to aerodynamic torque in LEO, it must be accounted for and is mainly influenced by the geometry of the spacecraft, its reflectivity, and the location of its center of gravity. Wertz and Larson model's solar radiation torque as follows [4].

$$T_{sp} = \frac{F_s}{c} A_s \cos(i) \left(1 + q_r\right)\left(c_{pa} - c_g\right) \tag{3}$$

The equation consists of T_{sp} as the solar radiation torque on the CubeSat, the Earth's incident solar radiation $F_s = 1367$ W/m^2, c as the speed of light, A_s is the surface area affected by the radiation, c_{ps} is the location of the center of solar pressure, c_g is the center of mass, q_r is the reflectance factor, and i is the angle of incidence of the Spacecraft-sun unit vector.

The torque resulting from a gravity gradient is given by Equation 4. It is most influenced by the spacecraft's moments of inertia and its altitude [4].

$$T_g = \frac{3\mu}{2r^3}|I_z - I_y|\sin(2\theta) \tag{4}$$

T_g is the gravity gradient torque on the CubeSat, the Earth's gravity constant is $\mu = 3.986$ $\times 10^5$ km^3/m^2, r is the orbital radius in km, θ is the maximum deviation of the axis relative to the nadir pointing vector in radians, and I_z and I_y are minor moments of inertia for the spacecraft. This torque is typically deemed negligible for space spacecraft such as a CubeSat, due to the small mass of the satellite. For the purposes of collecting data, this disturbance torque was not neglected when doing calculations.

The last disturbance torque results from the Earth's magnetic field acting on any residual magnetic dipole the spacecraft may produce. This disturbance torque is influenced by the vehicles orbital altitude, the spacecraft's residual dipole, and the orbital inclination. Equation 5 from Wertz and Larson can be used to estimate the disturbance torque due to the magnetic field [4].

$$T_m = D\frac{2M}{R^3} \tag{5}$$

Here, T_m is the magnetic torque on the CubeSat, D is the residual dipole of the vehicle in Am^2, $M = 7.96 \times 10^{15}$ Tm^3 is the magnetic moment of the Earth, and R is the radius from the center of the Earth to the CubeSat. $2M / R^3$ is the Earth's magnetic field in Tesla, usually noted as B [4].

During STK simulation and analysis, when the sunlight was aligned with the X-axis (as shown in Fig. 16, the incidence angle was equal to zero. For missions above 500 km the greatest

disturbances are due to solar pressure and the magnetic field whereas for missions below 400 km, the aerodynamic torque becomes the most significant torque [32].
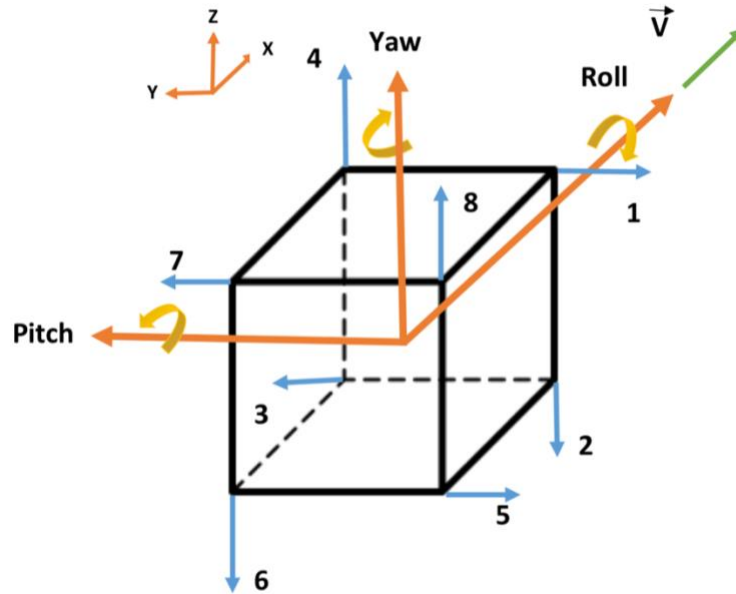
Figure 16: Diagram of μPPT placement

Table 10: Translational μPPTs firing couples

+ Roll	(6,8)	(7,5)	(5, 6, 7, 8)
- Roll	(1, 3)	(2, 4)	(1, 2, 3, 4)
+ Pitch	(4, 6)		
- Pitch	(2, 8)		
+ Yaw	(1, 7)		
- Yaw	(3, 5)		

In Figure 16, the placement of the μPPTs are shown by the blue arrows labeled 1-8 with their respective configurations to provide roll, pitch, and yaw movements in Table 10.

3.2.1.2 Maneuver Analysis

To determine thruster sizing, two maneuvers were analyzed for the CubeSat. The first of the two is the "detumble" or despin stabilization maneuver. This maneuver is the task of achieving a steady state after being ejected from the transport satellite. It is a crucial one since the mission

36

cannot begin if the spacecraft cannot stabilize and align with the proper velocity vector, especially in eLEO, the spacecraft will not be able to apply thrust in the correct direction and it will deorbit.

The second maneuver is a 180-degree slew maneuver that is a rotation about the CubeSat's minor axis. While a complete 180 turn is unlikely to be employed during the mission, it is useful as a baseline for thruster sizing in a trade study. The purpose of considering this maneuver is to evaluate the worse-case scenario so that if the thrusters were ever subjected to such conditions, they would be able to successfully perform that and any other maneuver with lower constraints.

To analyze these maneuvers, the equations of basic angular kinematics about a single axis were used. Equation 6 is used to calculate the required angular momentum rate (torque) required for slew maneuvers [32].

$$\dot{H}_{sl} = \frac{4I\Delta\theta}{(1+\alpha^2)\Delta t_{sl}}$$

(6)

Here, $\dot{H}_{sl}$ is the angular momentum required to complete the slew maneuver in radians/second, I is the moment of inertia, $\Delta\theta$ is the desired angle of rotation in radians, α is the idle time factor, and Δt_{sl} is the time required to complete the maneuver in seconds. It is important to note that these maneuvers were analyzed as a stop-to-stop rotation, meaning from start to finish.

The torque needed for spin stabilization is calculated using Equation 7 [32].

$$\dot{H}_{st} = \frac{I|\Delta\omega|}{\Delta t_{st}}$$

(7)

Here, $\dot{H}_{st}$ is the angular momentum rate required to achieve stabilization, I is the moment of inertia about the axis of rotation, $\Delta\omega$ is the change in angular velocity (i.e. the initial spin rate), and Δt_{st} is the time needed to complete the maneuver (i.e. bring it to rest).

In Equations 7 and 8 such as the time required to complete maneuvers, desired angle of rotation, and change in angular velocity were varied to determine the required torques for different

scenarios subject to different constraints. The primary constraint used was the time to complete

the maneuver, thus changing other parameters in the formulas. By applying these equations to the

maneuvers described at the beginning of this section, the thruster requirements were determined,

narrowing the range of propulsion technologies considered.

3.2.2 Propulsion Components Analysis

3.2.2.1 μPPTs

In order to size the μPPTs, ADN thrusters, and reaction wheels, a MATLAB code was

created based on the methods described in Wertz and Larson [4]. The code was first written to

calculate the torque required to counteract the disturbance torques described in Section 3.2.1.1. It

was then modified to calculate torques for maneuvers including a 180-degree slew maneuver with

0 and 90% idle time, and a despin stabilization maneuver with initial angular momentums of 5, 10,

and 20 degrees per second. The idle time refers to the span of time in between pulses used to

complete maneuvers. For the 90% idle time slew maneuver, the thrusters fire in one direction for

5% of the time, then idle for 90%, and then fire in the opposite direction for the remaining 5% to

stop the rotation. For the 0% idle, the thrusters pulse continuously for 50%, and then immediately

switch directions for the remainder of the rotation. The code also had the capability to evaluate

different actuators, including the μPPTs and the reaction wheels, and was coded to produce graphs

of the different useful parameters. These graphs were studied to help determine possible

improvements to the baseline which will be shown in Section 4.

The calculations were performed assuming a "worst-case scenario," with each maneuver

being performed around the minor moment of inertia, requiring more effort from the Reaction

Control System (RCS) being used. The moments of inertia were calculated assuming the

Rendezvous CubeSat could be represented by a 2x2x5 (20U) rectangular prism with a total

theoretical mass of 20 kg and a 1x1x4 (4U) rectangular prism with a 4kg theoretical mass for the eLEO mission. With the exception of the constant disturbance torques, the maneuver results were plotted for as a function of different execution times. The power required by the μPPTs calculated by evaluating the frequency required for a given maneuver and time-to-complete. This product represents the total number of pulses for the maneuver. This could then be multiplied by the power-per-shot according to Equations 8 and 9:

$$f_p = \frac{\dot{H}_T}{s \cdot I_{bit} \cdot n} \tag{8}$$

$$P = f_p \cdot E_d \tag{9}$$

Here, $\dot{H}_T$ is the angular momentum rate (torque) required for the maneuver, s is the moment-arm, I_{bit} is the (linear) impulse bit, n is the number of μPPTs firing (a multiple of two), f_p is the pulse frequency, E_d is the energy discharge per shot, and P is the power required. The baseline for the PPT was the same as the type used on the DAWGSTAR CubeSat, with an impulse bit of 70 μNs and an energy discharge per shot of 5 J [33].

3.2.2.2 ADN Thruster

The ADN thrusters were evaluated using the same required angular momentum rates for the maneuvers, as those values are independent of the actuators used. The hybrid thrusters would be placed in different positions than the μPPTs; they were set at the center of the faces rather than at the vertices. In order to evaluate the power used, the torque required by the maneuver was divided by the maximum torque available and multiplied by the max power consumption of the units, assuming the power consumed scales linearly with the thrust applied. This ignores the power used to open or close a valve, and other such usages. Since the maximum torque is higher than any torque required by any maneuver, the thrusters will never be drawing more power than their maximum.

3.2.2.3 Reaction Wheels

As a trade study, the team decided to explore reaction wheels and their possible application to the mission. The focus was on Blue Canyon Technologies (BCT) reaction wheels since the company has one of the most diverse options for the product ranging from 0.015 Nms to 0.10 Nms for CubeSats. Even though the use of μPPTs are the baseline option being considered for attitude control, reaction wheels also provide an efficient and high-performance solution. BCT offers brushless DC motors, ultra-smooth bearings, and a lubrication system which ensures low jitter performance and long life for the mission [34]. The three options we investigated were the RWP015, RWP050, and RWP100, as presented in Table 11.

Table 11: BCT Reaction Wheels Copyright © 2017 Blue Canyon Technologies

MicroWheel		RWP050		RWP100	
Momentum	0.015 Nms	Momentum	0.050 Nms	Momentum	0.10 Nms
Mass	0.130 kg	Mass	0.24 kg	Mass	0.35 kg
Volume	43x43x18 mm	Volume	58x58x25 mm	Volume	70x70x25 mm
T_tot	1.543E-7 Nms	T_tot	1.543E-7 Nms	T_tot	1.543E-7 Nms
DeSat_num	24.11	DeSat_num	7.23	DeSat_num	3.62
DeSat_times	1.29 days	DeSat_times	4.28 days	DeSat_times	8.57 days

3.3 Telecommunications Subsystem

3.3.1 eLEO

3.3.1.1 Telecommunications System Requirements

The telecommunication subsystem is responsible for the communication between the CubeSat and Earth. Due to the short duration of the eLEO mission, the subsystem objective was to maximize the amount of data that can be transferred over a determined timespan. Even though it did not fulfill past data transmission requirements, nor was it expected to be sufficient to ensure an appropriate data link budget for the current mission, the 2017 MQP's Telecommunications subsystem was adopted as a baseline for the present study [5]. From the baseline, trade studies were evaluated to determine system subsystem options that will have a maximized data link budget ensuring proper uplink and downlink and making telemetry and crucial mission data available to operators on the ground.

3.3.1.2 Telecommunications Component Selection and Trade Study

The hardware architecture consists of the transceiver and the antenna. The baseline included the ISIS VHF uplink/UHF downlink Full Duplex Transceiver and the ISIS Hybrid Antenna System [25] [35]. Table 12 details the baseline hardware and its main characteristics. Due to insufficient data link budget from previous year's MQPs [5], the hardware trade study considered additional options that would increase communications rates. A new state of the art transmitter from ISIS was analyzed, its main advantage being a fast data rate, and other characteristics listed in Table 13. The ISIS TXS S-Band Transmitter [36] was analyzed due to its compatibility with the Space Network Communication System, which is evaluated as a Communication Network option in Section 3.3.1.3. It is important to note that this is only a transmitter and not a full duplex transceiver as is the case for the baseline option. This S-band

transceiver is not a replacement receiver, but an addition to the baseline system. For the S-band option study, the same baseline transceiver board was kept as a receiver. For both the baseline and the S-band option, the hybrid antenna was kept unchanged.

Table 12: Telecom hardware (baseline) characteristics

Full Duplex Transceiver (VHF Uplink/ UHF Downlink)/Hybrid Antenna

Transmitter		
Operation Frequency	435 - 438	MHz
Power	4	W
Data Rate	9.6	Kbps
Modulation	BPSK	-
Pointing Loss	-1	dB
Price	11375	USD
Receiver		
Operation Frequency	435 - 438	MHz
Power	0.48	W
Data Rate	9.6	Kbps
Modulation	AFSK	-
Pointing Loss	-1	dB
Price	Comes with Transceiver	USD
Antenna		
Length	0.55	m
Length/Wave Length	0.799	-
Efficiency	0.55	-
Refraction Model	ITU-R P.834-4	-
Range Limit	3000	Km
Price	6356	USD

Table 13: Telecom hardware option 2 (S-Band Transmitter) characteristics

Hardware S-band Option (Trade Study 1):
S-Band Transmitter/ VHF Uplink / Hybrid Antenna

Transmitter		
Operation Frequency	2200-2290	MHz
Power	9.2	W
Data Rate	3.4	Mbps
Modulation	OQPS/ OQPSK	-
Pointing Loss	-1	dB
Price	Upon Request	USD
Receiver		
Operation Frequency	435-438	MHz

Power	0.48	W
Data Rate	9.6	Kbps
Modulation	AFSK	-
Pointing Loss	-1	dB
Price	11375	USD
Antenna		
Length	0.55	m
Length/Wave Length	0.799	-
Efficiency	0.55	-
Refraction Model	ITU-R P.834-4	-
Range Limit	3000	Km
Price	6356	USD

3.3.1.3 Ground Station Network Analysis

To complete the definition of the telecommunication subsystem architecture, a ground station network is essential. The 2017 MQP group's final ground station network consisted of a set of university operated, amateur ground stations. These did not provide enough access time for the data link requirement to be fulfilled [5]. A recommendation from that year was to add mobile ground stations in Worcester as well as in a WPI IQP site. For the present set of missions under study, characterized by relatively short mission time, it was decided to drop the baseline amateur ground stations and instead only consider professional, commercially available ground station networks, both operated by NASA. Option #1 is the NASA Near Earth Network (NEN) comprised of 15 ground stations around the globe. Option #2 is the NASA Space Network (SN) comprised of 2 ground stations and 8 geostationary TRDS satellites. Table 14 describes both network's main characteristics.

The fundamental considerations that lead to selection of these two networks for the present work included the following: First, being NASA's reputable, professionally operated network, state-of-the-art technology and services would be provided. Second, due to their flight heritage, NEN and SN combine to downlink 98% of NASA's telecommunication sensitive mission data

[37]. The NEN was analyzed first as an immediate upgrade from past year's amateur ground station network. The SN was also analyzed as a more exotic candidate to accommodate the CubeSat mission's data link budget requirements.

Table 14: Ground Station Network options (NEN & SN) characteristics

Ground Station Network Options

\	Option #1 (NEN)	Option #2 (SN)
Ground Stations	15	2
Satellite Constellation	N/A	8 TRDS
Coverage	Partial	Complete
Price	490 USD per Access	136.37 USD per Minute
Operated by	NASA	NASA
Proficiency	Varies	99.90%

3.3.1.4 STK Analysis

To perform the trade studies that would enable the selection of a communication architecture capable of fulfilling the data link budget requirements, different computational tools were needed. STK and MATLAB were used together to produce a data link budget for each of the assumed hardware and GSN options. To generate the data link budget, STK was used to establish a mission scenario and generate access reports. Then, MATLAB was used to integrate the data from these reports and produce total data transfer estimate per mission's day.

Scenario Set-up

A scenario for the mission was created using STK. To define the scenario and generate desired reports, several STK objects (elements that interact within a scenario) were defined and added. First, the main component of the mission, the CubeSat, was added using the Orbit Wizard and the classical orbital parameters provided by the graduate student mission leader, described in Table 15. Afterwards, the NASA NEN facilities were added into the scenario from the facilities database. Antenna arrays in single locations were deleted to eliminate redundancies and streamline the analysis. The final selection included 15 ground stations around the globe. For the Option 2

Network, a similar process was followed. Eight TRDS satellites were imported from the STK Standard Object Database [38]. With the CubeSat and Networks defined, the base STK scenario definition was complete, see Figure 17. Using the base scenario, Telecommunication specific objects (antennas, transmitters and receivers) were added to generate access and data link reports. First, transmitter, receiver and antenna objects were created for the satellite. Then their object parameters were specified according to the data in Tables 12 and 13. Next, receiver, transmitter, and antenna objects were added to the ground stations. Their properties were defined as a simple receiver and simple transmitter with auto tracking for frequency. This was based on the assumption that the professional has the optimal equipment needed to match the CubeSat's transmission. NEN ground station antenna size average is 10 meters. This average was used to define the antenna size for all NEN locations. All the ground stations were assumed to have the same characteristics. Finally, the receiver, transmitter, and antenna objects were added to the TRDS constellation. All TRDS were assumed simple receivers with auto tracking for frequency as the limiting end is the transmitter on the CubeSat.

Table 15: eLEO Mission classical orbital parameters

eLEO CubeSat mission Classical Orbital Parameters

Inclination	51.63	deg
Right Ascension of the Ascending Node	352.6	deg
Eccentricity	0.0022	-
Argument of Perigee	76.15	deg
True Anomaly	323.7	deg
Semi-major Axis of the Target Orbit	6603.1	km
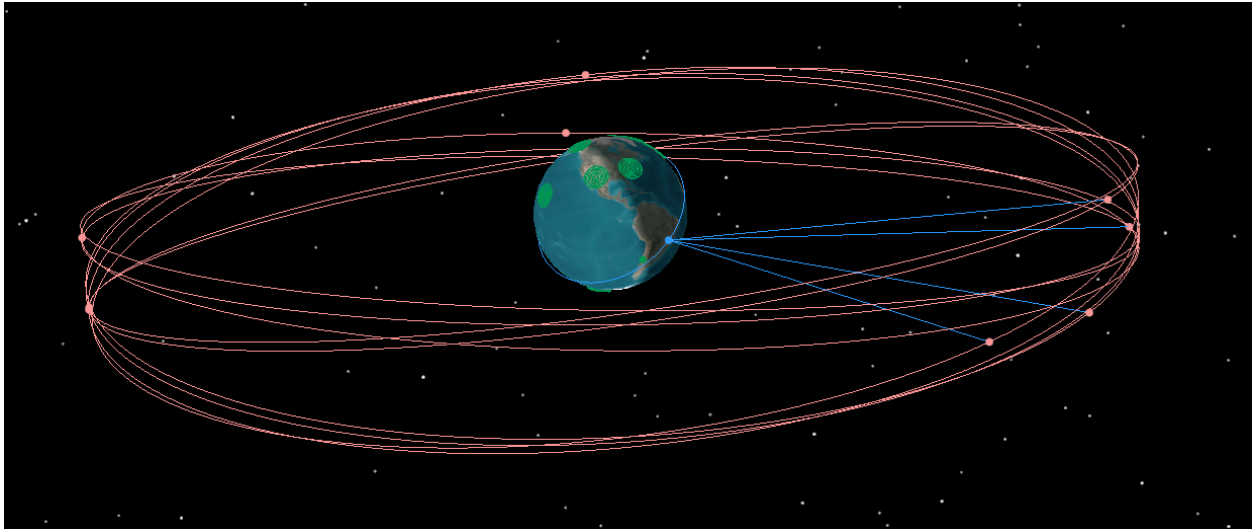
Figure 17: eLEO STK scenario

Report Generation

With the scenario defined for telecommunication analysis, the uplink and downlink Data Link Budget were generated for both the NEN and SN cases. An access report was generated from the analysis tool in STK. In this report, each of the different downlink opportunities was detailed. Links were sorted by ground station and numbered according to when on the day they connected. Columns show the Start and Stop time of connection on UTCG (Coordinated Universal Time in Gregorian Format) and the duration of each of the links (Appendix B). The analysis also provides a graphical access report where the access periods graphically represented on a map, shown color coded corresponding to their respective ground stations vs. UTCG time for the day (Appendix B). The last report produced was a Data Budget report that provided telecommunication specific

parameters for each of the connections. These parameters include the link quality, represented as the gain in decibels, bandwidth, and frequency among others (Appendix B).

Data Link Budget Calculation

With the different reports generated Data Link budget for uplink and downlink was calculated for both of the network cases, the NEN and the SN. First, the access report from the STK analysis was imported into MATLAB to be used with the Data Link Budget calculation code (Appendix C). The code takes the start time and stop time of each access period as date formats and subtracts them to calculate a duration. This duration is multiplied by the data rate in megabytes per second, producing an array of data transfer per connection in megabytes. This array was then plotted vs. time to generate daily data link budget. Finally, all the access duration times and data links per access were summed, generating the total link time and total data link per day.

3.3.2 Rendezvous

3.3.2.1 Telecommunications Component Selection

The Telecommunication team conducted trade studies for three different orbital inclinations. Those inclinations were 0, 45, and 90 degrees. The different inclinations produce different orbits, and these varying orbits result in differing coverage capabilities for uplink and downlink. Each inclination requires a specific communication architecture in order to analyze the total uplink and downlink capability per 24-hour period. For the 45 and 90 degree inclinations, the Telecom team began with the ISIS VHF uplink/UHF downlink Full Duplex Transceiver as well as the Hybrid Antenna System, both described in Section 2.4.1, as a baseline for trade studies. The 0-degree inclination would require an additional transmitter, the ISIS TXS S-Band Transmitter, as described by the eLEO sub-team in Section 3.3.1.3. The explanation regarding the need for this transmitter for the Rendezvous mission is outlined in Section 3.3.2.3.

3.3.2.2 Ground Station Network Analysis

The most challenging obstacle to overcome for the 2017 Telecom team was the limited access time for uplink and downlink given their selection for the ground station network. The few ground stations the 2017 team modeled did not have sufficient connection time for mission requirements. The suggestion for future teams was to investigate the possibility of more ground stations and updated hardware.

For the present study, ground stations that are part of the NASA Near Earth Network, which consists of more than ninety available ground stations for CubeSats, were investigated. Twelve ground stations were selected to receive data from the CubeSat in order to keep the parameters realistic for the Telecom trade studies. The ground stations and their locations are shown in Figure 18.
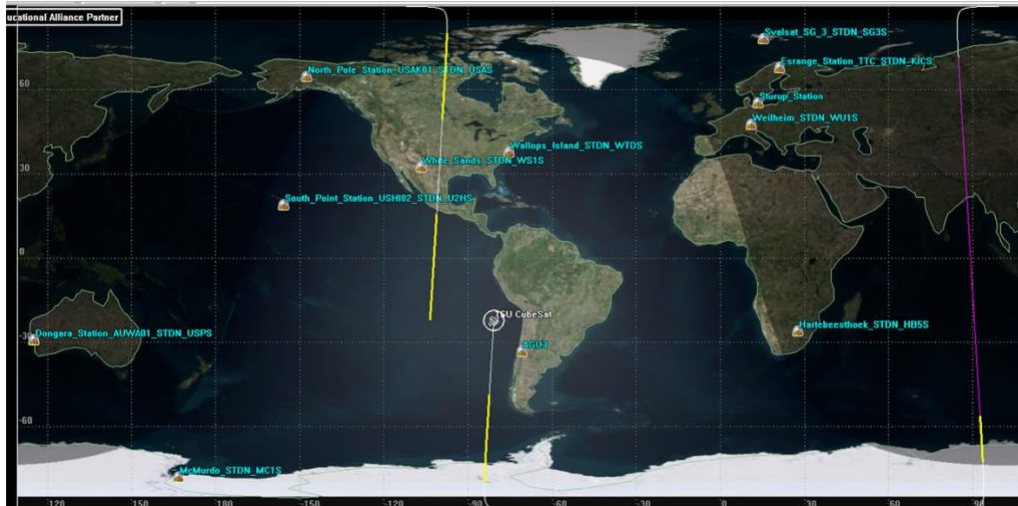
Figure 18: NASA NEN Ground Stations for the 2018 Telecom Analysis

As described in Section 3.3.1.3, the Space Network was investigated as a possible solution for telecommunication data transfer given the relatively short anticipated lifetime for the eLEO mission. The Space Network is not necessary for Rendezvous mission because the time in orbit is much longer for this mission. However, because the Rendezvous mission will have no downlink

48

access for the 0-degree orbit, (as outlined in Section 4.3.2.1) the Space Network offers a potential solution to conduct this mission at that inclination.

3.3.2.3 STK Analysis

An STK scenario was developed for the Rendezvous mission in order to estimate the available access time and potential uplink and downlink budgets. To account for the three inclinations, three STK scenarios were created, each having their own specific inclination. The twelve NASA NEN ground stations provide an array of coverage for the CubeSat at various inclinations. The STK scenarios with the three possible inclinations and ground station coverage are pictured in Figures 19 through 21. The yellow line in these images represents the track of the CubeSat's orbit for the specified inclination. The transition of the yellow line to the purple line represents the point where the CubeSat transitions from sunlight into darkness. The blue lines represent the access between the CubeSat and possible ground station when the scenario was run over a 24-hour period.
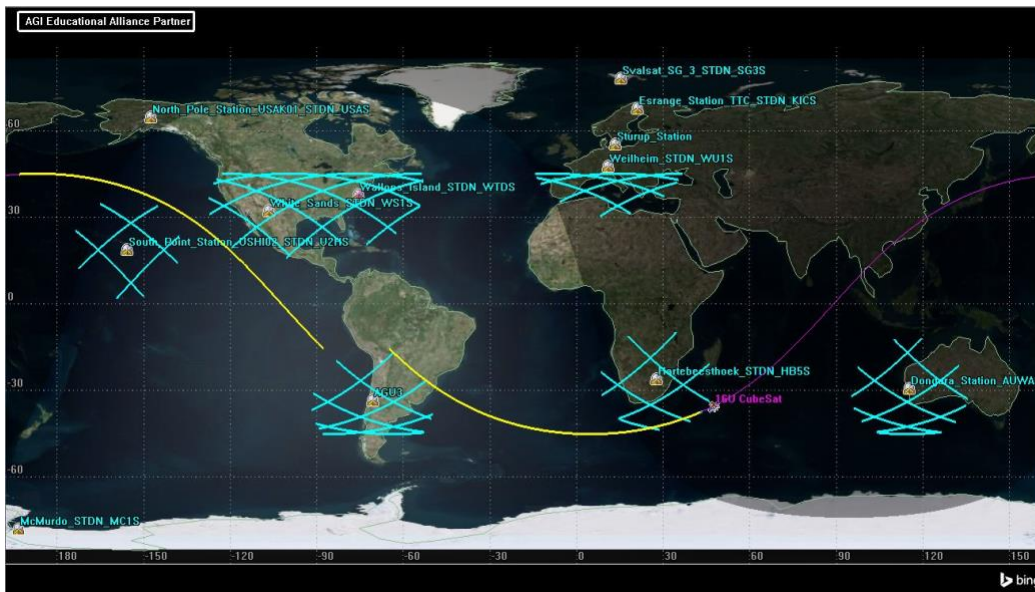
Figure 19: NASA NEN Ground Station access for a CubeSat at 45-degree inclination
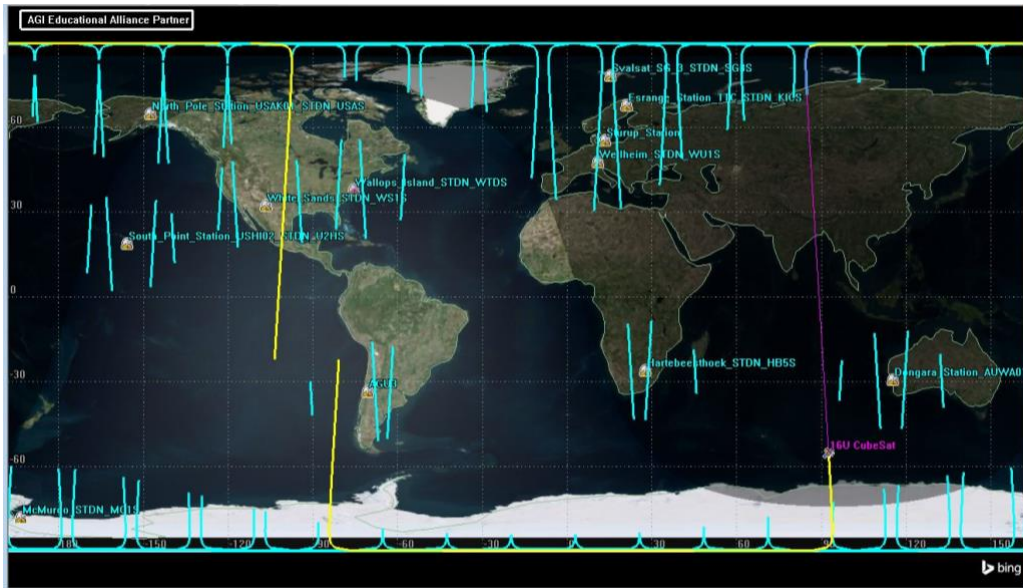
Figure 20: NASA NEN Ground Station access for a CubeSat at 90-degree inclination

Figure 21: NASA NEN Ground Station access for a CubeSat at 0-degree inclination

Once the STK scenario was executed over a 24-hour period, the access time between the satellites at different inclinations and the available ground stations could be extracted as an Excel file from the STK generated access report. It was then imported into MATLAB to calculate total data per connection as well as total downlink potential per 24-hour period.

4   Results

4.1 Power Subsystem

4.1.1 eLEO

4.1.1.1 Final Hardware Configuration

The hardware for the CubeSat power subsystem was determined earlier in the design process for the mission. After analyzing the performance and capability of the hardware, these components would later be switched out if they were deemed inadequate.

The final choice for the EPS remained as the 3rd Generation 3U EPS produced by Clyde Space [29]. This EPS board offers complete control over power distribution and conversion. This includes maximum power point tracking (MPPT), a Power Distribution Module (PDM), and protections from overcurrent and under-voltage protections. The EPS board was able to include all these features saving both weight and space while other EPS boards require physically separate modules.

For power storage, the 40 W-hr Clyde Space battery was chosen to handle all eclipse power requirements. Initial analysis showed that due to power generation, the size of the battery could be downsized. Another option was the 30 W-hr battery from Clyde Space, that was used by the 2013 team. However, like the 2016 team, due to the high demand for component activity, it would be safer to use the 40 W-hr as it can handle higher amperage [1]. The battery also has its own protections including overcharge, overdischarge, overcurrent, overvoltage and undertemperature [28].

The 2018 eLEO Power subsystem required custom manufactured solar arrays by Clyde Space. Using their Spectrolab Ultra Triple Junction (UTJ) Solar Cells, which are advertised to have a 28.3% efficiency at 28° C for cells less than 32cm^2, or 27.7% efficiency at 28° C for cells

greater than 50cm^2 [39]. The reason for the custom arrays was to add flexibility to the design due to certain components requiring exposure to space to function, such as the PPTs and sun sensors. Although these custom panels do include sun sensors and temperature sensors, it was decided to monitor these from other components as backups. The custom panels would cover all four side-faces of the CubeSat, leaving the front face for a sun sensor and the back face open for the thruster. Table 16 summarizes the power requirements for each subsystem.

Table 16: Subsystem power requirements (eLEO Mission)

Group	Component	Manufacturer	Part no.	Peak Power	Nominal Power	Quiescent Power	Current	Voltage
C & DH	OBC	Clyde Space	01-02928	1	0.35	0.165	150	Batt
ADC	Coarse Sun Sensor	Space Micro	CSS-01	0	0	0	3.5	-
	Fine Sun Sensor	New Space Systems	NSS-CSS	0.05	0.05	0	10	5
	Gyroscope	Analog Devices	ADXRS453	0.04	0.03	0.03	8	5
	GPS	Surrey Satellite Technology	SGR-05U	0.8	0.8	0	160	5
	Magnetometer	Honeywell	HMC5883L	<0.01	<0.01	0	0.1	3.3
Power	EPS	Clyde Space	CS 25-02452	0.2	0.2	0.2	24	Batt
	Battery	Clyde Space	CS 01-02686	-	-	-	2400	7.6
	Solar Panels	Clyde Space	25-02873	-	-	-	-	-
Telecomm	Transceiver	ISIS	TRXUV VHF/UHF	1.9	1.7	0.2	600	6.5-12.5
Propulsion	BET1mN	Busek		15	10.5	2	-	9-12.6
	PPT	Custom Made		12.5	-	-	-	-

4.1.1.2 Power Profile Results

To determine if the selected hardware would perform as predicted, a MATLAB simulation was created to analyze the solar generation and the battery capacity as a function of time over a

representative set of orbits. To aid with some of the data required, STK models were used to gather sun intensity and spacecraft-sun unit vector data. The general inputs included component power draw, battery capacity, estimated efficiency of the solar panels, and area of the solar panels on each face. Together, these were used to calculate total power consumption, solar production, and battery charge at any given time for four orbits.

STK Models

Using STK, a model of the CubeSat was used to gather data in relation to the mission's orbit. Mission critical data that was required from STK were the sun intensity and spacecraft-sun unit vector data. Acquiring the sun intensity data was a simple request from STK, as it is a default report. The default spacecraft-sun unit vector data required changing a spacecraft-sun unit vector fixed data report due to the axes not following the spacecraft body-fixed frame. It is still undetermined what body the axes were relative to by default settings. After changing the spacecraft-sun unit vectors to the body fixed vectors of the CubeSat a proper analysis of power generation was analyzed. The solar intensity percentage as a function of time can be seen in Figure 22 and the spacecraft-sun unit vector can be seen in Figure 23. The components are referenced from the body-fixed frame (see Figure 24).
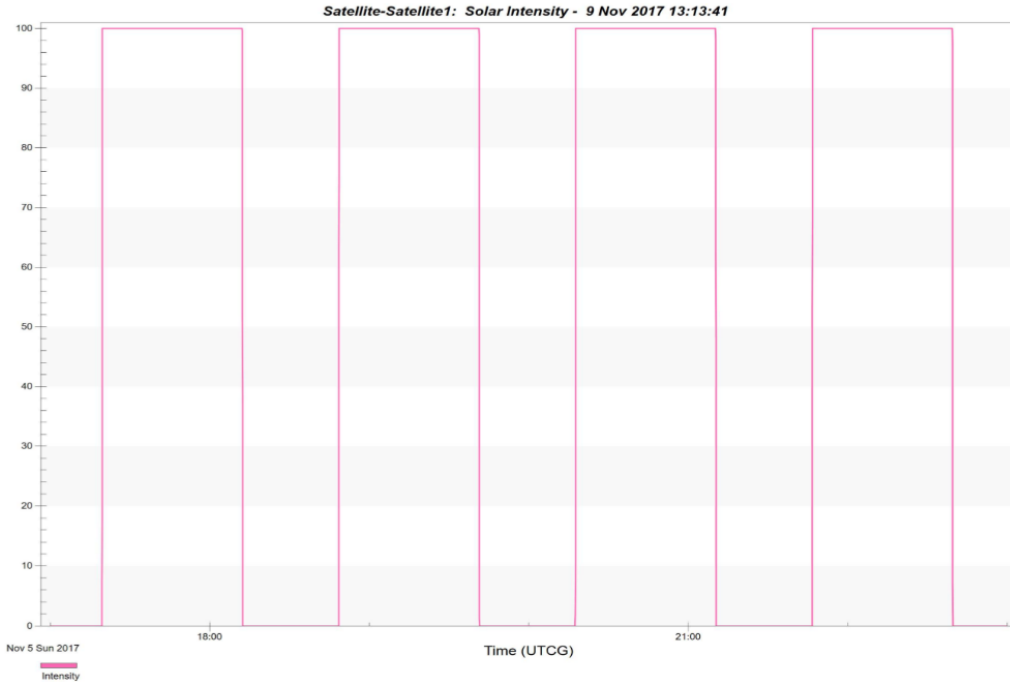
Figure 22: Solar intensity vs. time
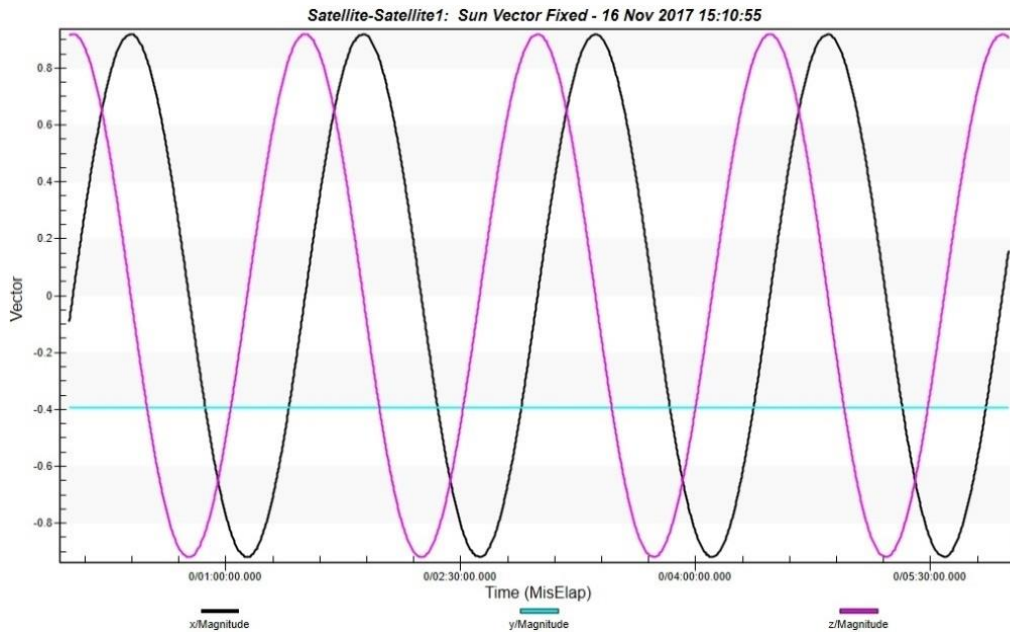
Figure 23: Spacecraft-sun unit vector components
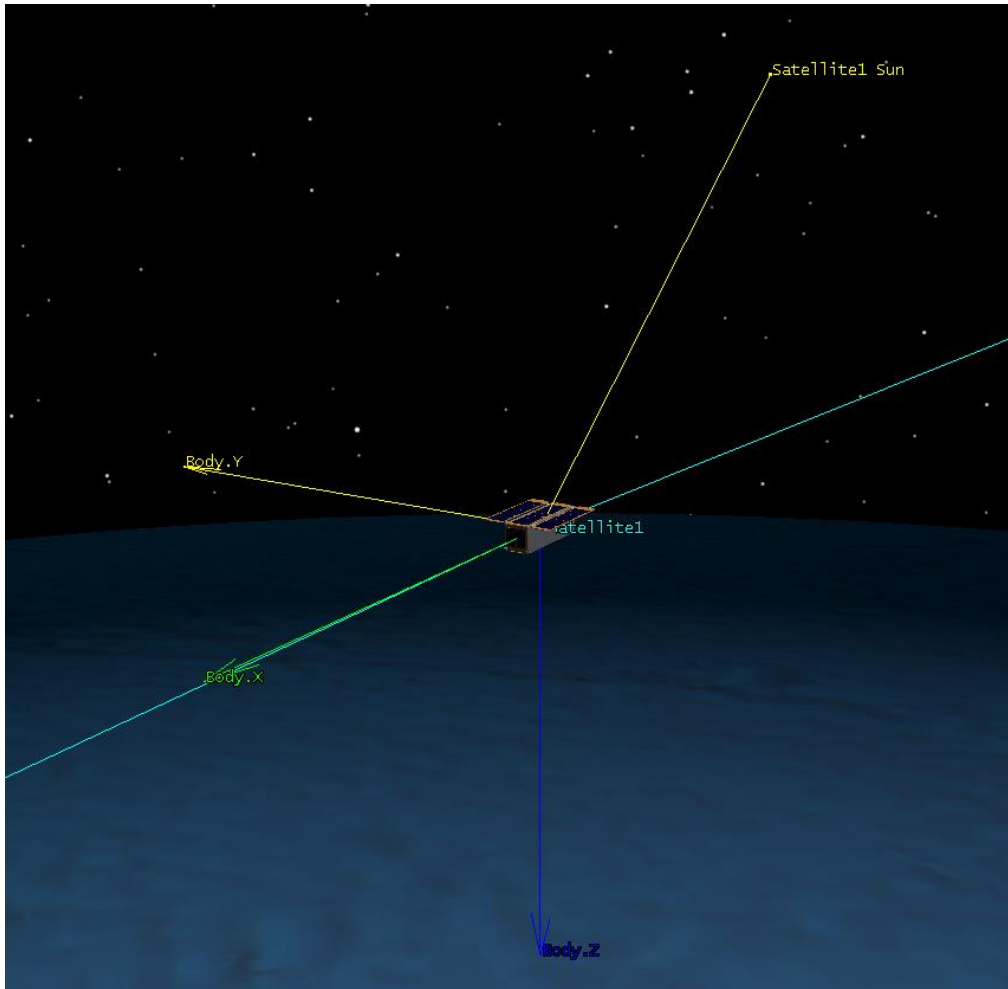
Figure 24: Spacecraft body-fixed frame visual

Solar Array Power Production

Evaluating the possible power production required the use of Equation 1. The calculations used the data from STK shown in Figure 23, an area of 214.9cm² solar panels per face, and an estimated of 25% efficiency for the solar panels. The 25% efficiency was a worst-case factor and assured the CubeSat could manage with a slightly lower efficiency than the Spectrolab UTJ cells efficiency. As the Spectrolab UTJ cells have an efficiency of 28.3% (or 27.7%) concerns on power production would be minimal if the battery was stable, would stay charged, at 25% efficiency. From this, the total solar generation averages out to 6.67 Watts in daylight with peak generation around 9.25 Watts and lowest at 2.90 Watts. This can be seen in Figure 25.
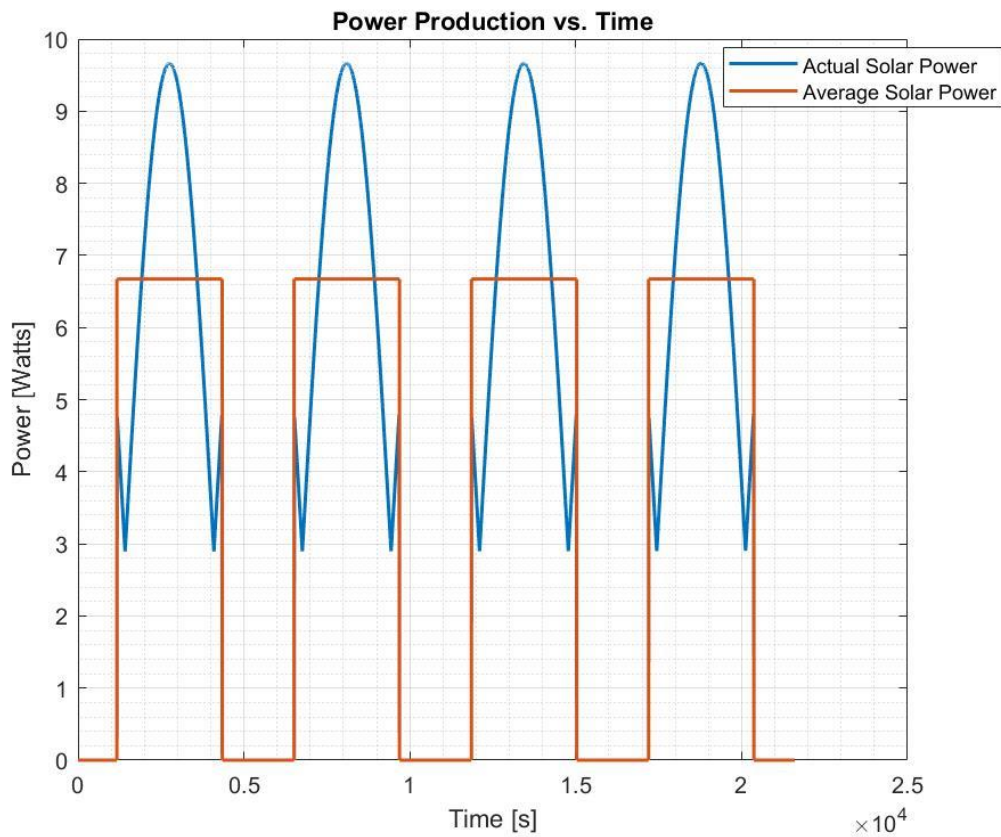
Figure 25: Power production vs. time graph

Battery Charge

Ensuring the CubeSat would have enough power during eclipse is crucial as the mission requires constant thrust and control. As such, it was determined that most of the components would require constant use through each orbit, the only exception being the transceiver as it required 9 Watts to function. The power required for each component is listed in Table 17. Most components listed in the table draw their peak power when in use except the OBC, which was tested at nominal power draws. It was tested at this power draw due to the activity of the computer would be nominal. Figure 26 shows the consumption in comparison to solar generation. Figure 27 shows the effects of consumption and generation on the battery capacity.

Table 17: Individual component power consumption

Component	Consumption (W)
OBC	0.35
Fine Sun Sensor	0.05
Gyroscope	0.04
GPS	0.8
Magnetometer	0.01
EPS	0.2
Transceiver	9
BET1mN	15
PPT	0.5
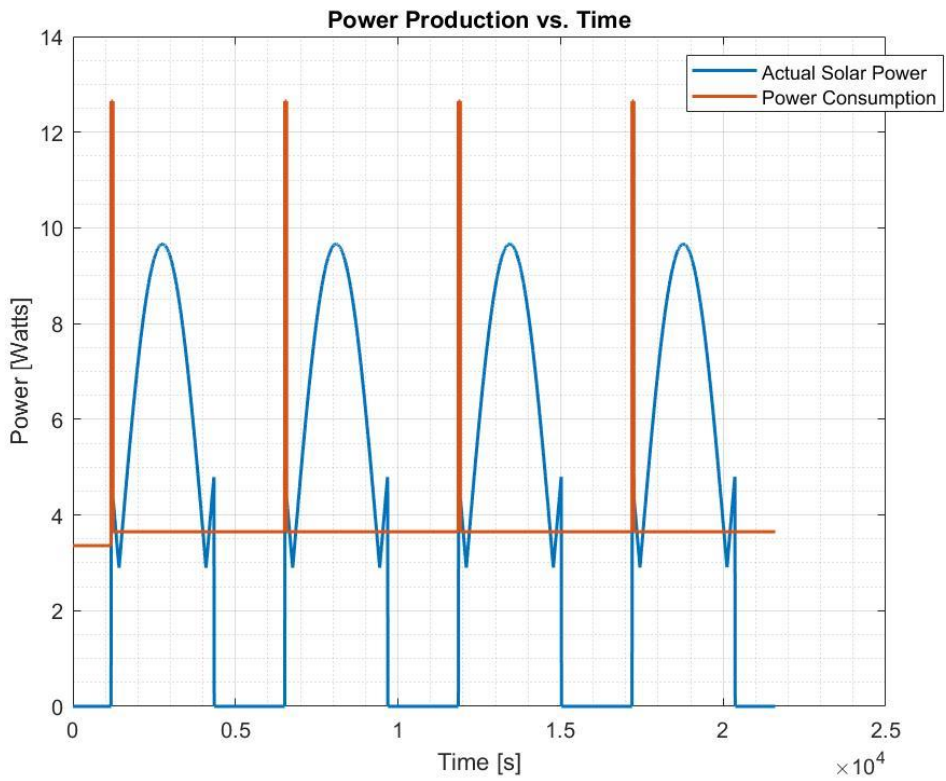
Figure 26: Power production and Power consumption as a function of time for four orbits
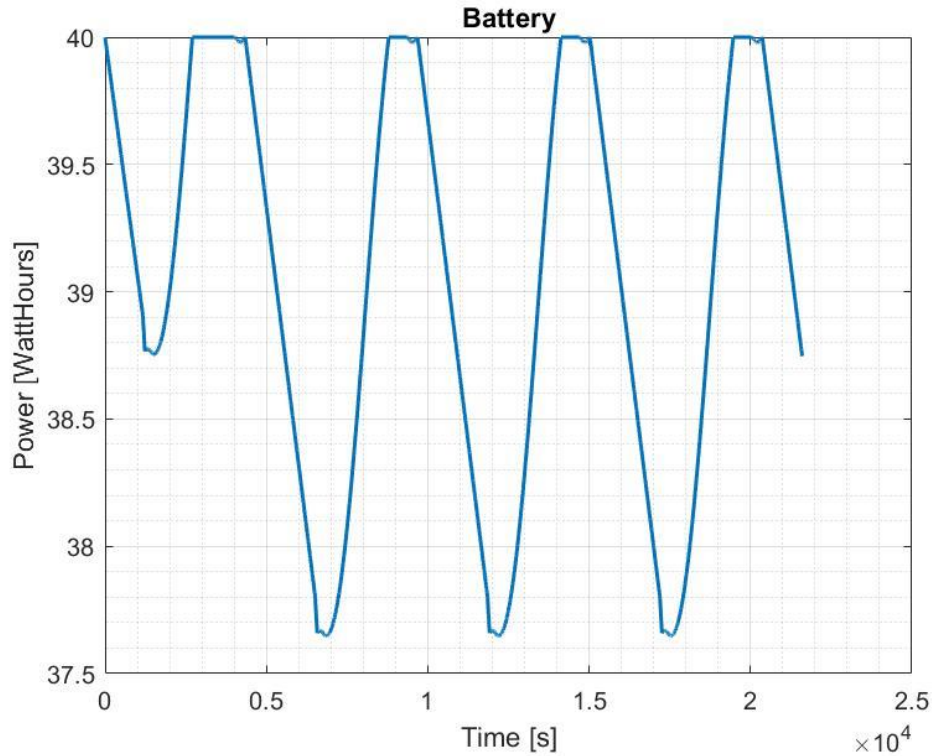
Figure 27: Battery charge as a function of time for four orbits

4.1.2 Rendezvous

4.1.2.1 Final Hardware Configuration

The final hardware selection is a refinement of the hardware selected to initially test the CubeSat design. This selection resulted from analysis based on simulations of the mission requirements.

The Clyde Space 40W-hr battery was selected as the battery for this mission. When initial simulations were conducted, there was doubt that the 40W-hr battery would be able to sustain flight through deployment and detumble. However, after testing both batteries through the simulations, the 40W-hr battery was able to sustain the maneuvers required to stabilize the CubeSat in a routine, steady-state manner. The Clyde Space Battery is shown in Figure 28.

58
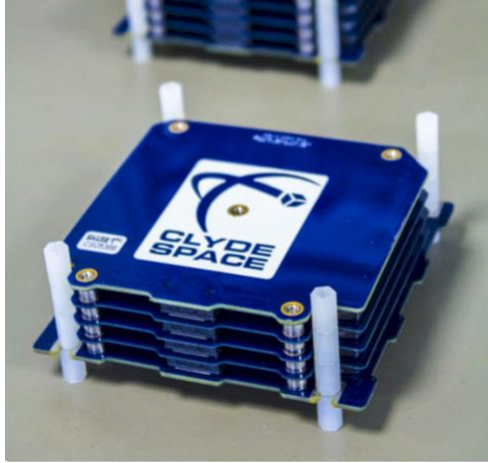
Figure 28: Clyde Space 40 W-hr Battery [31] Copyright © 2017 Clyde Space Ltd.

The Clyde Space 3rd Generation FlexU EPS was selected as the EPS board for the CubeSat. The Clyde Space EPS board is equipped with a Power Distribution Module, Maximum Power Point Tracking, and protection for battery charge and discharge. This EPS board is also compatible with the 40W-hr battery mentioned above. The selected battery and EPS board are both sold by Clyde Space in a High Power Bundle, reducing the cost of the CubeSat. The FlexU EPS can be seen in Figure 29.
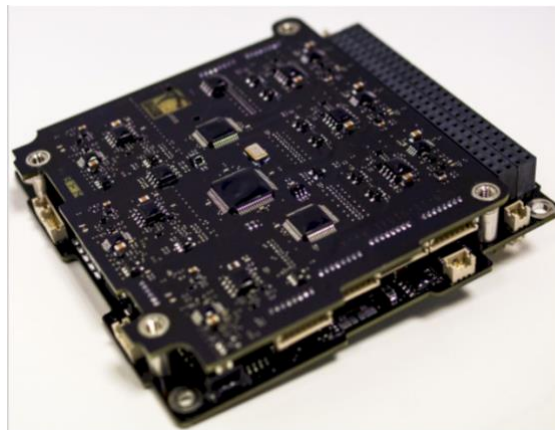
Figure 29: Clyde Space FlexU EPS [30] Copyright © 2017 Clyde Space Ltd.

In order to generate power, ISIS custom solar panels were selected. The custom solar panels were selected in order to allow for the most surface area to be covered on each face. The

ISIS custom solar panels are most compatible with the constraints of the Rendezvous mission, resulting from the placement of the ADN thrusters. These solar panels use GaAs triple-junction solar cells from AZUR space. These cells operate at 30% efficiency [31]. The ISIS custom solar panels integrate with the EPS system as well as with the ISIS Antenna System used for uplink and downlink, discussed in Section 4.3.2.1. The ISIS custom solar panels can be seen in Figure 30.
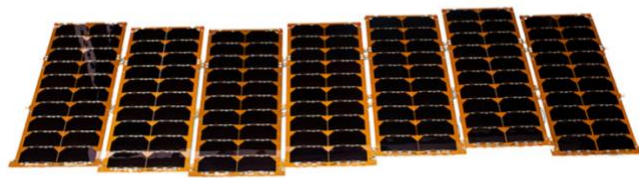
Figure 30: ISIS Custom Solar Panels [32] Copyright © 2017 Innovative Solutions in Space

Once all of the hardware was finalized, a power budget was created outlining these components for the Rendezvous mission. This budget reflects the power profile for each individual component on the CubeSat. The power budget generated for the Rendezvous mission is outlined in Table 18, followed by the cost breakdown for power components (prices current as of spring 2018).

Table 18: Subsystem power requirements (Rendezvous Mission)

Group	Component	Manufacturer	Part No.	Peak Power (W)	Nominal Power (W)	Quiescent Power (W)	Current (mA)	Voltage (V)
C&DH	OBC	Clyde Space	01-02928	1	0.35	0.165	150	Batt
ADC	Coarse Sun Sensor	Space Micro	CSS-01	0	0	0	3.5	-
	Fine Sun Sensor	New Space Systems	NSS-CSS	0.05	0.05	0	10	5
	Gyroscope (x3)	Analog Devices	ADXRS453	0.04	0.03	0.03	8	5
	GPS	Skyfox Labs	piNAV-NG	-	0.125	-	38	3.3
	Magnetometer	Adafruit	LSM03DLCH	3.96E-04	-	3.60E-06	0.11	2.16-3.6
Power	EPS	Clyde Space	CS 01-02698	0.2	0.2	0.2	24	Batt
	Battery (x1)	Clyde Space 40W-hr	CS 01-02698	-	-	-	5200 mAhr	8.4
	Custom Solar Panels	ISIS	-	-	-	-	-	-
Telecomm	Transceiver	ISIS	TRXUV VHF/UHF	4.8	3.3	0.4	600	Batt
	Antenna	ISIS	-		2	0.06		Batt
Propulsion	Thruster	VACCO	ADN		13.6			
	Attitude Control (x2 per orbit)	VACCO	ADN	5.25	0.2			

Table 19: Power hardware cost breakdown

Component	Part Number	Cost (each)	Number	Cost (total)	Ref.
CS High Power Bundle B	CS 01-02698	$12,500	1	$12,500	[4]
ISIS Custom Solar Panels	-	Based on request	1	~$30,000	[32]
Total				$42,500	

4.1.2.2 Power Profile Results

The results presented in this section were generated using the MATLAB simulation developed to simulate power profiles over two representative Rendezvous mission orbits. The inputs for this code include the spacecraft-sun unit vectors and intensity from STK, power usage for each component, the power states of each component (i.e. whether the component is on or off), battery operating parameters, solar array operating parameter, and the time for detumble and routine. These inputs are used to generate live and still simulations of the component state vectors, solar panel power production, battery charge/discharge status, and power consumption of components.

Power States

The power state simulations define the on/off states of each component on the CubeSat and the power that they consume. The OBC, EPS, Gyro, Magnetometer, GPS, and Fine Sun Sensor states throughout detumble and routine were identified by the sensors team and included in the code. In order to counter the disturbance torques during flight, it is assumed that there will be the equivalent of at least one thruster on, throughout the life of the mission. The Rendezvous mission includes an assumption that two slew maneuvers are required per orbit, these are carried out by the PPTs and reflected in the state vector. Finally, the radio (i.e. transceiver) state defines the uplink and downlink times carried out per orbit at the times identified in the STK scenario. These states are reflected in Figure 31.
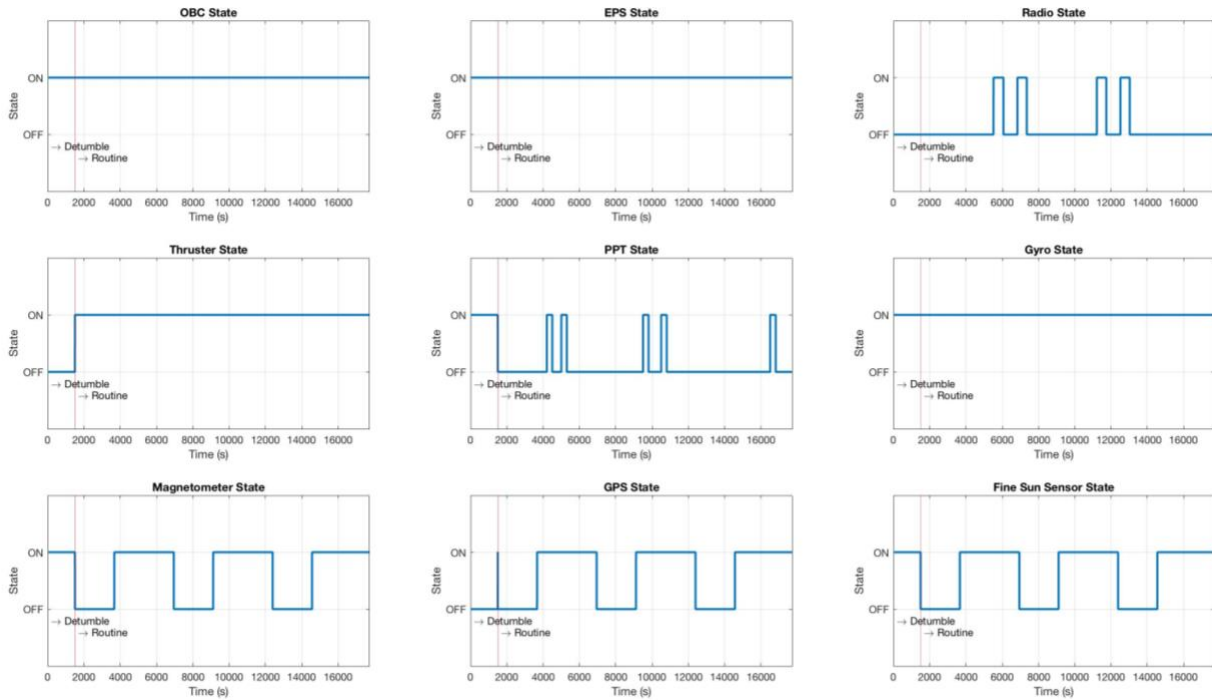
Figure 31: Component state vectors as a function of time for the Rendezvous mission, three orbits

After the state vectors for each component were defined, the instantaneous power consumption of each component was identified and included in the graph. This can be seen in Figure 32.
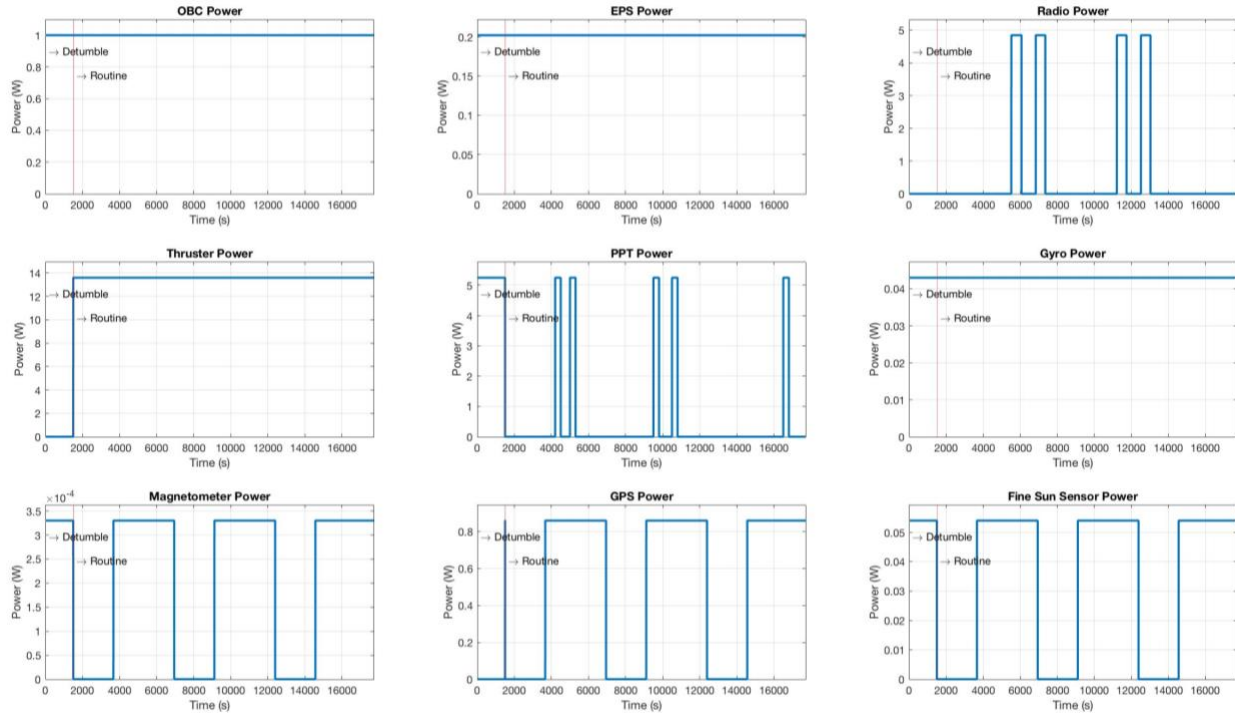
Figure 32: Component power consumption as a function of time for the Rendezvous mission, three orbits

Solar Power Production

The solar array power production model uses Equation 1 to determine the potential power generation throughout the Rendezvous mission. The ISIS custom solar panels have a cell efficiency of 30% [31]. The solar array power production was calculated and plotted for a 12U, 16U and 20U CubeSat, all using the ISIS custom solar panels. The coverage area was determined by the structures team for all three options and are listed in Table 20. In Table 20, the "coverage" represents the fraction of the area covered by active solar cells.

Side	Area (12U) [cm^2]	Area (16U) [cm^2]	Area (20U) [cm^2]	Solar Panel Coverage 12U	Solar Panel Coverage 16U	Solar Panel Coverage 20U	Total Solar Panel Area 12U [cm^2]	Total Solar Panel Area 16U [cm^2]	Total Solar Panel Area 20U [cm^2]
1	400	400	400	0.75	0.75	0.75	300	300	300
2	600	800	1000	0.5	0.625	0.7	300	500	700
3	600	800	1000	0.5	0.625	0.7	300	500	700
4	600	800	1000	0.5	0.625	0.7	300	500	700
5	600	800	1000	0.5	0.625	0.7	300	500	700
6	400	400	400	0.75	0.75	0.75	300	300	300

Using the cell efficiency, the coverage area, the spacecraft-sun vector with respect to the body-fixed CubeSat coordinate system, and the sun intensity data, a complete power generation plot was generated. The power production can be seen in Figures 33-35 for each of the three CubeSats configurations (12U, 16U, and 20U) evaluated.
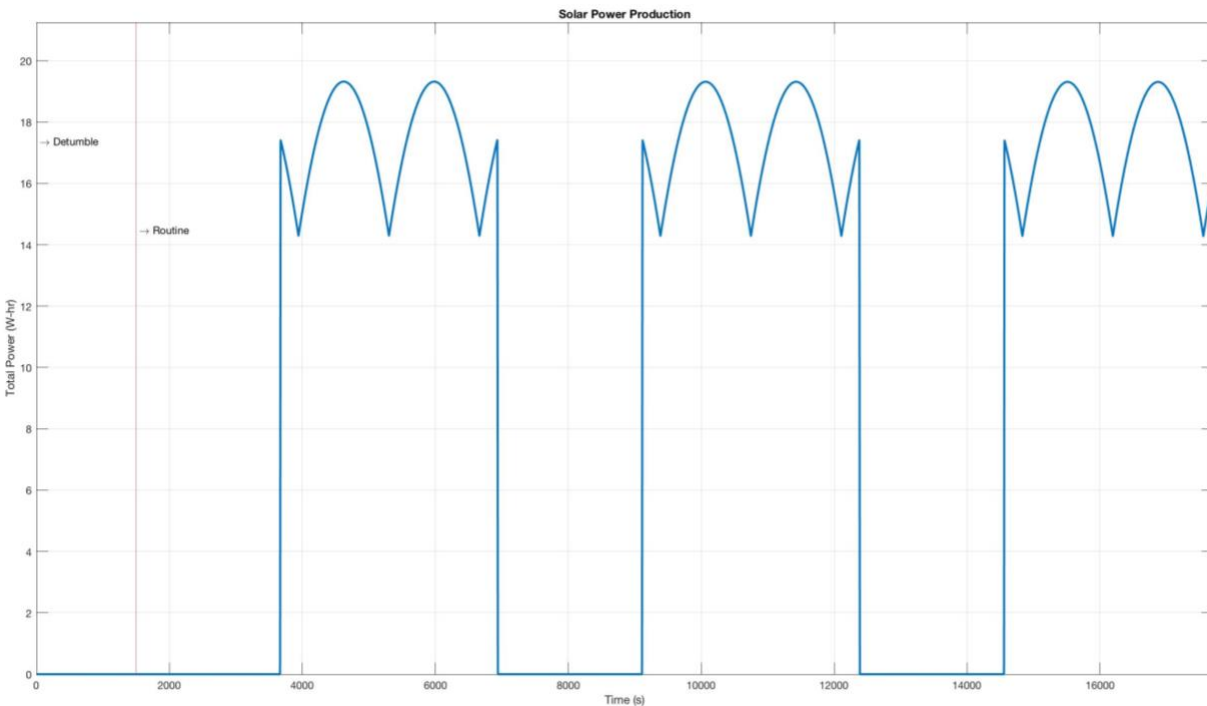
Figure 33: Solar Power production for three orbits (12U)
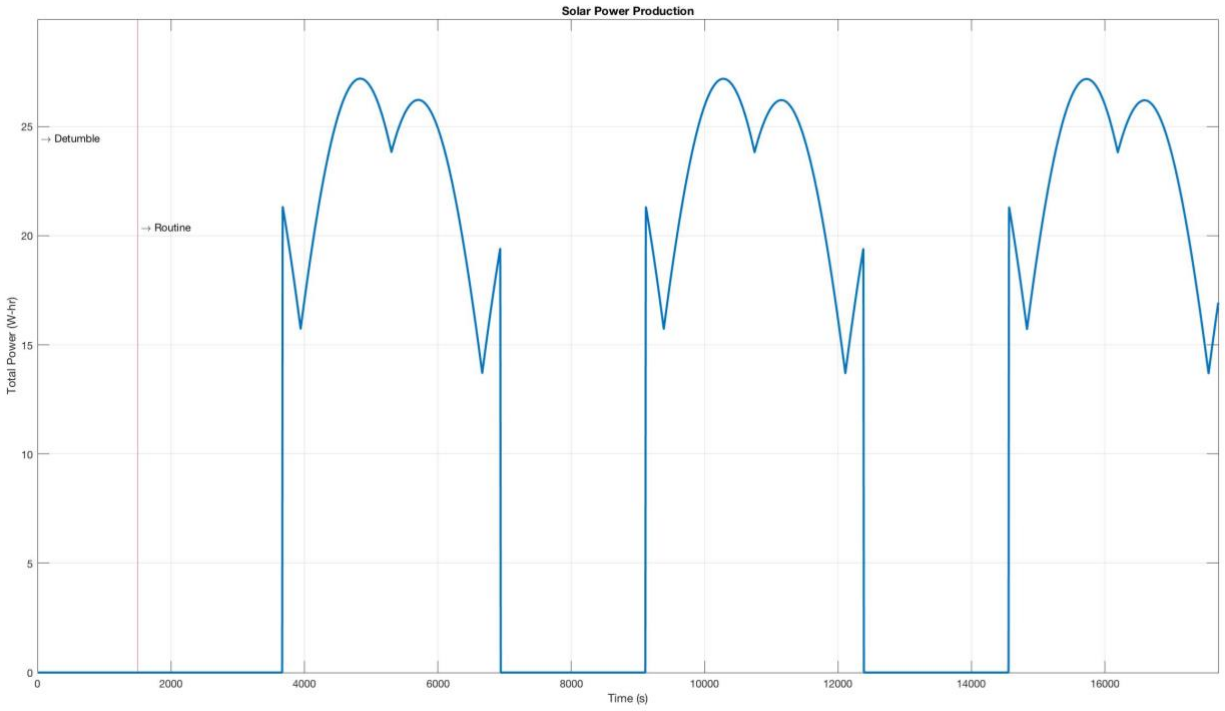
Figure 34: Solar Power production for three orbits (16U)
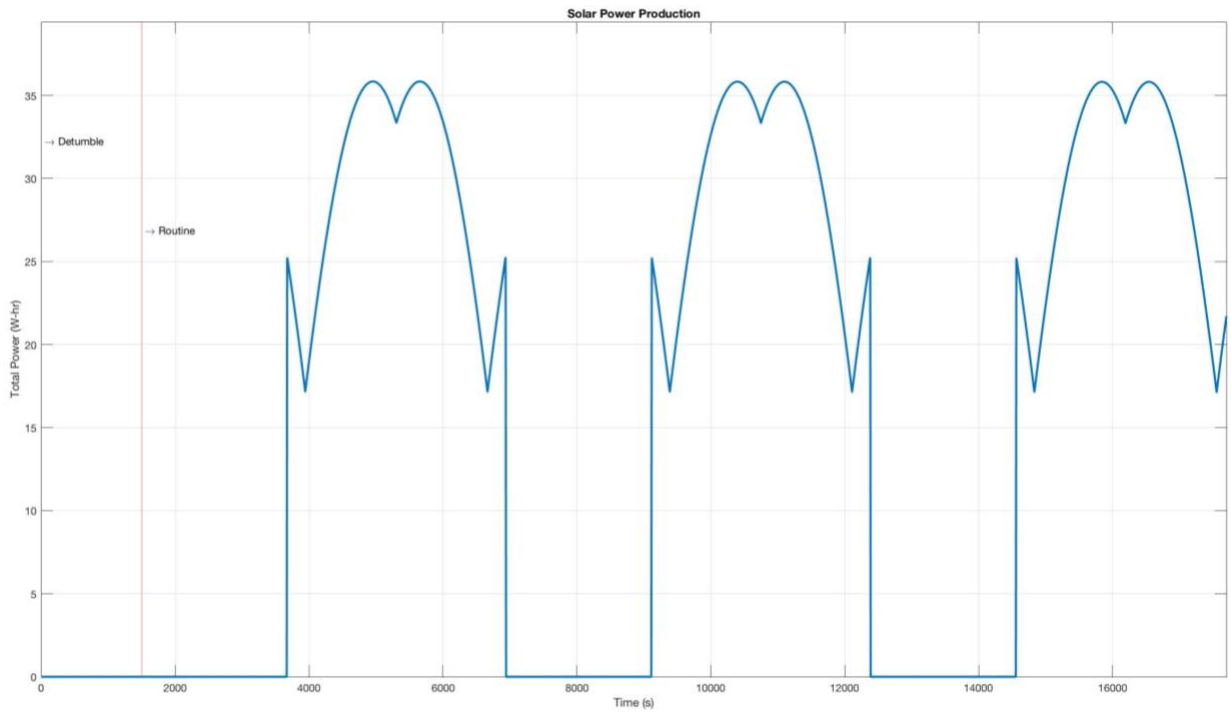
Figure 35: Solar Power production for three orbits (20U)

Power Profile

Combining the power states and the solar array models, a complete power profile was generated. The power profiles presented in this section depict the generation and consumption of power throughout a mission scenario consisting of detumble followed by three routine orbits as a function of time. The plotted power consumption represents the sum of the individual power states shown in Figures 31 – 32. The power profiles are presented in Figures 36 – 38 for the 12U, 16U and 20U respectively.
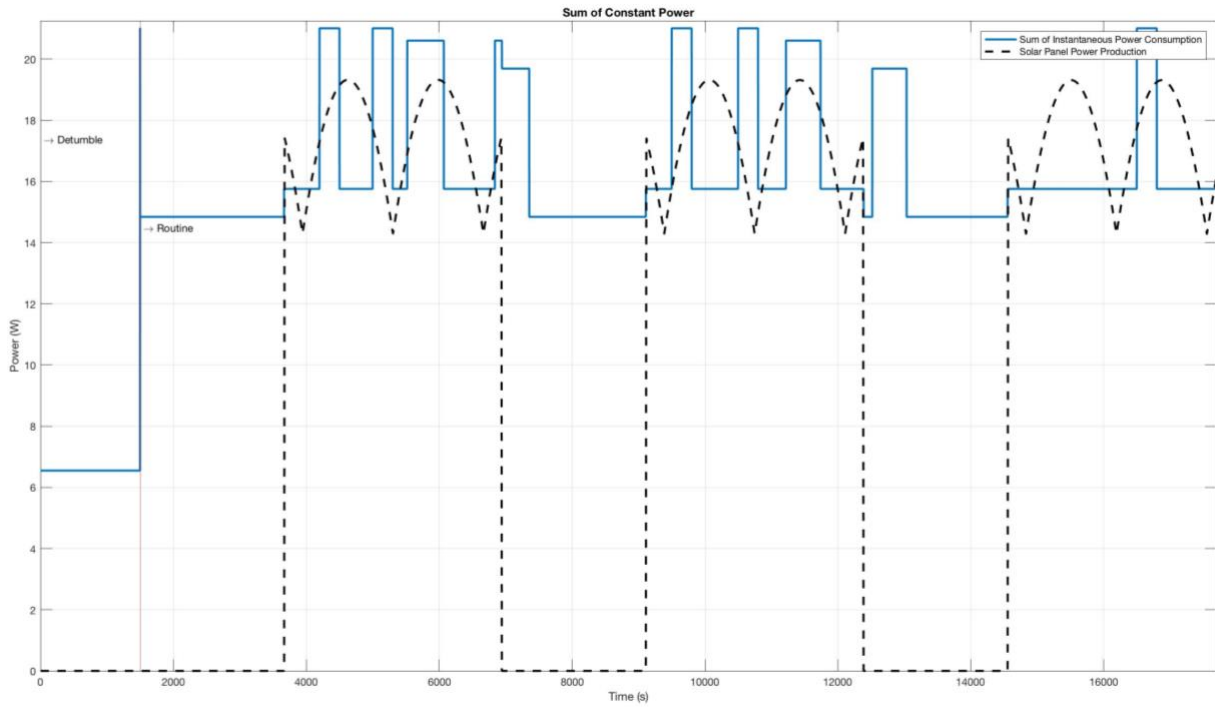
Figure 36: Power Profile for three orbits (12U)
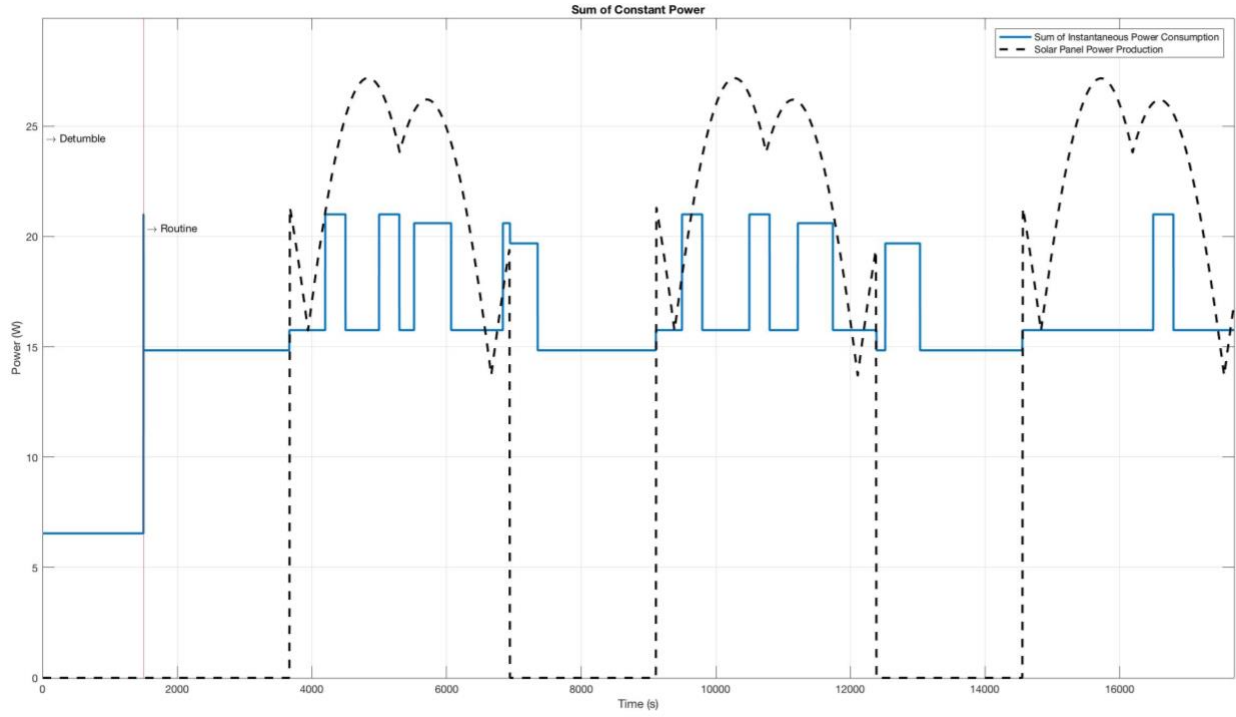
Figure 37: Power Profile for three orbits (16U)
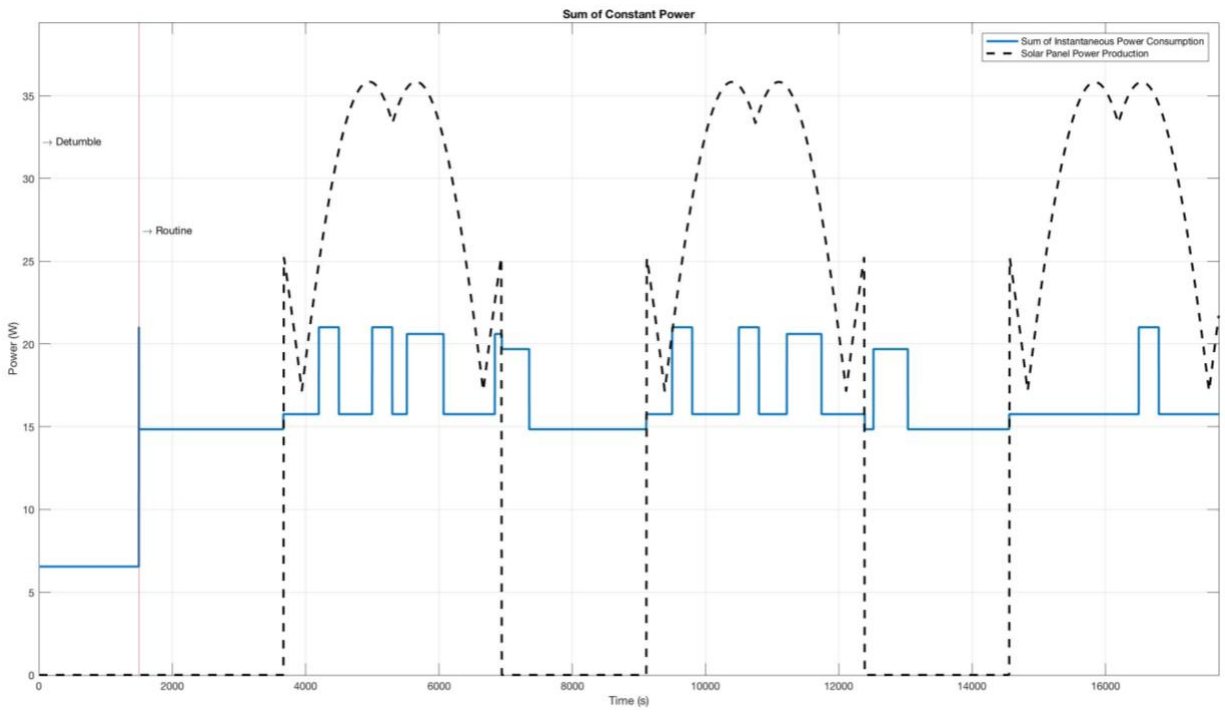
Figure 38: Power Profile for three orbits (20U)

In order for the battery to recharge, the area under the blue line in Figures 36 – 38 must be less than the area underneath the dotted black line. It can be clearly seen that the 12U CubeSat is not capable of generating enough power to recover from the discharge that occurs from the on-board components operating as assumed for this typical mission profile.

Battery Charge

The last important result generated came from simulating the charge and discharge of the battery throughout the Rendezvous mission. Using the data calculated from the power consumption and generation profiles, the MATLAB code evaluated the battery discharge during shadow required to operate all of the components on board the CubeSat. When the CubeSat was back in sunlight, the power consumption was subtracted from the power generation, with the assumption that the solar power would operate the components in sunlight, and that difference was then available to recharge battery energy that had been discharged in shadow. The battery charge and discharge graph can be seen for the 12U, 16U and 20U in Figures 39 – 41 below.
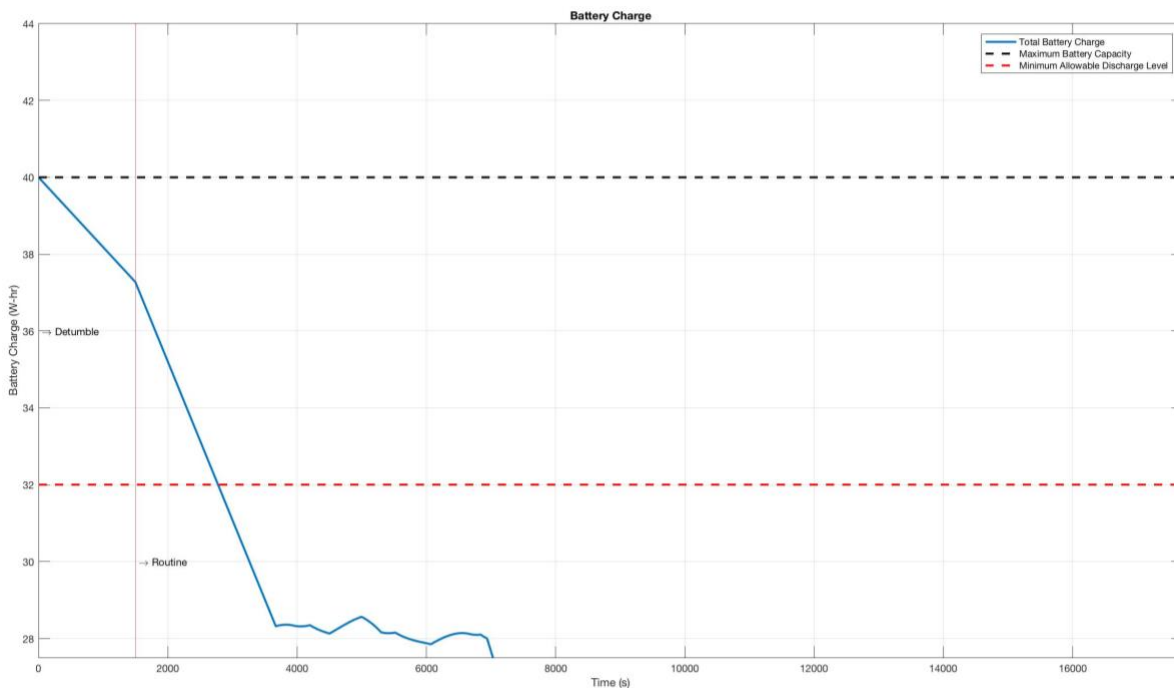
Figure 39: Battery Charge for three orbits (12U)
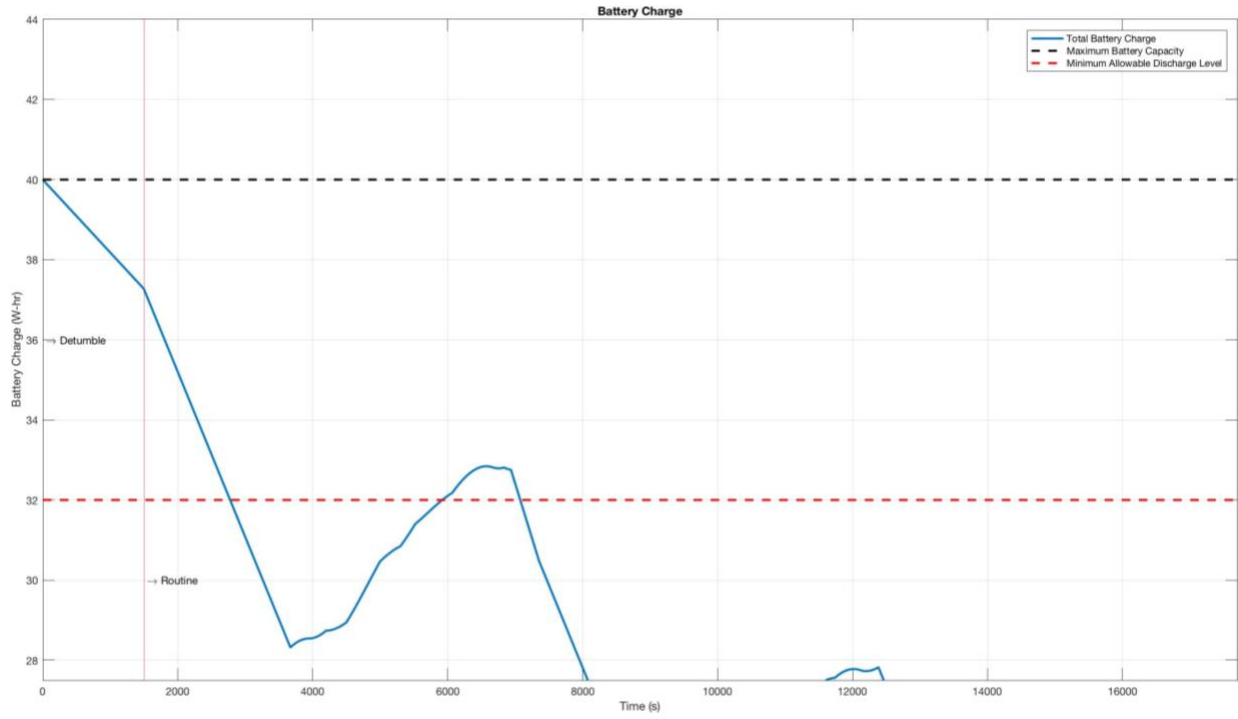
Figure 40: Battery Charge for three orbits (16U)
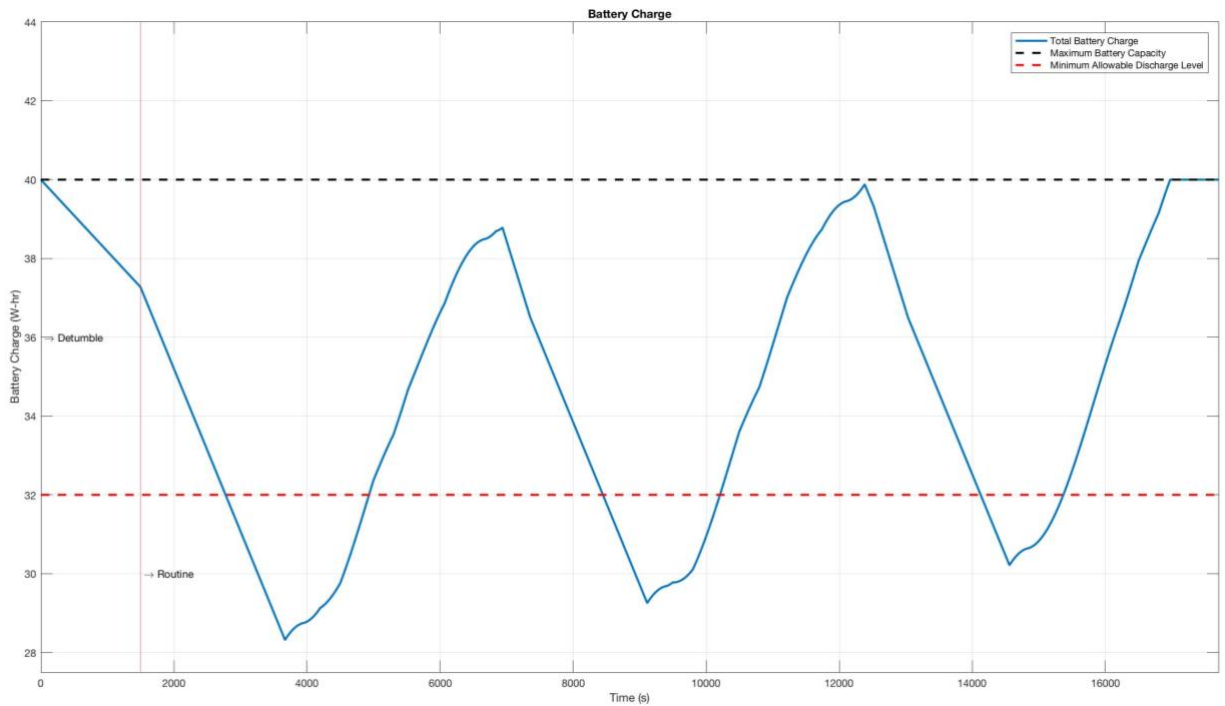
Figure 41: Battery Charge for three orbits (20U)

In these figures, a comparison can be made with respect to the power production capabilities for each of the CubeSat configurations. It can be seen that a 20U CubeSat is needed to support the Rendezvous mission requirements. The battery charge graph for the 12U CubeSat, confirms the results found in the power profile graphs, that the 12U CubeSat cannot generate enough solar power to recharge the battery. The battery charge graph for the 16U CubeSat shows that the CubeSat would be able to sustain flight in the sun, however, an excessive amount of power is required in the shadow. The 16U CubeSat cannot recover from the energy depletion when back in the sun and is therefore unable to support the Rendezvous mission. In order for the 16U CubeSat to sustain the Rendezvous mission flight, the thrusters cannot exceed a maximum of 10.3 W of power draw. It can be seen that in the 20U CubeSat, there is enough power generated to recover for the loss of battery power during detumble. In Figure 41, it is evident that the 20U CubeSat can generate sufficient power in the sun to make up for the energy expended during shadow.

Figure 41 also shows that on the third orbit, the CubeSat reaches a steady-state condition with respect to charging and discharging the battery. Over the first two orbits, the spacecraft is still recovering from the battery used during the detumble maneuver. The 20% recommended depth of discharge on the battery is highlighted by the red line in the Figures 39 – 41. Although the battery dips below this line during discharge, it only dips to ~25% depth of discharge, which will not harm the battery for the duration of the Rendezvous mission.

4.2 Propulsion Subsystem

4.2.1 Propulsion System Sizing

4.2.1.1 Mission Torque Requirements

In order to ensure that the propulsion system is able to meet the mission requirements, appropriate control authority, i.e. torque and/or thrust capability, needed to be determined. Figure

42, presents torque as function of time. This is an example of a plot used to determine required control authority. As is evident from Figure 42, if the mission does not require quick maneuvers, the maximum torque can be reduced by using slower maneuvers with longer idle times. Since it was assumed that the spacecraft would be performing two slews per orbit, the torque required for a slew maneuver determined the "average torque" that the CubeSat would need to perform the mission. The maximum torque would be determined by the detumble maneuver, and the minimum torque would be determined by the disturbance torques. Because the disturbance torques were substantially less than the required maneuver torques, they were not used for sizing the thrusters and are not discussed further in this section.
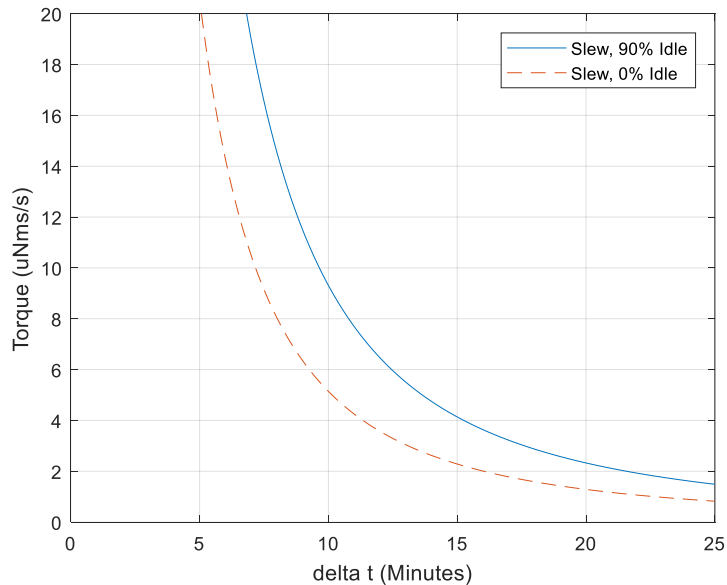
Figure 42: Torque vs. duration for slew maneuvers data used for sizing
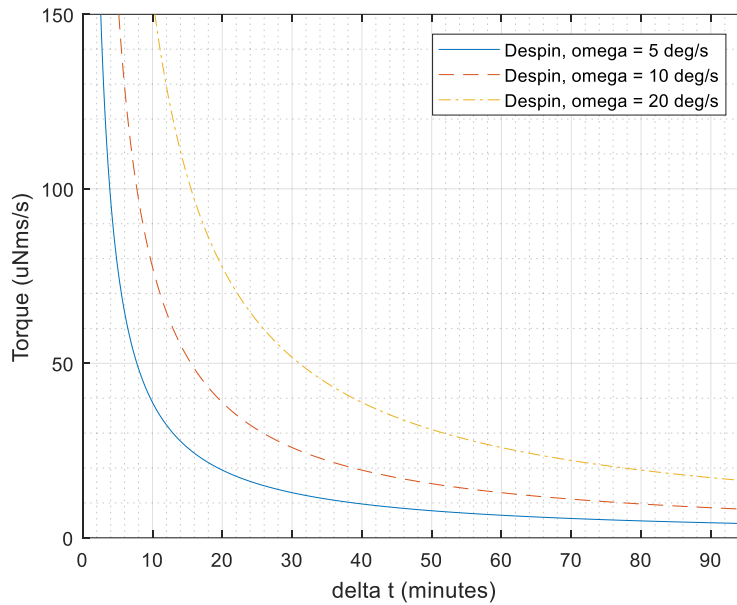
Figure 43: Torque vs. duration for detumble maneuver data used for sizing

The detumble maneuver requires a significantly higher torque to be completed in the same time as a slew maneuver. Ideally, the CubeSat would finish the detumble while it still has time to generate power from the solar arrays (i.e. before it is eclipsed by the Earth in at most half an orbit.) Since the orbital period of the CubeSat is approximately 90 minutes, a detumble time of 40 minutes or less would be preferred. Using this set of parameters, the max torque required would be about 40 or even 50 μNm.

4.2.1.2 PPT Sizing

Table 21: Trade thruster parameters

Model	Thrust (mN)	Isp (s)	Ibit (mN-s)	Power (W)	Mass (g)	Volume (cm^3)
DAWGSTAR PPT	0.01	500	0.07	12.5	475	24
PPTCUP	0.04	600	0.04	2	280	300
Hybrid AND/RCS Thruster	10	40	0.1	<1	1734	853

Knowing the maximum torque required for the mission from Figure 44 (torque displayed in the legend as an angular momentum rate in μNms/s), it can be determined how much power would be required by a PPT with a specific impulse bit to perform that maneuver. Table 21 lists the parameters of the PPTs (and the hybrid ADN/RCS thruster) that are to be used as reference when thruster systems are mentioned. The assumed discharge energy was 5 J/impulse; this could be varied by charging the capacitor to different voltages during the mission. Figure 45 was used to determine the frequency required to achieve a certain torque given the PPT's impulse bit. For this mission, we were limiting the pulse frequency to two Hz. Using this information, a set of PPT operating parameters can be found that meets the requirements for the mission.
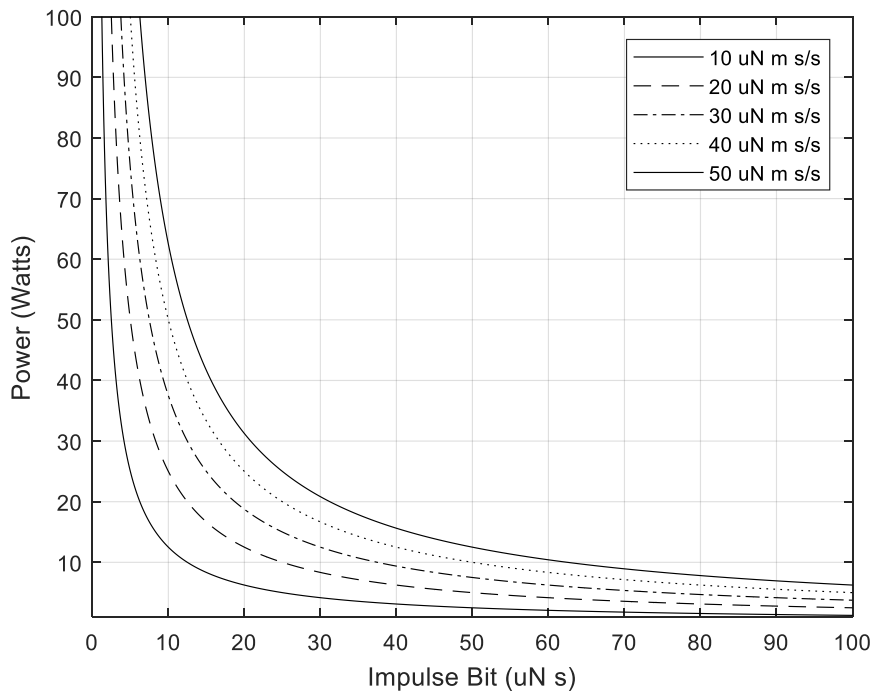
Figure 44: Power vs. impulse bit data used for system sizing
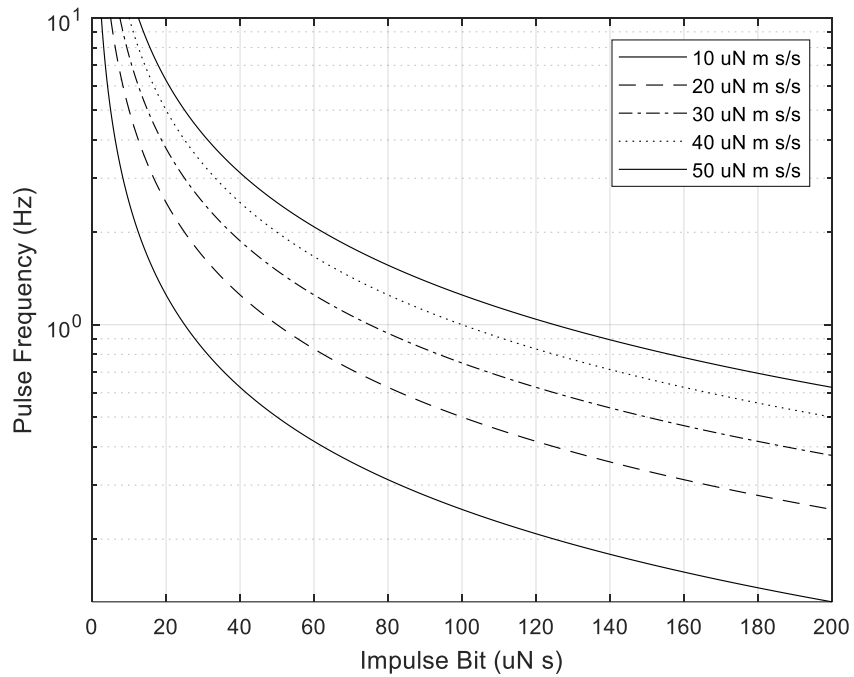
Figure 45: Pulse frequency vs. impulse bit data used for system sizing

4.2.2 eLEO

4.2.2.1 Detumble Maneuver

For all attitude control maneuvers, the eLEO mission adopted the Teflon-fueled µPPT from the design of Lu et al. (2015). These specific thrusters were designed with the accessibility of commercial-off-the shelf hardware. Table 22 shows the specifications for each thruster and Figure 46 demonstrates how they are arranged in the back portion of the CubeSat.
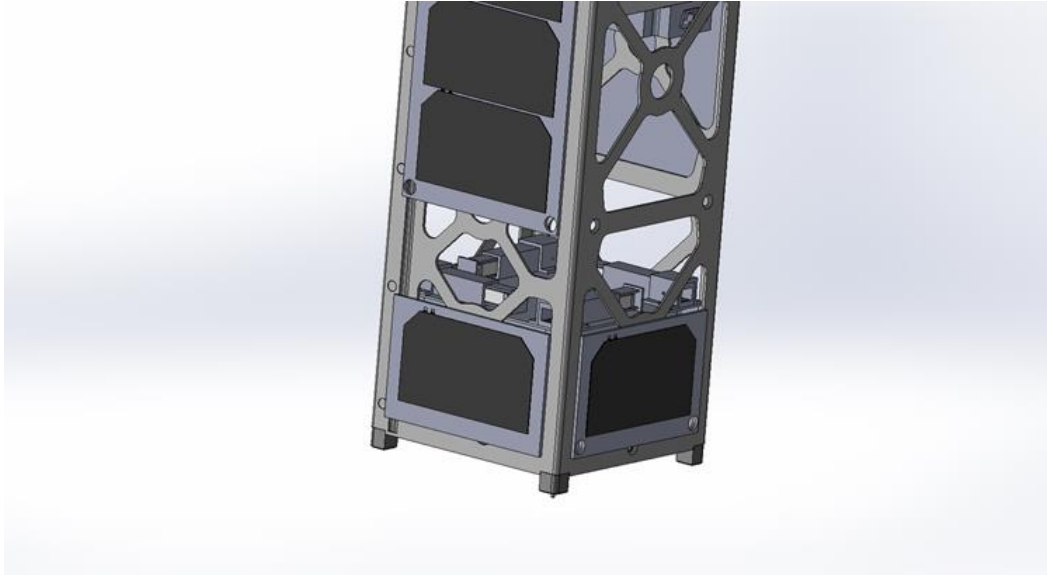
Figure 46: Location of μPPTs on CubeSat

Table 22: Teflon-fueled μPPT Specifications [32]

Name	Type	Thrust Level (mN)	Ibit [μNs]	Peak Power (W)	Dry Mass (kg)	Dimensions (cm)
μPPT	PPT	0.14	10-80	10	6.93	3.25x1.25x1.25

In order to regain stability and stop spinning once the CubeSat is released into eLEO orbit, it will take approximately 40 minutes to reach nominal stabilization with a 5 degree per second initial angular rate. Figure 47 shows the angular momentum rate (torque) necessary as a function of maneuver time for and initial angular rate of 5, 10 and 20 degrees per second. Figure 48 shows the detumble maneuver time and required torque as a function of available power. It highlights that it would be more beneficial to use higher power, closer to 1 watt, so that the maneuver can be completed in less time. On the other hand, if it was a priority to conserve power, it would be possible to take up to 190 minutes to complete the maneuver. This would be beneficial when the CubeSat emerges from eclipse and energy storage is low. The low power would also mean a lower angular momentum rate would be applied.
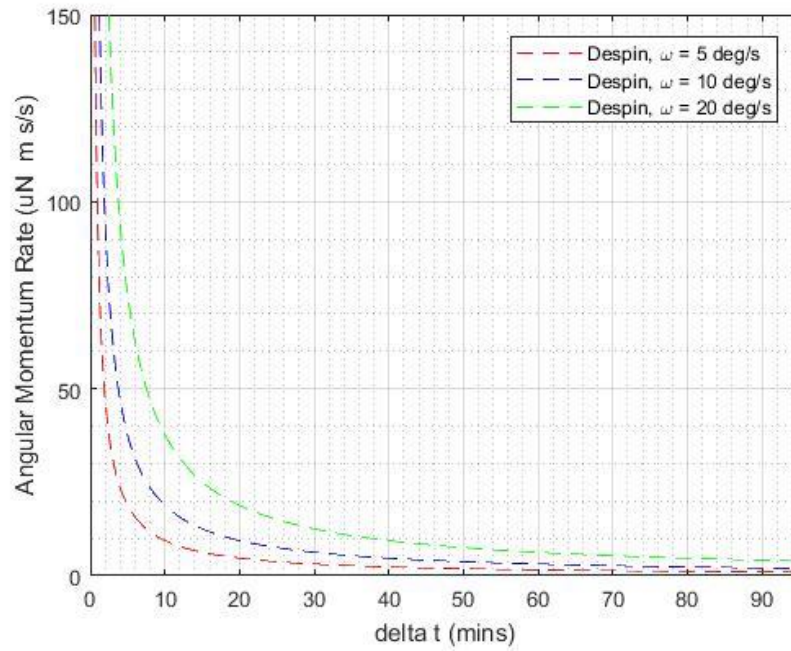
Figure 47: Angular momentum rate vs. duration for detumble maneuvers
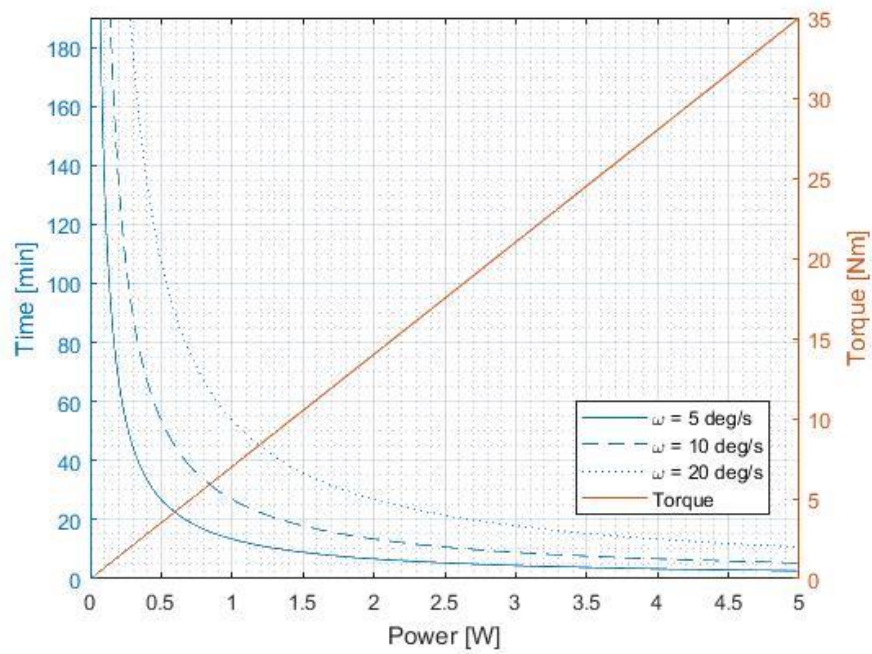
Figure 48: µPPT detumble maneuver time and required torque as a function of available power

4.2.2.2 Slew Maneuvers

In the unlikely event that the CubeSat will need to complete a 180-degree slew maneuver, Figure 49 demonstrates that it can be accomplished in 25 minutes if only minimal power is used, i.e. 5W corresponding to a torque of 20μNm, is available. Figure 49 also shows that there is no major difference when comparing the 90% idle vs. 0% idle, except for a slightly longer maneuver time for the former. The 90% idle assumes the PPTs are firing for 5% of the time at the beginning of the maneuver and then turning off for 90% of the time, after which the PPTs will fire again for 5% of the maneuver time to counteract the torque and bring it to rest. The 0% idle option requires the PPTs to fire all the time, with one couple for the first half and the opposing couples for the second half. The maneuver can also be completed as fast as 2.5 minutes but will require an angular momentum rate of approximately 20 micro-Newton m/s/s, which will require 5 watts demonstrated by Figures 49 and 50.
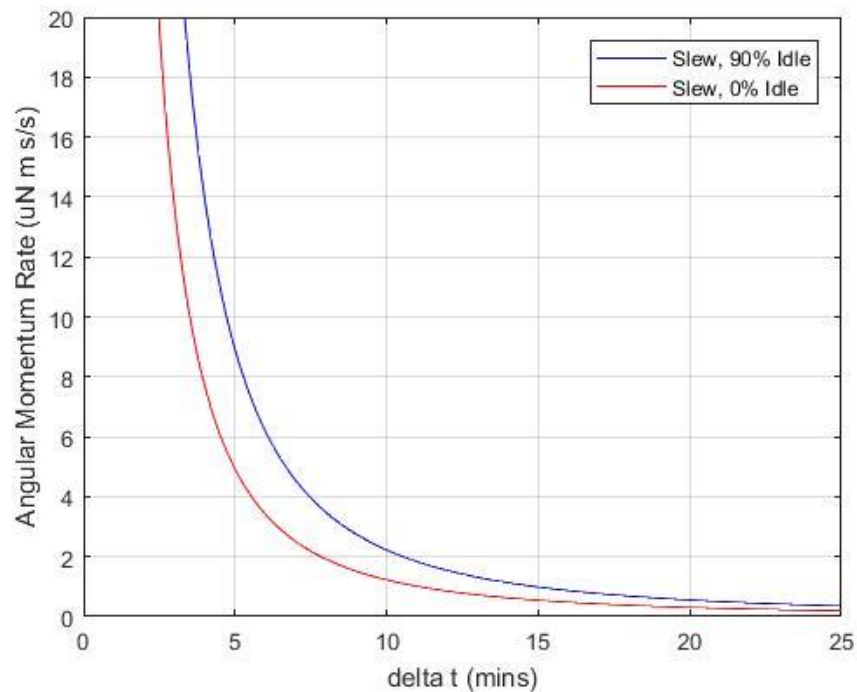
Figure 49: Angular momentum rate vs. duration for slew maneuvers
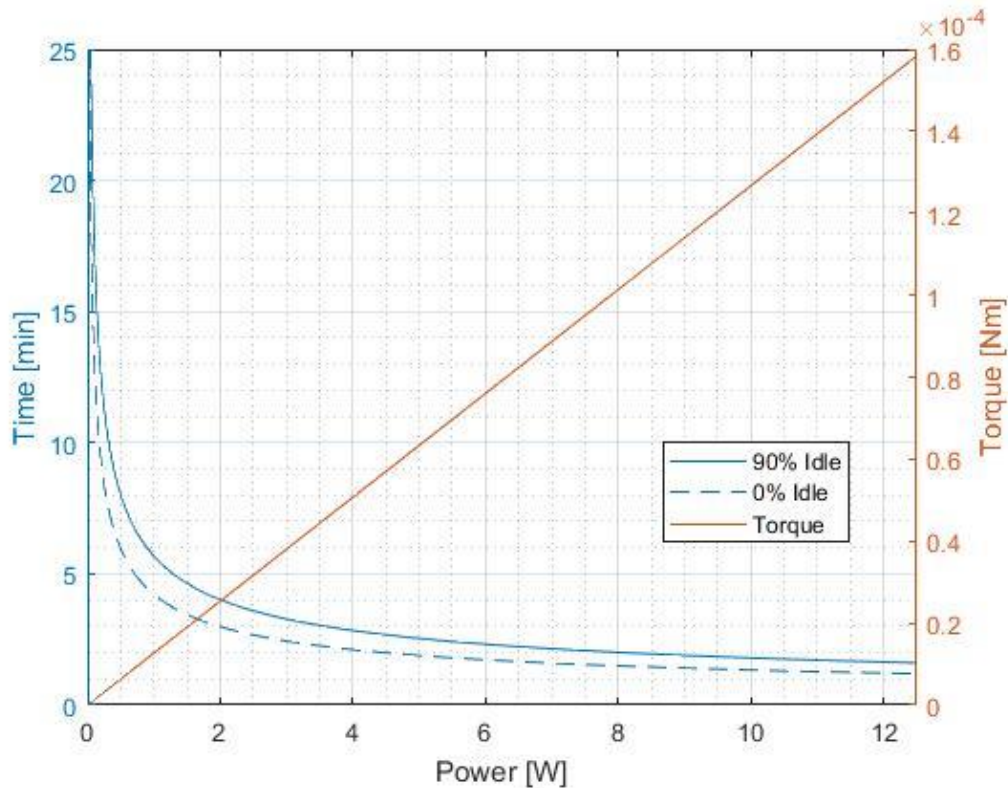
Figure 50: Power for a slew maneuver for a given time or torque

4.2.2.3 Disturbance Torque Compensation

Since the CubeSat will be traveling at 210km in the eLEO orbit, solar radiation, magnetic, and gravitational disturbance torques can be ignored. The greatest disturbance torque will originate from atmospheric drag, hence making it the total disturbance torque. For an overview of all disturbance torques taken into consideration on both missions see section 3.2.1.1 for the corresponding equations and descriptions.

The CubeSat was assumed to have a maximum inclination of 3 degrees about the pitch or yaw axes (see Figure 16), for the purpose of estimating the drag torque. When the velocity facing phase of the CubeSat was perpendicular to the velocity vector, there was only a $9.85 \cdot 10^{-8}$ Nm torque acting on the CubeSat, resulting from an assumed difference in the location of the center of mass (c.m.) and center of pressure (c.p.) of 0.47 mm. At a pitch inclination of 3 degrees, the total

disturbance increased to $2.59 \cdot 10^{-6}$ Nm. Due to the new shift in location of the c.m. relative to the c.p. (now 0.031 mm) created by the drag, rotations in the negative yaw and pitch directions resulted in torques of $6.0 \cdot 10^{-8}$ Nm and $2.59 \cdot 10^{-6}$ Nm respectively. To counteract these torques, it would be necessary to fire PPTs #1 and #7 to cause a positive yaw movement requiring $8.22 \cdot 10^{-7}$ N per PPT. PPTs #4 and #6 would result in a positive pitch movement requiring $4.29 \cdot 10^{-5}$ N per PPT.

4.2.2.4 Propulsion Options Results

For a trade study, a reaction wheel actuator (RWA) was studied to compare to the μPPT. Blue Canyon's RWP015 was used, as it was the smallest RWA offered that met the power and torque requirements for the mission. Figure 51 and Table 23 provides information about the RWA used for the eLEO mission. The aerodynamic drag torque encountered throughout the mission is well below the threshold of the max torque of the RWA. Table 23 also shows the number of desaturations the RWA would have to complete in its lifespan throughout the mission.

Figure 51: RWP015 © 2017 Copyright Blue Canyon Technologies

Table 23: RWP015 Specifications

RWP015 (MicroWheel)	
Momentum	0.015 Nms
Max Torque	0.004 Nm
Mass	0.130 kg
Volume	43x43x18 mm
Drag Torque	$2.597 \cdot 10^6$ Nm
# of Desats	463.69
Desat Period (Days)	0.0669

Using Figures 52 and 53, one can gain a better understanding of the reaction wheel performance. The torque and power axis are scaled proportional to the RWA's given values and the max time for completion of a maneuver is 30 seconds. Both of these figures can be used to determine how much torque and power it would take to perform a maneuver in a given period of time.
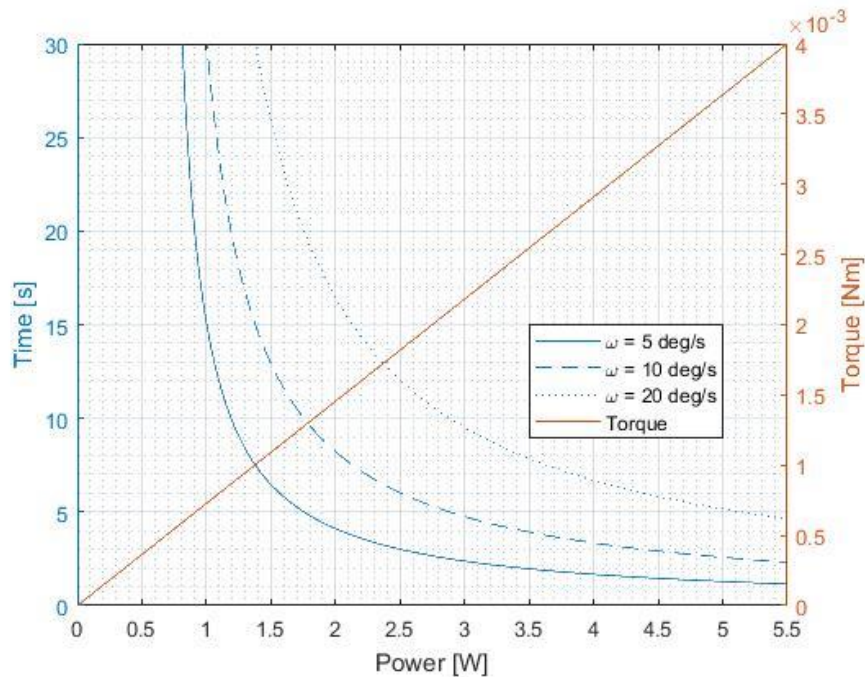
Figure 52: RWA detumble maneuver time and required torque as a function of available power
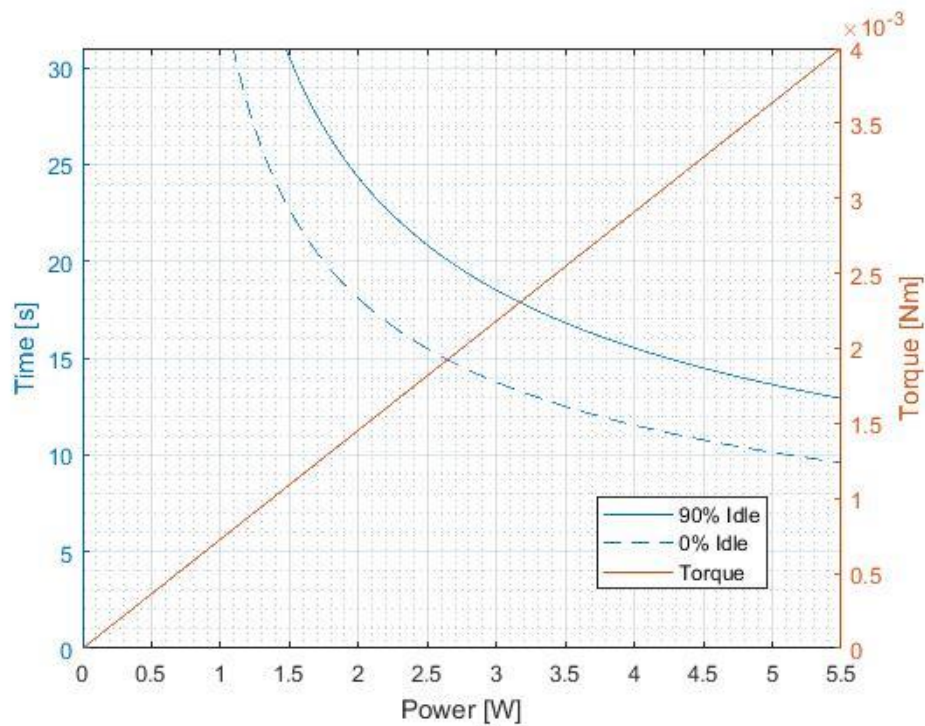
Figure 53: RWA slew maneuver time and required torque as a function of available power

From the data gathered, it was concluded that based on the necessities of the mission, both µPPTs and RWAs were beneficial. If the mission called to conserve power, it would require a longer maneuver completion time, making the µPPTs the safest bet. If the mission required to complete a maneuver at a faster rate, the RWAs offer a good choice for reasonable power consumption, shown by its 30 second completion time using a maximum of 5.5W.

Table 24: Trade-study comparison between the µPPT and the RWA for 2 orbits

Option	µPPT	RWA
Dry Mass (g)	6.93 (each)	130 (each)
Propellant Mass (g)	8.99	----
Total Mass (g)	64.43	390
Peak Power (W)	10	5.5

4.2.3 Rendezvous

4.2.3.1 Detumble Maneuver

The Rendezvous mission will also have to undergo a detumble maneuver to achieve a stable attitude. Since the Rendezvous CubeSat is more massive than the eLEO CubeSat, the required forces to reach a stable state are larger. As is evident from Figures 54 - 56, it is possible to despin within 95 minutes, which is much longer than the eLEO's detumble time. All the maneuver performance data provided in this section assume the micro PPT thruster as the baseline technology. The performance parameters for this thruster have already been summarized in Table 21.
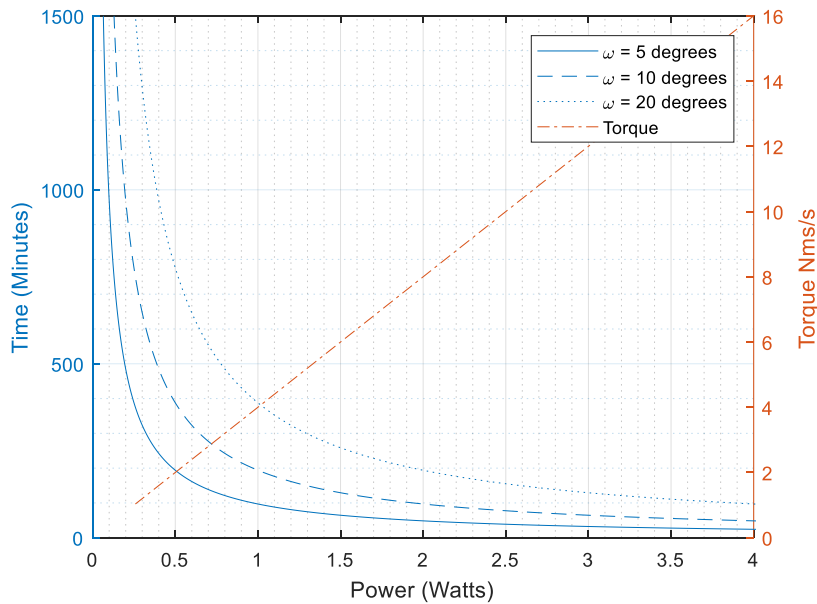
Figure 54: Rendezvous detumble time and torque vs. power with the PPTCUP thruster
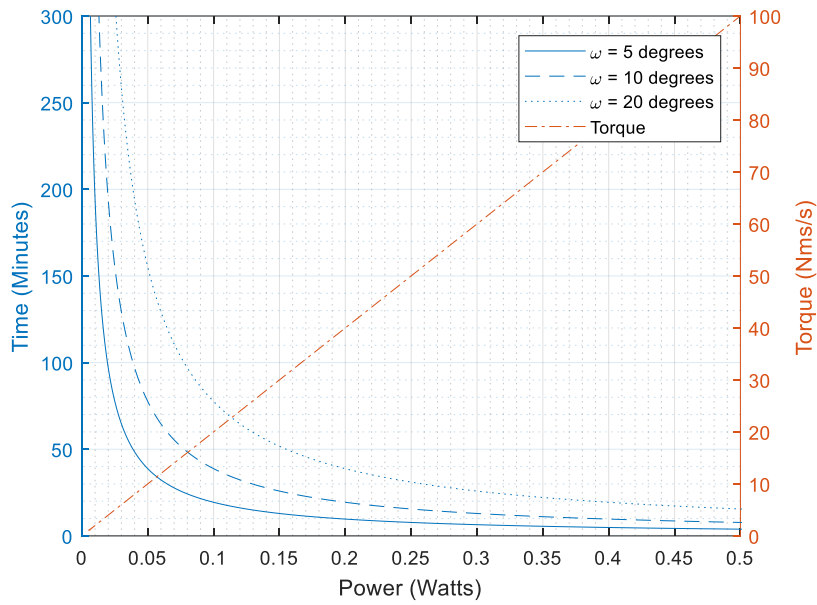
Figure 55: Rendezvous detumble time and torque vs. power with the Hybrid ADN/RCS thruster
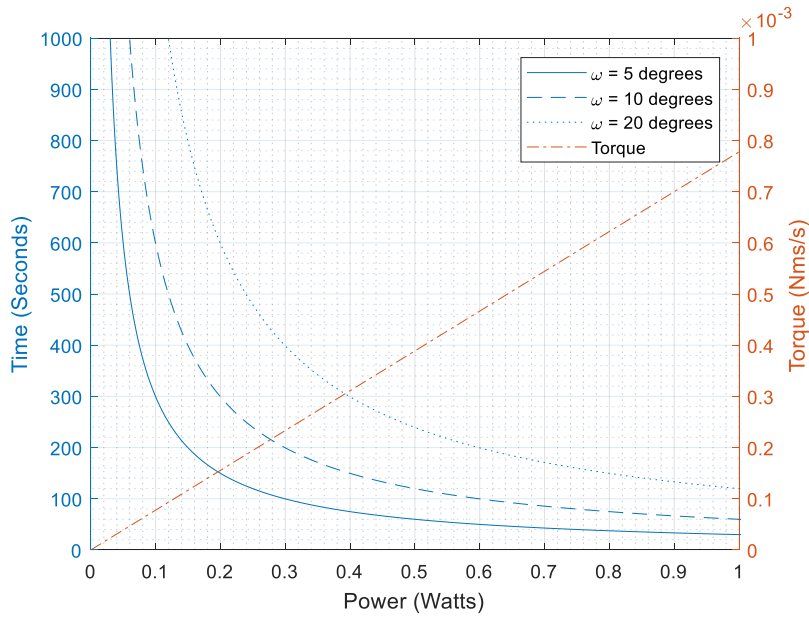
Figure 56: Rendezvous detumble time and torque vs. power with the Blue Canyon Tech RWP100 reaction wheels

Figures 54-56 are plots of the shows power required for a maneuver on the x-axis, with detumble duration on the left y-axis and angular momentum rate is on the right y-axis. For a given torque available from an ACS actuator, the corresponding time to detumble can be determined. The different colored lines represent the different initial spin rates, as listed in the legend. These

values refer to the initial angular rate at which the CubeSat is spinning when it is deployed. The 10 and 5 degrees/second cases correspond to more probable situations, with the initial spin rate of 20 degrees/second representing a worst-case scenario. These rotations were assumed to be about a minor axis. For the Rendezvous mission CubeSat, this is the yaw or pitch (Z or Y) axes, as shown in Figure 16. Each ACS system actuator option produced different results for the detumble procedure.

4.2.3.2 Slew Maneuvers

In Figures 57 - 59, torque is displayed on the right y-axis and time to complete is on the left y-axis. Both time and torque are plotted against power, denoted on the x-axis. The 180-degree slew maneuver is an end-over-end, repositioning maneuver that is considered a worst-case scenario so as to learn the capabilities and maneuverability of the CubeSat. Figures 57 - 59 show a comparison of the 90% idle versus the 0% idle, the difference between the two was described in section *3.2.1.2 Maneuver Analysis*. These plots show how each of the actuator options that were chosen for trade studies performed completing one of these maneuvers, starting with the PPTCUP thruster and working through the Hybrid ADN/RCS thrusters and reaction wheels.

Of note in Figures 57-59, there is not a large difference between the required maneuver times for the two idle options. While the 90% idle uses less power per second over a longer time to complete the maneuver, it ends up using the same amount of power using either method. As noted from Figures 57 – 59 the power versus torque line is linear. Therefore, the use of one type of idle option over the other is entirely based on the time that is needed to complete the maneuver.
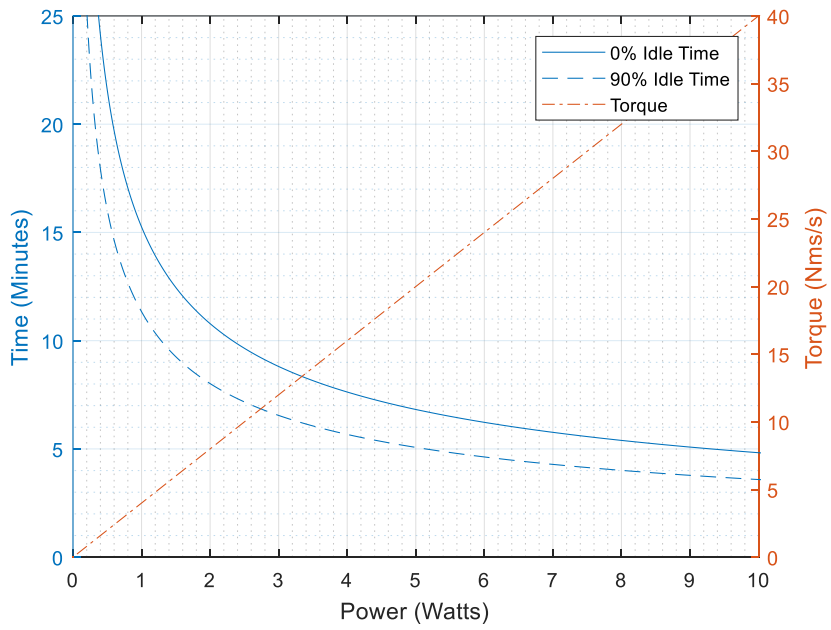
Figure 57: Rendezvous 180-degree slew maneuver with PPTCUP thrusters.
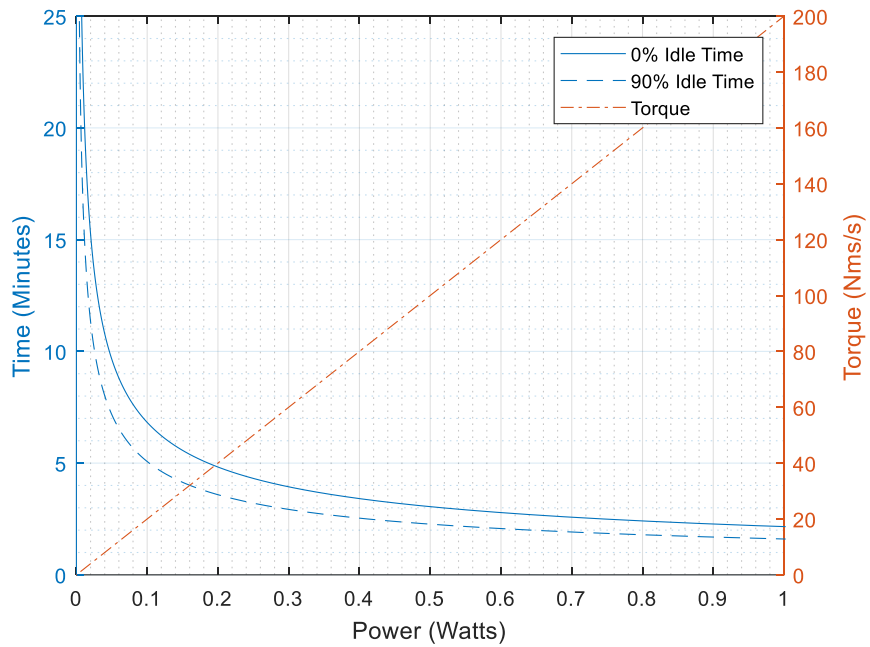
Figure 58: Rendezvous 180-degree slew maneuver with the Hybrid ADN/RCS thruster
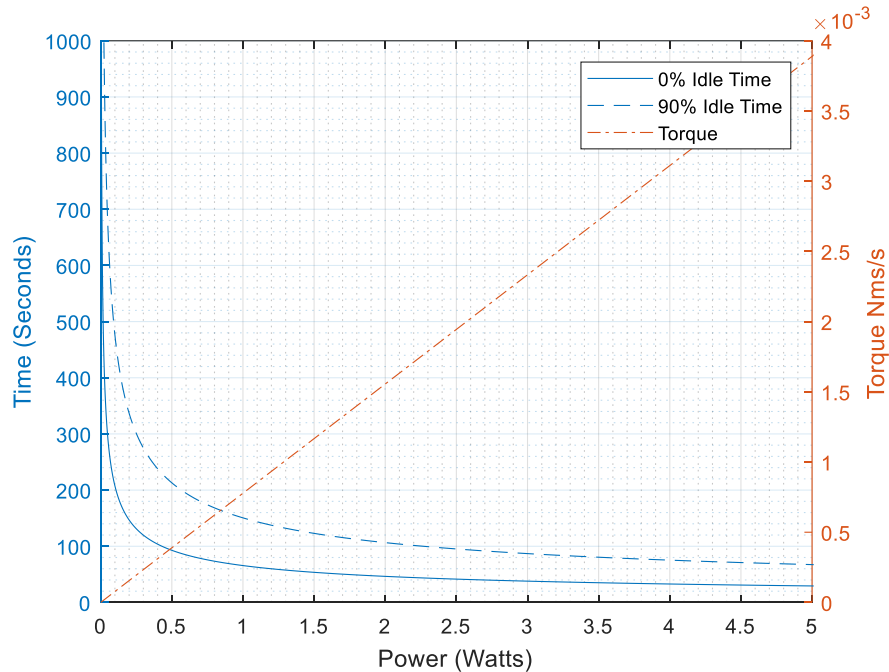
Figure 59: Rendezvous 180-degree slew maneuver with the Blue Canyon Tech RWP100 reaction wheels

4.2.3.3 Disturbance Torque Compensation

Spacecraft in both the eLEO and Rendezvous missions experience all the disturbance torques outlined in Section 3.2.1.1. As already described in Section 4.2.2.3 for the eLEO mission, the disturbance torque due to atmospheric drag is significantly larger than the other disturbances and was therefore the only disturbance considered for that mission. For the Rendezvous mission, it was necessary to consider all disturbance torques. The reason for this is that for the Rendezvous CubeSat, all of the disturbance torques are of similar orders of magnitude.

Figure 60 shows all of the disturbance torques that act on the Rendezvous CubeSat. The values shown in Figure 60 are the accumulated angular momentum rates over two orbits. Bars 1 through 4 show each of the individual disturbance torques on the CubeSat in increasing order. Torques are shown in different colors to differentiate between them. Bar 5 is the total disturbance torque acting on the CubeSat, and this bar shows the different colors of the other torques to show their contribution to the total torque.
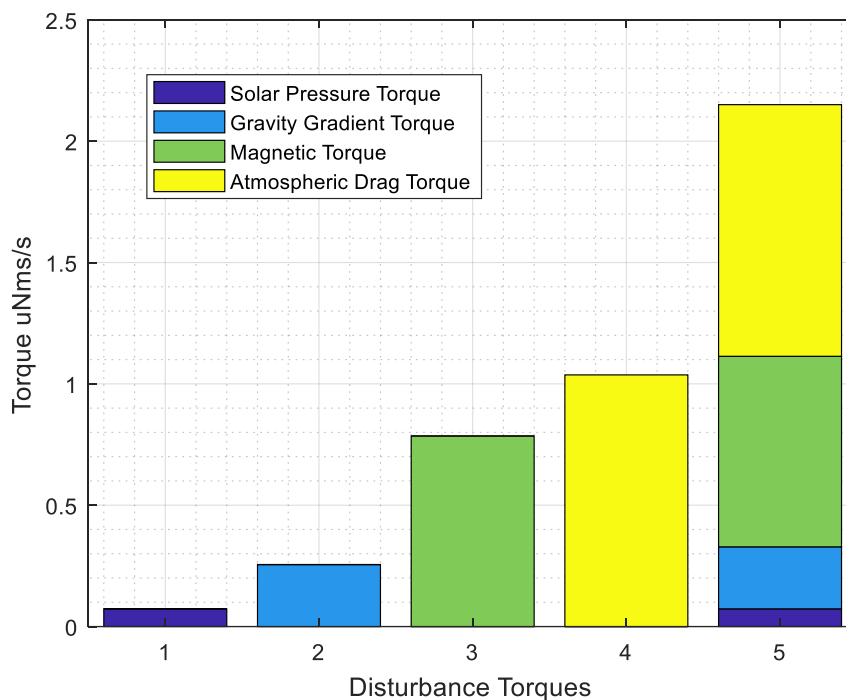
Figure 60: Disturbance torque magnitudes

Over the course of the mission, the disturbance torques will create an accumulating angular momentum on the CubeSat. To counteract these, the propulsion system must apply a torque to the spacecraft to ensure that it doesn't reach a point where it will be spinning out of control. It is important to also note that the CubeSat must remain pointed in such a way that the antennae can send and receive signals from the ground station. Disturbance compensation can be achieved by applying corrections in short periodic pulses that act opposite to the sum of the induced disturbance torques. An alternative recommendation is to have the thrusters apply a continuous torque to the craft, though this method will yield issues with power consumption and require more complex ACS control algorithms.

These options work for both the Hybrid ADN/RCS thruster and the PPTCUP, as they do not require desaturation. The reaction wheels do require desaturation, so there will be a time that the spacecraft is experiencing the disturbance torques and have no stabilizing

capability. There are two solutions recommended for this issue. The first is to use PPTs to counteract the forces while the wheels are desaturating. This would easily provide the torque required to the CubeSat to remain stable. This option is slightly unnecessary since the PPTs can complete the stabilizing maneuver and do not require desaturation, therefore making the reaction wheels superfluous. The second option is to add magnetorquers to the craft to create a torque for desaturating. This is the better option as the reaction wheels and the magnetorquers can work independently of each other and both provide sufficient torque to the satellite.

4.2.3.4 Propulsion Options Results

The recommended configuration for this CubeSat is still uncertain because of uncertainty in the mission requirements. Ultimately, results for the trade study will depend on the allowable mission time. For a mission where fast maneuvers are required, and power and mass are constrained only by the size of the CubeSat, the Hybrid ADN/RCS thrusters would be ideal. They provide an additional advantage of being integrated with the main propulsion system, saving on real estate for additional systems within the CubeSat. This spacecraft may also be larger and more massive since the hybrid RCS thrusters can generate much higher torques than the other systems, at the expense of a significant power draw.

Reaction wheels offer a middle ground between speed and efficiency, where efficiency refers to using the least amount of resources as possible. They will be useful for a mission that would require several rotations more often, rather than a mission that requires extremely precise pointing maneuvers. They require a low constant power draw (see Table 11) and can produce high-frequency vibrations (jitter), but they can deliver sufficient torque and ensure that any maneuvers are completed within the allowed time. Due to the design of the CubeSat affecting available

internal volume, the reaction wheels cannot all be placed in line with the principal axes of the bus, resulting in some loss in control authority and possibly inducing undesired components of torque. Likewise, a massive payload will decrease the effectiveness of the reaction wheels. The reaction wheels will also need to be desaturated approximately twice a day, during which time the magnetorquers will only be able to counter the disturbance torques, leaving the spacecraft with limited maneuvering capability.

The PPT systems use less power overall but are weaker in terms of control authority. The main disadvantage of the PPTs is the significant amount of time to detumble; they would require at least a full orbit firing at full power (in the worst-case scenario of 20 degrees/second initial spin rate around the minor axis of inertia). Overall, the PPTs take much longer to perform maneuvers, but can provide more precise control due to the low Ibit of the PPT. Since the PPTs occupy a small volume and have low mass, it is possible to double up on them. This may prove effective as the extra power usage may be made up for in the ability to orient solar panels to produce power sooner.

4.3 Telecommunications Subsystem

4.3.1 eLEO

After analyzing the Telecommunication Subsystem requirements for the eLEO mission, components were selected, and operation trade studies were performed. The results of these studies will be presented in this chapter.

4.3.1.1 Hardware Architecture Component Selection

The adopted baseline total mission data link budget was insufficient due the short duration of eLEO mission. The state-of-the art "ISIS TXS S-Band Transmitter" [36] was selected as an addition to the baseline system. This transmitter was selected because of its ability to interface with the NASA Space Network, which was chosen as the downlink network (detailed in section

4.3.1.2). It was also chosen because it can operate at higher data rates (3.4 Mbps), which increased the CubeSat's downlink capabilities. This will ensure critical mission information is transmitted to ground operators.

The baselined ISIS VHF uplink/UHF downlink Full Duplex Transceiver and the ISIS Hybrid Antenna System [25] [35] were kept as part of the final hardware architecture. The duplex transceiver board was kept as the only receiver onboard. Additionally, the receiver can interface with the NASA Near Earth Network, which was chosen as the uplink ground station network. The hybrid antenna was kept as it matched the CubeSat's mechanical design and interfaced adequately with both the transmitter and the duplex transceiver cards onboard. A complete set of characteristics of the selected hardware architecture are detailed in Table 12.

4.3.1.2 Mission Modeling and Timelines

The telecommunication subsystem scenario was modelled using STK. The model was composed of the NEN Ground Station Network, the Space Network TDLRS constellation, and the eLEO CubeSat. The subsystem configuration is illustrated in Figure 61, which shows the CubeSat in orbit with the blue lines representing instant connection to a TDLR Satellite and the red lines representing TDLRS respective geosynchronous orbits.
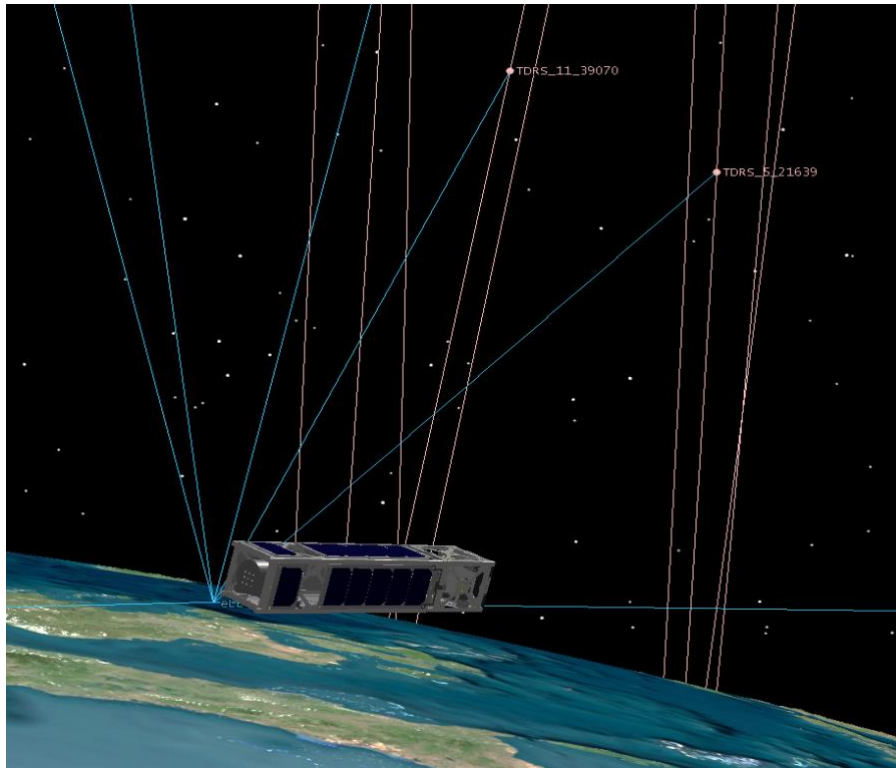
Figure 61: eLEO CubeSat communicating with TDLRS

Downlink Data Link Budget

As previously stated, the eLEO mission is inherently short (i.e. less than 31 days). Since exploration missions investigating the eLEO portion of the atmosphere are limited, high importance is placed on the ability to collect as much data from the payload as possible. Conventional ground-station-based downlink systems were deemed not suitable due to the low data rate (9.6 kbps). Because of this, NASA's Space Network was selected as the communication network. Its connection availability throughout the day and its fast data rate provide flexibility when transmitting from the CubeSat to Earth. Figure 62 shows all the possible access to a TDLR satellite and how much data would be transmitted if connected. The available power for the CubeSat constrains the total data transfer. A full mission day connection would result in approximately 300 gigabytes of transmitted data. Using the transmitter once per orbit at peak

power for one minute is sufficient to transmit approximately three gigabytes per day. This is a conservative approach that has little effect on the power subsystem operation. An optimal operations plan would need to be implemented to maximize data transmission while minimizing power consumption and the cost related to the use of the network.
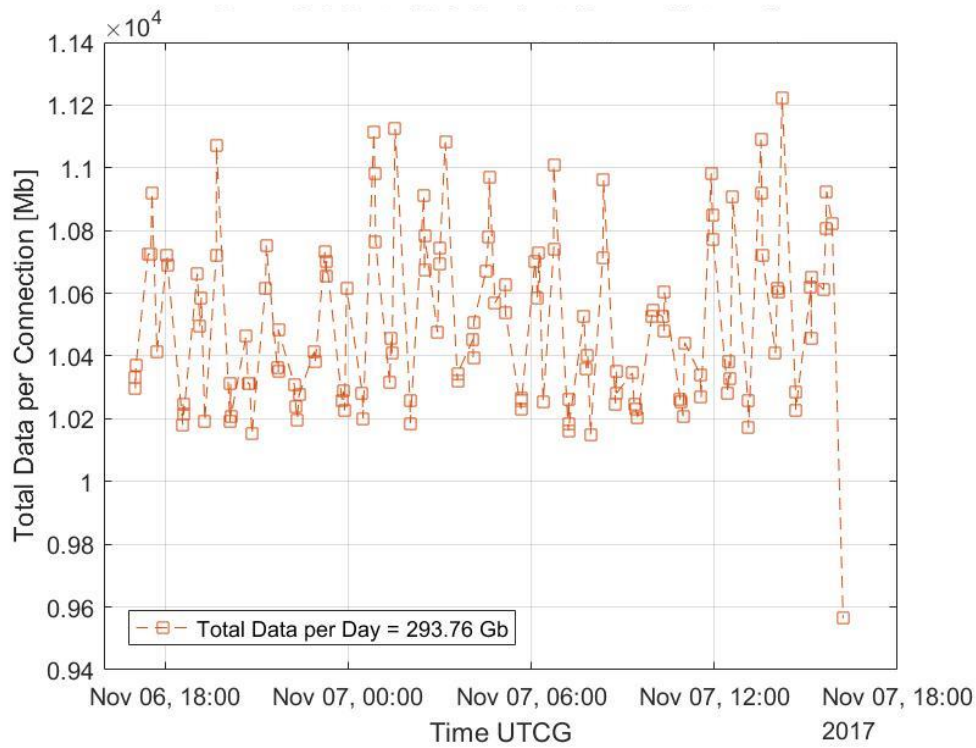
Figure 62: Downlink Data Link Budget (Space Network) for a one-day period

Uplink Data Link Budget

Uplink will utilize the Near Earth Network as the receiver does not operate on S-band. The lower data rate will not be an issue as the mission does not expect critical messages or commands to be sent from Earth. All firmware and commands are expected to be onboard for the short mission span. If an external data packet has to be sent and received by the CubeSat, there would be a possibility of using the NEN. This emergency data packet size is assumed to be small (i.e. < 1.0 Mb). Figure 63 shows each point of access between the CubeSat and one of the Ground Stations

on the NEN, corresponding to the total data transmission possible over a one-day period, with an average of 3.4 Mb per connection. The locations of optimum data transfer are purple colored, these are Australia and New Mexico. These connections occur during the day time and provide 4.53 Mb and 4.52 Mb, respectively The New Mexico ground station was the most convenient as it was the same station that would receive transmission from the Space Network, requiring ground operations to be handled from one only ground location inside the United States. Figure 64 shows all the access locations and times and duration for each connection.
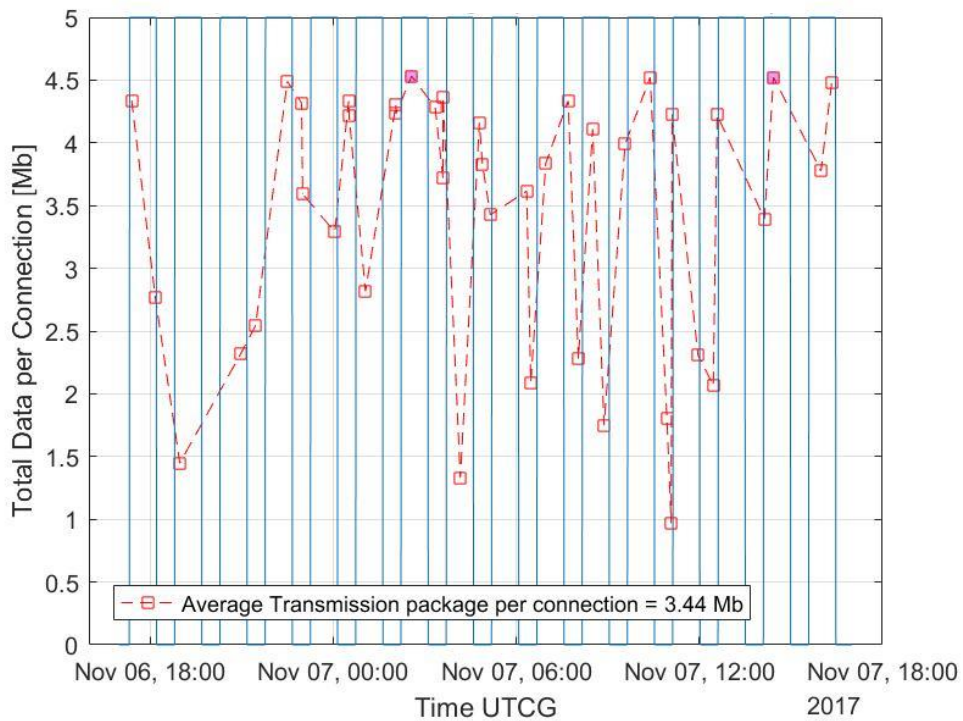
Figure 63: Uplink Data Link Budget (Near Earth Network) for a one-day period
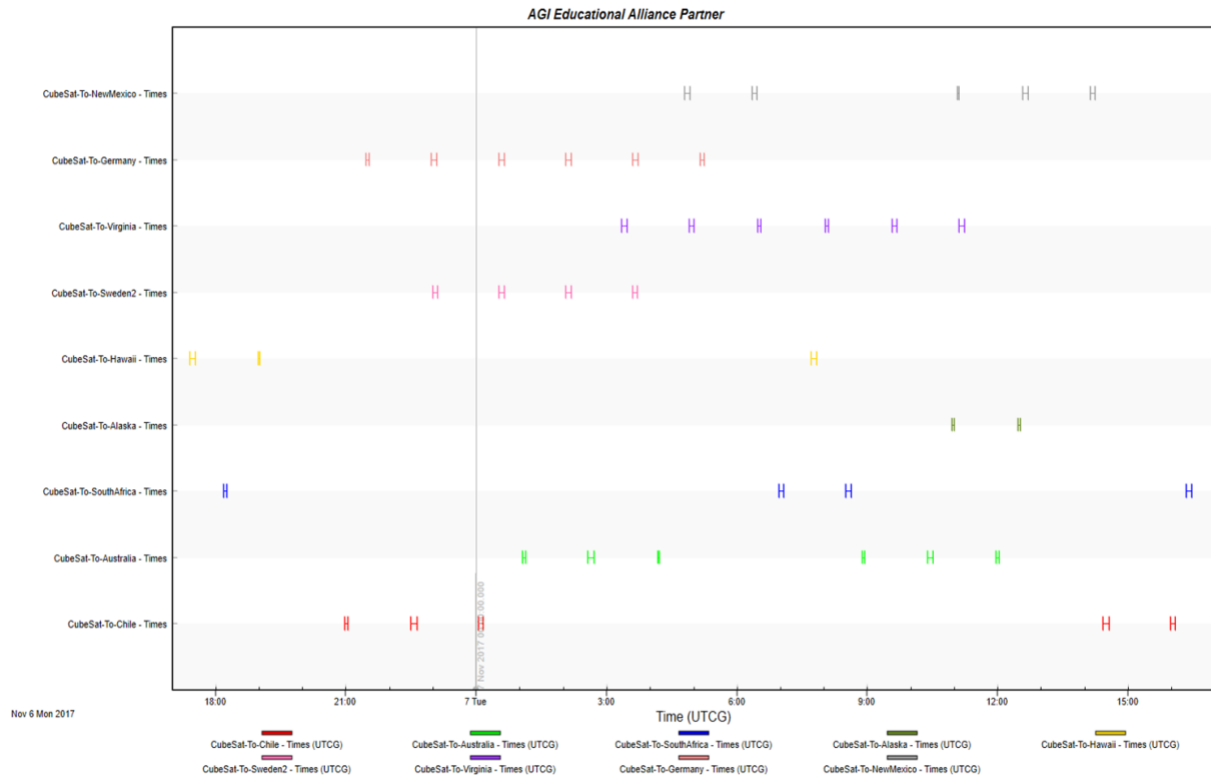
Figure 64: NEN access and connections, locations and duration for a one-day period

4.3.2 Rendezvous

4.3.2.1 Hardware Architecture Component Selection

The baseline hardware components described in Section 2.4.1 were chosen as the final hardware architecture for the Rendezvous mission. These hardware components included the ISIS Full Duplex Transceiver (VHF Uplink / UHF Downlink) and the Hybrid Antenna system. These hardware components are readily available and provide an acceptable data rate (9.6 Kb/s) that produced a satisfactory data link budget for the Rendezvous mission. Details and specifications of the selected hardware are outline in Table 12.

4.3.2.2 Mission Modeling and Timelines

Uplink and Downlink Opportunities

As outlined in section 3.3.2.3, an STK scenario was developed to determine the uplink and downlink access times for the CubeSat as it orbited at various inclinations. During a 24-hour

period, the occurrence of access times and their duration varied based on the inclination of the orbit studied. It was important for the 2018 Telecom team to extract and analyze all possible access times, so that various uplink and downlink times could be accounted for in the power budget.

Figure 65 depicts the uplink and downlink opportunities for a 45-degree inclination orbit. The colored marks on the figure represent when these access times occurred, and which ground station these access times are associated with. This figure was the first step in determining when uplink and downlink for the CubeSat could take place and proved there were many instances and ground stations to choose from.
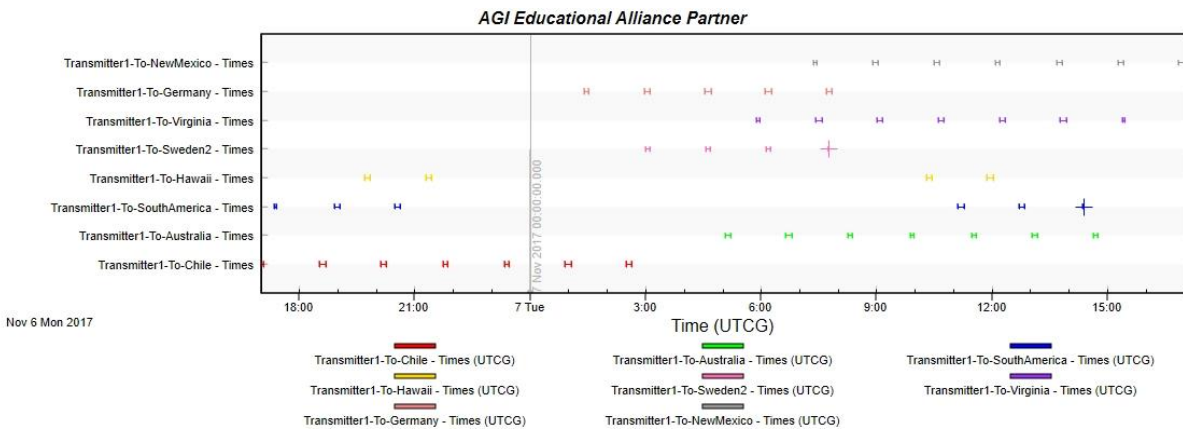
Figure 65: Uplink and downlink opportunities for a 45-degree inclination for a period of 16 orbits

Similarly, Figure 66 represents the uplink and downlink opportunities for a 90-degree inclination orbit. The colored marks also represent when the access times occurred during a 24-hour period, and these access times correspond to the ground station listed on the left.
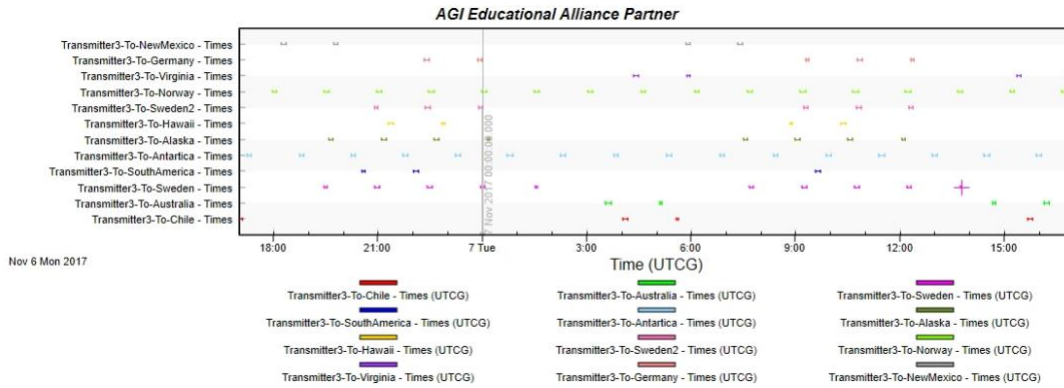
Figure 66: Uplink and downlink opportunities for a 90-degree inclination for a period of 16 orbits

Notably, when an attempt was made to produce uplink and downlink opportunities for a 0-degree orbit, STK could not generate a report. This remains true with the STK coverage depicted in Section 3.3.2.3. If there is no coverage available, no access times can be plotted, and no data can be transferred via uplink or downlink. Since transfer of data is mission critical, the Space Network (described by the eLEO Telecom team) would be the only datalink option for a 0-degree inclination mission.

After the uplink and downlink opportunities were plotted for both 45 and 90-degree inclinations, it was clear that the 90-degree inclination provided more coverage over the ground stations, which is consistent with the coverage maps in Section 3.3.2.3. With this information, the access times from a 24-hour period needed to be used to calculate the data that can be transferred via uplink or downlink during the respective access time with one of the ground stations.

Uplink and Downlink Data Link Budget

The uplink and downlink opportunities depicted above were extracted in the form of Excel worksheets from STK. These worksheets listed the duration of each uplink or downlink opportunity, and when this opportunity occurred during a 24-hour period. This information was combined with data rate in a MATLAB code developed by the Telecom team and was then plotted over a 24-hour period. The MATLAB code uses data rate and these uplink and downlink durations

to plot the total data per connection over a 24-period. Figures 67-68 depict these instances and are the culmination of the 2018 Telecom trade study, evaluating the two networks and three inclinations.
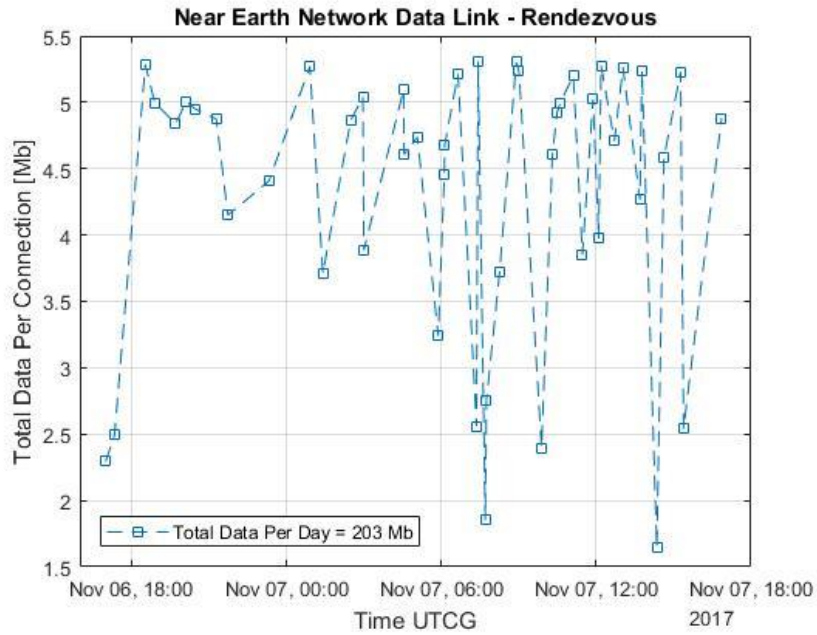
Figure 67: Uplink and downlink potential for a 45-degree inclination for a period of 16 orbits
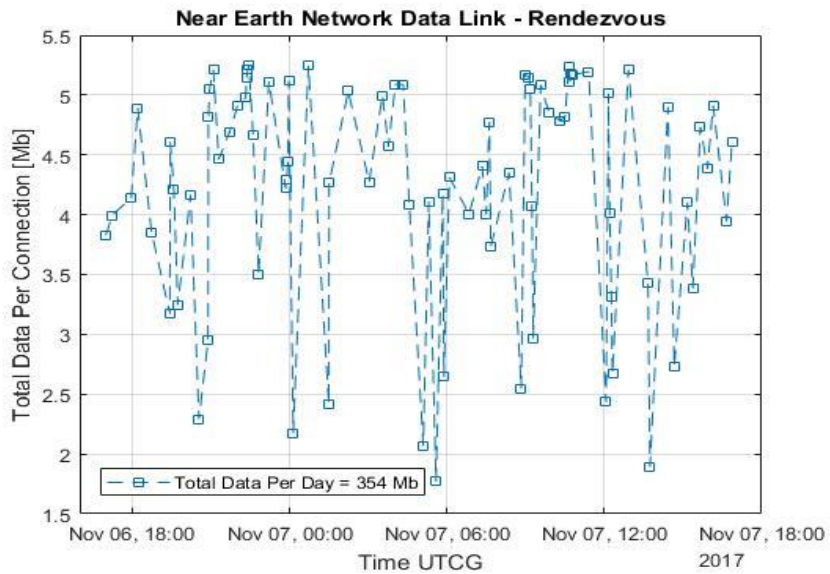
Figure 68: Uplink and downlink potential for a 90-degree inclination for a period of 16 orbits

In Figures 67-68, each data point represents a connection that lasts a certain duration. The instances that result in 5 Mb or more last approximately 500-600 seconds, whereas the instances with less than 2.5 Mb last approximately 100-200 seconds. As expected, the 90-degree inclination contains more data points in the plot, representing the larger number of access times available for this inclination. Furthermore, the total data per day was calculated and shown on each figure, to demonstrate the total uplink and downlink potential for each of the inclinations. However, the Rendezvous CubeSat would likely never have sufficient power to uplink or downlink during all of these opportunities.

To accommodate the power restrictions, the Telecom team chose two data link sessions per orbit as a baseline for the mission. These two instances, for both 45 and 90-degree inclinations, provided 5-5.25 Mb per instance. Therefore, the total data transferable via uplink or downlink per orbit is approximately 10 Mb. These instances were added into the power budget to account for the telecom system power usage and did not negatively affect the power budget. With approximately 16 orbits per 24-hour period, the total available data transfer for either uplink or downlink is approximately 160 Mb per 24-hour period. Due to the Rendezvous mission's ample time in orbit compared to the eLEO mission, the 160 Mb per day of data transmission serves as an acceptable baseline that leaves room for flexibility and improvement for future missions.

5   Conclusions & Recommendations

5.1 Power Subsystem

5.1.1 eLEO

The next iteration of this comprehensive CubeSat study should involve testing options for a payload. The 2018 CubeSat MQP was focused on identifying the minimum resources to keep the CubeSat in orbit, whereas a payload was deemed unnecessary for power analysis. Future work would include better options for solar panels if needed or budgeting of the payload power activity. As this was the first introduction of propulsion, power models of such were limited and require further analysis to be efficient.

5.1.2 Rendezvous

The power system described in this report provides a baseline to build upon; some improvements still need to be made. The most important future steps include combining the CubeSat thermal analysis with the thermal efficiency rating of the solar arrays in order to further refine the precision of the power generation.

Additionally, further work with the propulsion group will help identify other possible scenarios in the power budget in order to determine if other attitude control or primary thrusters are more beneficial for the Rendezvous mission.

Finally, importing the SolidWorks model for the CubeSat into STK would allow users to simulate the solar arrays on the face of the CubeSat and generate power generation reports directly from STK.

5.2 Propulsion Subsystems

5.2.1 eLEO

As shown by the analysis presented, although the drag torque dominated the disturbance torques, it is possible to compensate for it. It is also important to note that the life of the CubeSat is around 25 days in orbit, with a heavier payload (greater than 2kg) surprisingly extending the life of the mission due to the higher ballistic coefficient. The longer life results in a higher consumption of fuel and power, due to the higher torques and forces the μPPTs and RWAs would need to exert for a heavier CubeSat. It would be useful and interesting to explore how much mass could be added to the CubeSat before the lifetime is adversely impacted. This would be possible by partnering with the design and power groups to calculate the necessary adjustments that would need to be made to batteries and solar arrays. In conclusion, this CubeSat is a cost-effective way to gather at least three weeks' worth of data at a low cost, allowing easy accessibility to a strategic and unexplored area of Earth's thermosphere.

5.2.2 Rendezvous

For future CubeSat MQPs, it would be advised to establish the trade space early on. This would include chemical, electrical, and internal torquers (i.e. reaction wheels and magnetorquers) for attitude control systems, and chemical and electrical thrusters for primary propulsion. Furthermore, increased communication with other teams to ensure that the systems being traded with are compatible into the design and the effects of the specific locations of the system for use in comparison are known to enhance the fidelity of design trade considerations. Additionally, use of STK to more precisely simulate orbital maneuvers would provide more data for trades.

5.3 Telecommunications Subsystem

5.3.1 eLEO

Within the constraints of the analysis and the STK model, the selected hardware as well as the communication network, both for downlink and uplink, fulfills the mission requirements. The data link capability was maximized considering the short mission duration. Utilizing the Space Network ensures that all data to be collected during the mission is transmitted to Earth each orbit continuously. This continuous access would be particularly beneficial in the event of an unexpected failure, allowing some mission science to be recovered. Once a payload is selected, further studies should be performed to optimize the interface with the telecommunication subsystem. Further implementations of the Space Network are recommended to future MQP groups as it has potential benefits for multiple types of missions. High data rates can be used for information intensive missions, a low data-to-power ratio can be a solution to the problem of limited power production. It can also make mission operation costs cheaper as its data-to-cost ratio is smaller to that of the conventional Ground Station Network.

5.3.2 Rendezvous

As technology advances, the Telecommunication subsystem hardware for the Rendezvous CubeSat should also progress forward. Depending on mission or customer requirements, 25 Mb per day might not be sufficient. Continuing to research and update the CubeSat with the most advanced transceiver and antenna will ensure optimal data rate for uplink and downlink budgets. If hardware advances plateau, and more data transfer is still needed, then additional uplink and downlink instances would need to be prioritized in the power budget, rather than other maneuvers.

The ground stations that the 2018 Telecom team chose proved to work sufficiently and provide adequate coverage for a long duration mission at inclinations such as 45 and 90 degrees.

However, the limitations for a 0-degree inclination were evident in the analysis. Future Telecom teams should further investigate how realistic it is to use the advanced Space Network system. These future groups should compare and contrast whether or not it would be worth pursuing this advanced form of data transfer in order to accommodate an equatorial orbit.

Works Cited:

[1] J. J. Blandino, N. Martinez-Baquero, M. A. Demetriou, N. A. Gatsonis and N. Paschalidis, "Feasibility for Orbital Life Extension of a CubeSat in the Lower Thermosphere," *Journal of Spacecraft and Rockets,* 2014.

[2] J. W. Conklin, "The Drag-Free CubeSat," *26th Annual AIAA/USU Conference on Small Satellites,* 2012.

[3] A. Mehrparvar, "CubeSat Design Specification," California Polytechnic State University.

[4] J. R. Wertz and W. J. Larson, Space Mission Analysis and Design, 3rd Edition ed., New York, NY; Hawthorne, CA: Springer; Microcosm Press, 1999.

[5] D. H. Ko, S. Laudage, M. Murphy, D. Pelgrift, S. Young and J. Advisor: Blandino, "Design and Analysis of the Sphinx-NG CubeSat," 2017.

[6] Analytical Graphics Inc., *Systems Tool Kit,* 2017.

[7] The Mathworks Inc., *MATLAB,* 1994-2018.

[8] K. Cote, J. Gabriel, B. Patel, N. Ridley, Z. Taillefer and S. Tetreault, "Mechanical, Power, and Propulsion Subsystem Design for a CubeSat," 2011.

[9] National Instruments, "Using NI CompactRIO to Design a Maximum Power Point Tracking Controller for Solar Energy Applications," [Online]. Available: http://sine.ni.com/cs/app/doc/p/id/cs-11738. [Accessed October 2017].

[10] J. Kalde, "System architecture of the ESTCube-1 satellite power system," July 2012. [Online]. Available: http://jaanus.tech-thing.org/space/more-details-electrical-power-system/. [Accessed October 2017].

[11] N. Navarathinam, R. Lee and H. Chesser, "Characterization of Lithium-Polymer batteries for CubeSat applications," *Acta Astronautica,* vol. 68, pp. 1752-1760, 2011.

[12] G. Horváth, G. Marosy, S. Glisics and D. Czifra, "Battery characterization for CubeSat missions with battery tester application.," in *2012 IEE Electronics Conference*, 2012.

[13] C. Clark and E. Simon, "Evaluation of Lithium Polymer Technology for Small Satellite Applications," in *21st AIAA Conference on Small Satellites*, 2007.

[14] B. Seifert, N. Buldrini, A. Reissner, C. Scharlemann, D. Krejci, F. Plesescu and F. Hörbe, "Integrated Electric Propulsion Systems for Small Satellites," in *Space Propulsion Conference, At Cologne*, Cologne, Germany, 2014.

[15] C. Carpenter, D. Schmuland, J. Overly and R. Masse, "Test Results for the MPS-120 and MPS-130 CubeSat Propulsion Systems," in *28th Annual AIAA/USU Conference on Small Satellites*, 2014.

[16] J. D. DeSain, "Green Propulsion: Trends and Perspectives," *Aerospace,* July 2011.

[17] B. Yost, "State of the Art of Small Spacecraft Technology," 13 September 2017. [Online]. Available: https://sst-soa.arc.nasa.gov/04-propulsion. [Accessed 9 October 2017].

[18] Aerojet Rocketdyne, "MPS-120™ CubeSat High-Impulse Adaptable Modular Propulsion System (CHAMPS)," Aerojet Rocketdyne, [Online]. Available: http://www.rocket.com/cubesat/mps-120. [Accessed October 2017].

[19] VACCO, "Hybrid ADN Delta-V / RCS System," VACCO, [Online]. Available: http://www.cubesat-propulsion.com/hybrid-adn-delta-v-rcs-system/. [Accessed October 2017].

[20] Clyde Space, "CubeSat Pulsed Plasma Thruster," [Online]. Available: https://www.clyde.space/products/50-cubesat-pulsed-plasma-thruster. [Accessed October 2017].

[21] "MIT SPL delivers the Scalable ion Electrospray Propulsion System (S-iEPS) for CubeSats to NASA," MIT, 2 July 2015. [Online]. Available: spl.mit.edu/news/mit-spl-delivers-scalable-ion-electrospray-propulsion-system-s-ieps-cubesats-nasa. [Accessed October 2017].

[22] BUSEK, "ELECTROSPRAY THRUSTERS," Busek Co. Inc., [Online]. Available: http://www.busek.com/technologies__espray.htm. [Accessed October 2017].

[23] Mars Space Ltd., "PPTCUP - Pulsed Plasma Thruster for CUbesat Propulsion," [Online]. Available: http://www.mars-space.co.uk/projects/pptcup. [Accessed October 2017].

[24] Innovative Solutions In Space (ISIS), "Full Ground Station Kit VHF/UHF/S-band," [Online]. Available: https://www.isispace.nl/product/full-ground-station-kit-for-vhfuhfs-band/. [Accessed 9 October 2017].

[25] Innovative Solutions In Space (ISIS), "Hybrid antenna system," [Online]. Available: https://www.isispace.nl/product/antennas/. [Accessed 9 October 2017].

[26] R. F. J. P. A. C. W. P. K. U. F. Charles Cooper, *The CubeSat Ground Station at the University of Arizona,* University of Arizona, 2002.

[27] A. Campbell, Ed."Near Earth Network (NEN)," 10 March 2016.

[28] "40Whr CubeSat Battery," [Online]. Available: https://www.clyde.space/products/49-40whr-cubesat-battery. [Accessed 7 December 2017].

[29] "3rd Generation FlexU EPS," [Online]. Available: https://www.clyde.space/products/19-3rd-generation-flexu-eps. [Accessed December 2017].

[30] Clyde Space, "CS High Power Bundle B: EPS + 40Whr Battery," [Online]. Available: https://www.clyde.space/products/44-cs-high-power-bundle-b-eps-40whr-battery. [Accessed February 2018].

[31] "Custom solar panels," [Online]. Available: https://www.isispace.nl/product/custom-solar-panels/. [Accessed 7 December 2017].

[32] Y. Lu, "CubeSat Design and Attitude Control with Micro Pulsed Plasma Thrusters," Worcester Polytechnic Institute, Worcester, MA, April 2015.

[33] J. R. Cassady, A. W. Hoskins, M. Campbell and C. Rayburn, "A Micro Pulsed Plasma Thruster (PPT) for the "Dawgstar'' Spacecraft," IEEE, Seattle, WA, 2000.

[34] "Blue Canyon Technologies," 2017. [Online]. Available: http://bluecanyontech.com/reaction-wheels/.

[35] Innovative Solutions In Space (ISIS), "ISIS VHF uplink/UHF downlink Full Duplex Transceiver," [Online]. Available: https://www.isispace.nl/product/isis-uhf-downlink-vhf-uplink-full-duplex-transceiver/. [Accessed 9 October 2017].

[36] Innovative Solutions in Space (ISIS), "ISSI TXS S-Band Transmitter," [Online]. Available: https://www.isispace.nl/product/isis-txs-s-band-transmitter/. [Accessed December 2017].

[37] NASA, "Exploration & Space Communications," [Online]. Available: https://esc.gsfc.nasa.gov/. [Accessed February 2018].

[38] AGI.Inc, "Insert an Object from the Standard Object Database," [Online]. Available: http://help.agi.com/stk/index.htm#stk/InsertFromSOC.htm. [Accessed February 2018].

[39] Spectrolab, "28.3% Ultra Triple Juntion Solar Cells," 2010. [Online].

[40] U. Kvella, M. Puusepp, F. Kaminski, J.-E. Past, K. Palmer, T.-A. Grönland and M. Noorma, "Nanosatellite orbit control using MEMS cold gas thrusters," in *Proceedings of the Estonian Academy of Sciences*, 2014.

[41] J. J. Blandino, N. Martinez-Baquero, M. A. Demetriou, N. A. Gatsonis and N. Paschalidis, "Feasibility for Orbital Life Extension of a CubeSat in the Lower Thermosphere," *Journal of Spacecraft and Rockets,* 2016.

[42] W. A. De Groot, "Propulsion Options for Primary Thrust and Attitude Control of Microspacecraft," Nyma Inc., Brook Park, OH, 1998.

[43] J. Mueller, R. Hofer, M. Parker and J. Ziermer, "Survey of Propulsion Options for CubeSats," Pasadena, CA, 2010.

[44] Busek, "Products," Busek Co. Inc., [Online]. Available: http://www.busek.com/technologies__main.htm. [Accessed October 2017].

Appendices

Appendix A: MPS-Thruster Option Master Table

Name	Type	Thrust Level (mN)	Isp (s)	Impulse Capabilities (Ns)	Power (W)	Wet Mass (kg)	Dry Mass (g)	Dimensions (cm)	Manufacturer	Heritage	Reference #
MPS-120	Chemical	260-2790	206-217		<4 (Startup); <1 (Operation)	1.48		10x10x11.35	Aerojet Rocketdyne	In Development/NASA Funded	1
ADN Delta-V MPS	Chemical	400		1036	<15(hot-fire); <0.055(Standby)	1.8		4.15x3.54x3.54	VACCO/ECAPS	TRL8	2
HYDROS-C	Chemical	2.1	310		5-25	1.76		0.092cm^3	Tethers Unlimited	Flight qualification targeted for Q4 201	3
100mu	Electric	0.1	2300		5	0.55		9x9x4	Busek	TRL5/NASA ST-7	4
BIT-1	Electric	0.1	2250		10				Busek	TRL5	5
mu-CAT	Electric	50	3000		0.1	0.24		200cm^3	GWU and USNA	TRL7	6
NANOPS	Chemical	35	46				480	5x5x10	SFL	CanX-2	9-11
CNAPS	Chemical	12.5-50	45				240	7x12.5x18	SFL	CanX-5	12-13
MEMS	Chemical	100	30				188	9.1x9.1x2.2	SFL	MEPSI-3	14-15
MarCO MIPS	R236fa	25							VACCO		4,21
MIPS	R134a (Cold Gas)	10	40					3.33x3.33x3.33 - 10x10x10	Aerospace Corporation		4,21
Micro-Propulsion	Chemical	1 per nozzle	32				-	-	Microspace Rapid Pte Ltd	POPSAT-HIP1	16
T3-μPS	Chemical	6	69				<10	100cm^3	TNO, U. Twente, & TU Delft	Delfin-3xt	17-19
AFRL PUC	SO2	3.5	47		.542-1.245		434-835	2.5x2.5x2.5 - 10x10x10	VACCO		4,21
RIT-uX	Ion	10-15000	3000-4500		6	1.4		-	ALTA SpA		7
MEPSI MIPS	Isobutane	53	65				456	9.1x9.1x2.5	VACCO		4,21
IPL MEP	Electrospray	0.2	3744		8.16			140cm^3	JPL		7
MIXI	Xenon	0.1-1.553	3000-7000		20-60			1000cm^3	California Polytech State U		8
Green Monopropellant	Green Monopropellant	500	220		15(initial)	<1		<500cm^3	Busek		22
uPPT	PTFE	0.01 - 0.02	1000		0.5 - 4		25	202.5cm^3	Austrian Research Centers		20
Clyde Space PPT	Pulsed Plasma	0.038	590		0.5			250cm^3	Clyde Space		24
BGT-5X	HAN-based	0.5	220-225					-	Busek		23
BGT-1X	HAN-based	0.1	214					1U	Busek		24
MRI	Ammonia	2-10	150		3-15	1.25		810cm^3	Busek		22
CAT	Helicon Plasma (Xenon)	0.5-4	400-800		10-50			250cm^3	University of Michigan		25
Busek pressure-fed elec Electrospray (Ionic liquid)	Electrospray (Ionic liquid)	0.7	800		9	1.15		560cm^3	Busek		22
SNAP-1 Butane System	Cold Gas (Butane: stored as liquid)	40-120	43-70		15			5300 (thruster + propellant)			22
Micro-PPT	Pulsed-Plasma (Teflon)	0.14	500		12.5	3.8		-	Dawgstar	-	22
MPS-130	Chemical	250-1250	206-235	6000	10	1.66	1060	10x10x10	Aerojet Rocketdyne	In development	28,29
Water Propellant	Water	3						-	Aerospace Corporation		27
Bong Palomar MIPS	Isobutane	35 per nozzle	-				890	10x10x10.7	VACCO		26
FEMTA	Water	0.006 - 0.068	>80		<1	0.0368	34	10x10x10	Purdue University		30
CHIPS	Cold gas (R236fa or R134a)	17-31	38-76	287-498				10x10x2.5	CU Aerospace	In development	31
BmP-220 ppt	PPT teflon propellant	0.02-0.14	536	220	1.5 @ 1Hz, 7.5 @ 7hz	0.5		330 cm^3	Busek	FalconSat-3, MPACS	32
NASA C-POD	Cold gas (R134a)	25	40	186	5	1.244		9.8x9.8x10.15	VACCO		33
MPS-220	Cold gas (Rt134)										

Ref. Number	
1	"MPS-120™ CubeSat High-Impulse Adaptable Modular Propulsion System (CHAMPS)," MPS-120™ CubeSat High-Impulse Adaptable Modular Propulsion System (CHAMPS), Aerojet Rocketdyne, www.rocket.com/cubesat/mps-120.
2	"ADN Micropropulsion System." Vacco Industries, www.vacco.com/images/uploads/pdfs/MicroPropulsionSystems.pdf.
3	"HYDROS™ Water Electrolysis Thruster Green Propellant, High-Thrust Propulsion for Orbit-Agile CubeSats." HYDROS Propulsion System, Tethers Unlimited, www.tethers.com/HYDROS.html.
4	"BET-100 Busek Electrospray Thrusters." Electrospray Thrusters, Busek, www.busek.com/technologies__espray.htm.
5	Yost, Bruce. "State of the Art of Small Spacecraft Technology." NASA, NASA, 13 Sept. 2017, sst-soa.arc.nasa.gov/04-propulsion.
6	Keidar, Michael. "Micro-Cathode Arc Thruster for Small Satellite Propulsion." dcspacegrant.org/affiliatemeeting2016/GWU2016.pdf.
7	https://arc.aiaa.org/doi/pdf/10.2514/1.A33564
8	http://digitalcommons.calpoly.edu/cgi/viewcontent.cgi?article=1021&context=aerosp
9	K. Sarda, C. Grant, S. Eagleson, D.D. Kekez, R.E. Zee, Canadian Advanced Nanospace Experiment 2: On-orbit experiences with a three-kilogram satellite, in: Proceedings of the 22nd AIAA/USU Conference Small Satell., Logan, UT: SSC08–II–5, 2008.
10	S. Mauthe, F. Pranajaya, R. Zee, The Design and Test of a Compact Propulsion System for CanX Nanosatellite Formation Flying Conference on Small Satellites, in: Proceedings of the 19th AIAA/USU Conference Small Satell., Logan, UT: SSC05– VI–5, 2005.
11	K. Sarda, C. Grant, S. Eagleson, D. Kekez, R. Zee, Canadian Advanced Nanospace Experiment 2 Orbit Operations: One Year of Pushing the Nanosatellite Performance Envelope, in: Proceedings of the 23rd Annu. AIAA/USU Conference Small Satell., Logan, UT: SSC09–IV–6, doi:http://dx.doi.org/10.1089/ees.2013.0409, 2009.
12	G. Bonin, N. Roth, S. Armitage, J. Newman, B. Risi, R.E. Zee, CanX-4 and CanX-5 Precision Formation Flight: Mission Accomplished!, in: Proceedings of the 29th AIAA/USU Conference Small Satell., Logan, UT: SSC15-I-44, doi:http://dx.doi.org/10.1016/j.jcrysgro.2014.02.053, 2015.
13	B.W. Risi, Propulsion System Developemnt for the CanX-4 and CanX-5 Dual Nanosatellite Formation Flying Mission, University of Toronto, Toronto, Canada, 2014.
14	D. Hinkley, A Novel Cold Gas Propulsion System for Nanosatellites and Picosatellites, in: Proceedings of the 22nd AIAA/USU Conference Small Satell., Logan, UT: SSC08–VII–7, 2008.
15	D. Hinkley, Chapter 20: picosatellites at The Aerospace Corporation, in: H. Helvajian, S.W. Janson (Eds.), Small Satell. Past, Present. Futur., Aerospace Press, El Segundo, CA, 2008.
16	G. Manzoni, Y.L. Brama, Cubesat Micropropulsion Characterization in Low Earth Orbit, in: Proceedings of the 29th AIAA/USU Conference Small Satell., Logan, UT: SSC15–IV–5, 2015.
17	J. Guo, J. Bouwmeester, E. Gill, In-orbit results of Delfi-n3Xt: Lessons learned and move forward, Acta Astronaut. 121 (2016) 39–50, http://dx.doi.org/10.1016/j.actaastro.2015.12.003.
18	J. Guo, J. Bouwmeester, E. Gill, From Single to Formation Flying CubeSats: An Update of the Delfi Programme, in: Proceedings of the 27th Annu. AIAA/USU Conference Small Satell., Logan, UT: SSC13–WK–Flight Results, 2013.
19	B.T.C. Zandbergen, A. Cervone, Cubesat Micro-Propulsion Systems for Extending the Capabilities of Academic Projects, in: Proceedings of the 65th International Astronaut. Congr., Toronto, Canada, 2C
20	S. Pottinger, D. Krejci, C. Scharlemann, Development of a µPPT for CubeSat Applications, in: Proceedings of the 44th AIAAASMESAEASEE Jt. Propuls.Conference Exhib., Hartford, CT, doi:10.2514/6.200
21	Lemmer, Kristina. "Propulsion for CubeSat." Elsevier 134.Acta Astronautica (2017): 231-43. Web.
22	Hudson, Jennifer, and Sara Spangelo. "Mission Analysis for CubeSats with Micropropulsion." Journal of Spacecraft and Rockets 53.5 (2016)Web.
23	Busek, BGT-X5 Green monopropellant Thruster, Datasheet. 16) 2016.(http://www.busek.com/index_htm_files/70008517 BGT-X5 Data Sheet RevD.pdf) (accessed16), 2016. 16.06.
24	R.K. Masse, C.B. Carpenter, D.T. Schmuland, J. Overly, M.Y. Allen, CubeSat HighimpulseAdaptable Modular Propulsion System (CHAMPS) Product LineDevelopment Status and Mission Applications, in:
25	Sheehan, J. P., Collard, T. A., Longmier, B. W., and Goglio, I. M., "New Low-Power Plasma Thruster for Nanosatellites," 50th AIAA/ASME/SAE/ASEE Joint Propulsion Conference, AIAA Paper 2014-3914
26	VACCO ChEMS Micro Propulsion Systems, in: Proceedings of the CubeSat Dev.Work., 2015 CubeSat Developers Workshop, San Louis Obsipo, CA, 2015
27	G. Maul, C. Coffman, S.D. La Lumondiere, I. Nicolette, D. Hinkley,Satellites, Logan, UT: SSC16–III–03, 2015.The NASA Optical Communications and Sensor Demonstration Program: InitialFlight Results, in: Proceedings of the 29th Annu. AIAA/USU Conference Small Satellites, Logan, UT: SSC16–III–03, 2015.
28	S. Janson, R. Welle, T. Rose, D. Rowen, B. Hardy, R. Dolphus, P. Doyle, A. Faler, D.Chien, A. Chin, G. Maul, C. Coffman, S.D. La Lumondiere, I. Nicolette, D. Hinkley,Chien, A. Chin, www.rocket.com/files/aerojet/documents/CubeSat/MPS-130%20data%20sheet%20crop.pdf
29	"MPS-130 Innovative Propulsion Solutions for SmallSats", MPS-130 Propulsion System, Aerojet Rocketdyne, www.rocket.com/cubesat/mp
30	Fowee, K., Pugia, S., Clay, R., Fuehne, M., Linker, M., Cofer, A., & Alexeenko, A. (n.d.). Quad-Thruster FEMTA Micropropulsion System for CubeSat 1 ... Retrieved October 6, 2017, from http://www.bing.com/cr?IG=0FDEA04A033940EC92453DAF6F7F3DCD&CID=13FD2BD584EE64A7109B20C685E865BB&rd=18h= hS4x56fjstoLa2cO3hqg0lly3n4DUqr1sYLI7gHI4Il&v=1&r=http%3a%2F%2fdigitalcommons.usu.edu%2fcgi%2fviewcontent.cgi%3farticle%3d3544%26context%3dsmallsat&p=DevEx,5040.1
31	"CubeSat High Impulse Propulsion System (CHIPS)", CHIPS Propulsion System, CUAerospace, www.cuaerospace.com/Portals/2/SiteContent/pdfs/datasheets/CHIPS/CHIPS-Brochure-170718.pdf?ver=2017-07-18-234056-717
32	"BmP-220 Micro Pulsed Plasma Thruster", BmP-220 Propulsion System, Busek, www.busek.com/index_htm_files/70008502F.pdf
33	"VACCO Reaction Control Propulsion System", VACCO, www.cubesat-propulsion.com/wp-content/uploads/2015/10/Reaction-control-propulsion-module.pdf

Appendix B: Telecommunication STK Generated Reports

1. NASA Near Earth Network Data Link Budget Report (Uplink)

Time (UTCG)	EIRP (dBW	Rcvd. Freq	Rcvd. Iso.	CubeSat-T	CubeSat-T	CubeSat-T	B	C/N	Eb/No	B
11/6/2017	-1	435.5051	-211.317	-137.081	20	37.28226	19.2	-5.5508	-2.5405	1.46E-01
11/6/2017	-1	435.5041	-210.86	-136.624	20	37.73946	19.2	-5.0935	-2.0832	1.33E-01
11/6/2017	-1	435.5029	-210.482	-136.247	20	38.11669	19.2	-4.7163	-1.706	1.23E-01
11/6/2017	-1	435.5016	-210.23	-135.994	20	38.36925	19.2	-4.4638	-1.4535	1.16E-01
11/6/2017	-1	435.5002	-210.127	-135.891	20	38.47249	19.2	-4.3605	-1.3502	1.13E-01
11/6/2017	-1	435.4988	-210.184	-135.948	20	38.4153	19.2	-4.4177	-1.4074	1.15E-01
11/6/2017	-1	435.4975	-210.395	-136.16	20	38.20374	19.2	-4.6293	-1.619	1.20E-01
11/6/2017	-1	435.4962	-210.74	-136.505	20	37.85905	19.2	-4.974	-1.9637	1.30E-01
11/6/2017	-1	435.4952	-211.188	-136.952	20	37.41124	19.2	-5.4218	-2.4115	1.42E-01
11/6/2017	-1	435.4951	-211.232	-136.996	20	37.36755	19.2	-5.4655	-2.4552	1.43E-01
11/6/2017	-1	435.5102	-211.274	-137.038	20	37.32525	19.2	-5.5078	-2.4975	1.44E-01
11/6/2017	-1	435.5101	-210.194	-135.958	20	38.40524	19.2	-4.4278	-1.4175	1.15E-01
11/6/2017	-1	435.51	-208.973	-134.737	20	39.62648	19.2	-3.2065	-0.1962	8.34E-02
11/6/2017	-1	435.5097	-207.577	-133.342	20	41.02197	19.2	-1.811	1.1993	5.22E-02
11/6/2017	-1	435.5094	-205.968	-131.732	20	42.63134	19.2	-0.2017	2.8086	2.53E-02
11/6/2017	-1	435.5086	-204.113	-129.877	20	44.48642	19.2	1.6534	4.6637	7.77E-03
11/6/2017	-1	435.5072	-202.054	-127.819	20	46.54487	19.2	3.7119	6.7222	1.08E-03
11/6/2017	-1	435.5043	-200.144	-125.908	20	48.45548	19.2	5.6225	8.6328	6.65E-05
11/6/2017	-1	435.4996	-199.371	-125.136	20	49.22787	19.2	6.3949	9.4052	1.48E-05
11/6/2017	-1	435.4951	-200.414	-126.178	20	48.1853	19.2	5.3523	8.3626	1.06E-04
11/6/2017	-1	435.4925	-202.4	-128.165	20	46.19906	19.2	3.366	6.3763	1.61E-03
11/6/2017	-1	435.4912	-204.438	-130.202	20	44.16142	19.2	1.3284	4.3387	9.89E-03
11/6/2017	-1	435.4906	-206.253	-132.018	20	42.34576	19.2	-0.4873	2.523	2.93E-02
11/6/2017	-1	435.4902	-207.826	-133.591	20	40.77272	19.2	-2.0603	0.95	5.73E-02
11/6/2017	-1	435.49	-209.192	-134.957	20	39.40695	19.2	-3.4261	-0.4158	8.88E-02
11/6/2017	-1	435.4899	-210.39	-136.154	20	38.20943	19.2	-4.6236	-1.6133	1.20E-01
11/6/2017	-1	435.4898	-211.032	-136.796	20	37.56743	19.2	-5.2656	-2.2553	1.38E-01
11/7/2017	-1	435.5077	-211.156	-136.921	20	37.44284	19.2	-5.3902	-2.3799	1.41E-01
11/7/2017	-1	435.507	-210.384	-136.149	20	38.21467	19.2	-4.6183	-1.608	1.20E-01
11/7/2017	-1	435.5061	-209.624	-135.388	20	38.97541	19.2	-3.8576	-0.8473	9.98E-02

2. NASA Space Network Data Link Budget Report (Downlink)

Time (UTCG)	EIRP (dBW)	Rcvd. Freq	Rcvd. Iso.	CubeSat-T	CubeSat-T	CubeSat-T	Bandwidth	C/N (dB)	Eb/No (dB	BER
5:01:41 PM	-1	435.5089	-238.978	-164.742	20	9.621316	19.2	-33.2117	-30.2014	4.83E-01
5:02:11 PM	-1	435.509	-238.941	-164.705	20	9.65829	19.2	-33.1747	-30.1644	4.82E-01
5:02:41 PM	-1	435.5091	-238.903	-164.668	20	9.695783	19.2	-33.1372	-30.1269	4.82E-01
5:03:11 PM	-1	435.5091	-238.865	-164.63	20	9.733744	19.2	-33.0993	-30.089	4.82E-01
5:03:41 PM	-1	435.5092	-238.827	-164.592	20	9.772139	19.2	-33.0609	-30.0506	4.82E-01
5:04:11 PM	-1	435.5092	-238.788	-164.553	20	9.810934	19.2	-33.0221	-30.0118	4.82E-01
5:04:41 PM	-1	435.5093	-238.749	-164.514	20	9.850091	19.2	-32.9829	-29.9726	4.82E-01
5:05:11 PM	-1	435.5093	-238.71	-164.474	20	9.889572	19.2	-32.9434	-29.9331	4.82E-01
5:05:41 PM	-1	435.5093	-238.67	-164.434	20	9.929338	19.2	-32.9037	-29.8934	4.82E-01
5:06:11 PM	-1	435.5093	-238.63	-164.394	20	9.969347	19.2	-32.8637	-29.8534	4.82E-01
5:06:41 PM	-1	435.5093	-238.59	-164.354	20	10.00956	19.2	-32.8235	-29.8132	4.82E-01
5:07:11 PM	-1	435.5093	-238.549	-164.314	20	10.04992	19.2	-32.7831	-29.7728	4.82E-01
5:07:41 PM	-1	435.5093	-238.509	-164.273	20	10.0904	19.2	-32.7426	-29.7323	4.82E-01
5:08:11 PM	-1	435.5093	-238.468	-164.233	20	10.13094	19.2	-32.7021	-29.6918	4.82E-01
5:08:41 PM	-1	435.5092	-238.428	-164.192	20	10.17149	19.2	-32.6615	-29.6512	4.81E-01
5:09:11 PM	-1	435.5091	-238.387	-164.152	20	10.212	19.2	-32.621	-29.6107	4.81E-01
5:09:41 PM	-1	435.5091	-238.347	-164.111	20	10.25243	19.2	-32.5806	-29.5703	4.81E-01
5:10:11 PM	-1	435.509	-238.306	-164.071	20	10.29271	19.2	-32.5403	-29.53	4.81E-01
5:10:41 PM	-1	435.5089	-238.266	-164.031	20	10.33279	19.2	-32.5002	-29.4899	4.81E-01
5:11:11 PM	-1	435.5088	-238.227	-163.991	20	10.37262	19.2	-32.4604	-29.4501	4.81E-01
5:11:41 PM	-1	435.5087	-238.187	-163.952	20	10.41214	19.2	-32.4209	-29.4106	4.81E-01
5:12:11 PM	-1	435.5086	-238.148	-163.912	20	10.45129	19.2	-32.3817	-29.3714	4.81E-01
5:12:41 PM	-1	435.5084	-238.109	-163.874	20	10.49001	19.2	-32.343	-29.3327	4.81E-01
5:13:11 PM	-1	435.5083	-238.071	-163.835	20	10.52824	19.2	-32.3048	-29.2945	4.81E-01
5:13:41 PM	-1	435.5081	-238.033	-163.798	20	10.56591	19.2	-32.2671	-29.2568	4.81E-01
5:14:11 PM	-1	435.5079	-237.996	-163.761	20	10.60297	19.2	-32.23	-29.2197	4.80E-01
5:14:41 PM	-1	435.5078	-237.96	-163.724	20	10.63936	19.2	-32.1937	-29.1834	4.80E-01
5:15:11 PM	-1	435.5076	-237.924	-163.689	20	10.675	19.2	-32.158	-29.1477	4.80E-01
5:15:41 PM	-1	435.5073	-237.889	-163.654	20	10.70984	19.2	-32.1232	-29.1129	4.80E-01
5:16:11 PM	-1	435.5071	-237.855	-163.62	20	10.7438	19.2	-32.0892	-29.0789	4.80E-01

3. NASA Space Network Access Report (Downlink)

Access	Start Time (UTCG)	Stop Time (UTCG)	Duration (sec)
1	11/6/2017	11/6/2017	3038.568
2	11/6/2017	11/6/2017	2994.347
3	11/6/2017	11/6/2017	2997.396
4	11/6/2017	11/6/2017	3047.966
5	11/6/2017	11/7/2017	3156.611
6	11/7/2017	11/7/2017	3268.415
7	11/7/2017	11/7/2017	3209.819
8	11/7/2017	11/7/2017	3082.166
9	11/7/2017	11/7/2017	3009.147
10	11/7/2017	11/7/2017	2988.686
11	11/7/2017	11/7/2017	3014.14
12	11/7/2017	11/7/2017	3095.561
13	11/7/2017	11/7/2017	3230.133
14	11/7/2017	11/7/2017	3261.669
15	11/7/2017	11/7/2017	3131.153
16	11/7/2017	11/7/2017	899.184
Access	Start Time (UTCG)	Stop Time (UTCG)	Duration (sec)
1	11/6/2017	11/6/2017	3050.234
2	11/6/2017	11/6/2017	3004.105
3	11/6/2017	11/6/2017	3002.447
4	11/6/2017	11/6/2017	3044.036
5	11/6/2017	11/7/2017	3133.992
6	11/7/2017	11/7/2017	3229.638
7	11/7/2017	11/7/2017	3198.213
8	11/7/2017	11/7/2017	3090.747
9	11/7/2017	11/7/2017	3019.524
10	11/7/2017	11/7/2017	2995.769
11	11/7/2017	11/7/2017	3014.887
12	11/7/2017	11/7/2017	3082.258
13	11/7/2017	11/7/2017	3190.875
14	11/7/2017	11/7/2017	3228.637
15	11/7/2017	11/7/2017	3132.951
16	11/7/2017	11/7/2017	817.955

4. NASA Near Earth Network Access Report (Uplink)

Access	Start Time (UTCG)	Stop Time (UTCG)	Duration (sec)
1	11/6/2017	11/6/2017	241.864
2	11/6/2017	11/6/2017	467.71
3	11/7/2017	11/7/2017	342.522
4	11/7/2017	11/7/2017	471.134
5	11/7/2017	11/7/2017	393.249

Access	Start Time (UTCG)	Stop Time (UTCG)	Duration (sec)
1	11/7/2017	11/7/2017	293.512
2	11/7/2017	11/7/2017	472.07
3	11/7/2017	11/7/2017	138.64
4	11/7/2017	11/7/2017	182.2
5	11/7/2017	11/7/2017	471.066
6	11/7/2017	11/7/2017	240.352

Access	Start Time (UTCG)	Stop Time (UTCG)	Duration (sec)
1	11/6/2017	11/6/2017	287.879
2	11/7/2017	11/7/2017	399.599
3	11/7/2017	11/7/2017	428.086
4	11/7/2017	11/7/2017	466.331

Access	Start Time (UTCG)	Stop Time (UTCG)	Duration (sec)
1	11/7/2017	11/7/2017	187.573
2	11/7/2017	11/7/2017	215.314

| Access	Start Time (UTCG)	Stop Time (UTCG)	Duration (sec)
1	11/6/2017	11/6/2017	451.822
2	11/6/2017	11/6/2017	150.799
3	11/7/2017	11/7/2017	451.579

Appendix C: Telecommunication Code

1. Downlink Data Link Budget MATLAB Code

2. Uplink Data Link Budget MATLAB Code

```
clc; clear all; close all;
% WPI eLEO CubeSat MQP 2018
% Telecomunication Subsytem Data Link Budget
% Space Network

load('SN_LB.mat');
[T1, I1] = sort(StartTimeUTCG); [T2, I2] = sort(StopTimeUTCG);
T1(1 : 3) = []; T1(end-20 : end) = [];
T2(1 : 3) = []; T2(end-20 : end) = [];
datarate = 3.4;
Td = T2 - T1;
Tds = seconds(Td);
Tdst = seconds(days(1));
Tdl = Tds*datarate;
Tdlt = Tdst*datarate;
plot(T1, Tdl, '--s', 'Color', [0.8500    0.3250    0.0980]);
title('Downlink Data Link Budget (Space Network)');
xlabel('Time UTCG');
ylabel('Total Data per Connection [Mb]');
legend('Total Data per Day = 293.76 Gb', 'Location', 'southwest');
 grid on;
```
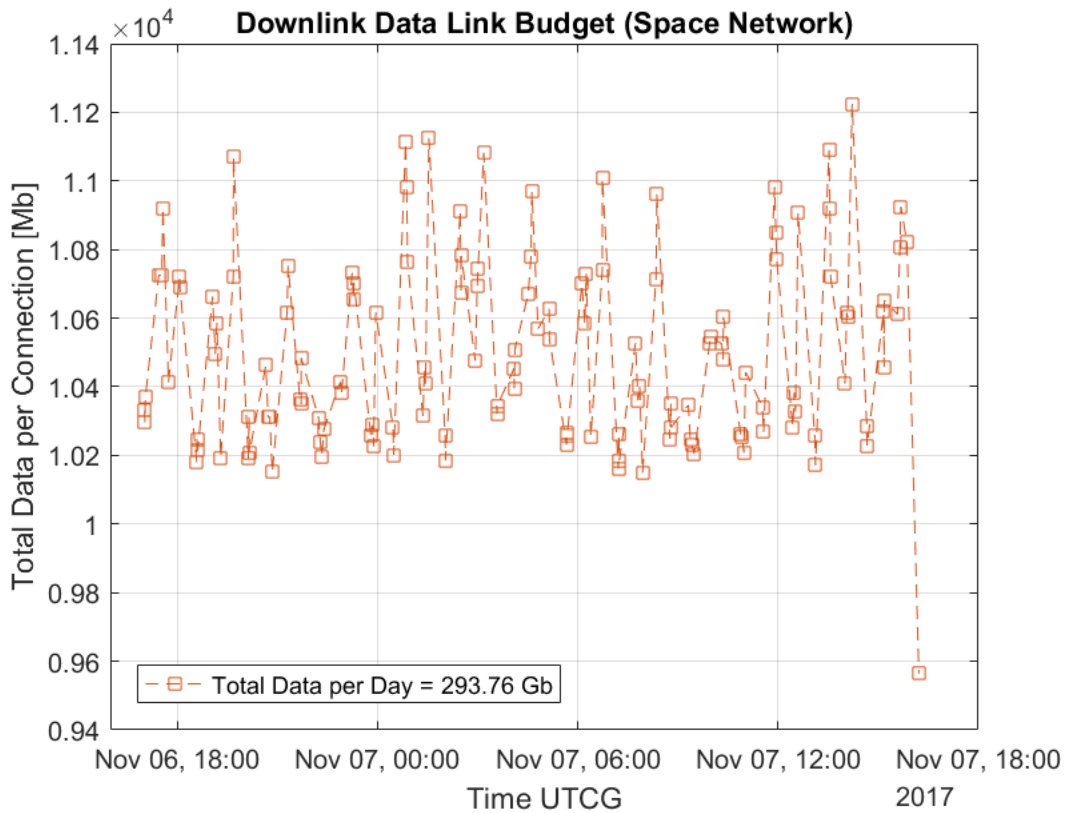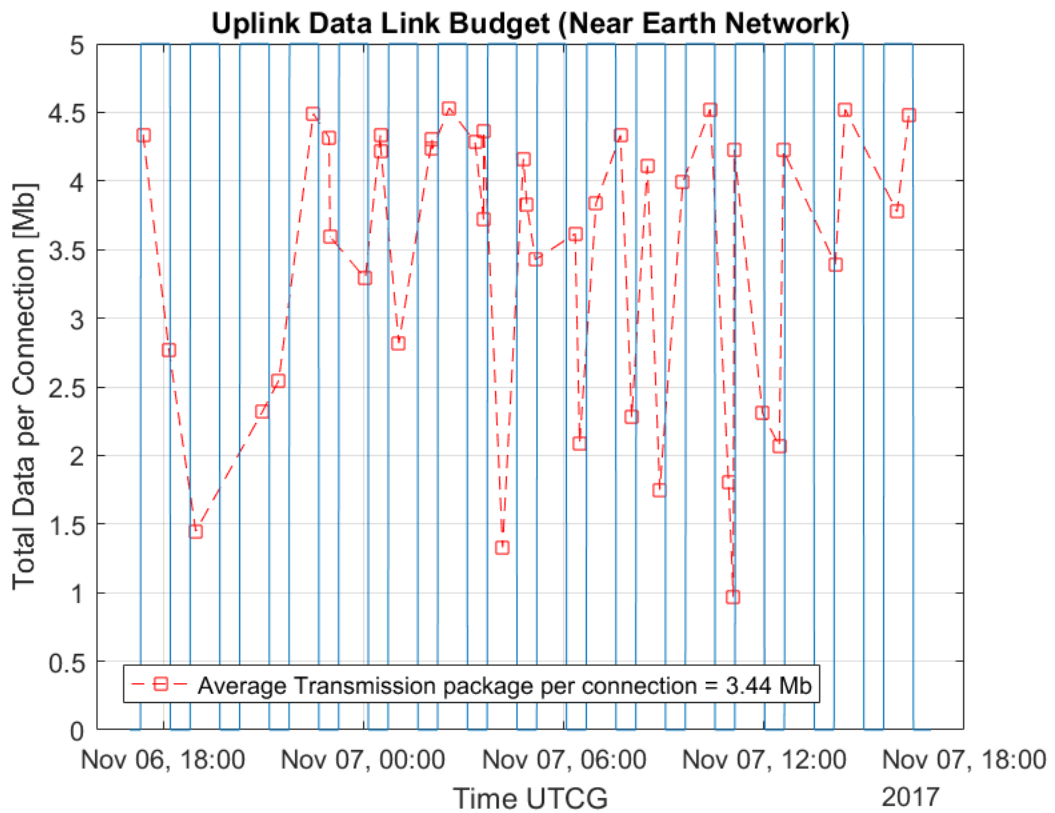
```matlab
clc; clear all; close all;
% WPI eLEO CubeSat MQP 2018
% Telecomunication Subsytem Data Link Budget
% Near Earth Network

load('Uplink_NEN.mat'); load('eLEO_Ilumination');
[T1, I1] = unique(StartTimeUTCG); [T2, I2] = unique(StopTimeUTCG);
Intensity = Intensity/20; datarate = 9.6/1000;
Td = T2 - T1;
Tds = seconds(Td);
Tdst = sum(Tds);
Tdl = Tds*datarate;
Tdlt = sum(Tdl);
plot(T1, Tdl, '--sr');
hold on;
plot(IluTime, Intensity);
title('Uplink Data Link Budget (Near Earth Network)');
xlabel('Time UTCG');
ylabel('Total Data per Connection [Mb]'); grid on;
legend('Average Transmission package per connection = 3.44
 Mb', 'Location', 'southwest')
```


Published with MATLAB® R2016b

Appendix D: eLEO Power Code

```matlab
clc; clear variables; close all;

%% Solar Panel Power Code eLeo

load ('Sun_Intensity_6.mat')
load ('Sun_Vector_Body_6.mat')
Gs = 1370; %Watts/m^2
eta = 0.25; % Solar Array Efficiency
RSE = 1.4831e+08; % km

if Time == TimeUTCG
    s = size(Time);
    t = 1 : s(1); % seconds
else
    disp('time arrays do not match');
end

gamma(t, :) = [sx sy sz]./RSE; %[unitless]
Psa = [1 1 1 1 1 1]; % Power Solar Face array
Psa_total = [0 0 0 ]; % Define Result Array
Psa_positive = [1 1 1 1 1 1]; % Define Positive Value array
Psa_face_sum = [0 0 0 ]; % Define Face sum array

An_u = [1 0 0; 0 1 0; 0 0 -1; 0 -1 0; 0 0 1 ; -1 0 0];
A = [000 161.17*(8/6) 161.17*(8/6) 161.17*(8/6) 161.17*(8/6) 000]'./10000;
An = An_u .* A;

for k = 1 : 1: s(1)

    for face = 1 : 6
        Psa(face) = eta*Gs*dot(gamma(k,:), An(face,:));

        if Psa(face) > 0
            Psa_positive(face) = Psa(face);
        else
            Psa_positive(face) = 0;
        end

    end

    Psa_face_sum(k) = sum(Psa_positive);

    Psa_total(k) = Psa_face_sum(k) * Intensity(k, :)/100;

end

Sum = 0;
kpositive = 0;
knegative = 0;
for k = 1:1:s(1)
```

D-2

```matlab
    if Psa_total(k) > 0
        Sum = Sum + Psa_total(k);
        kpositive = kpositive + 1;
        %k = k+1;
    else
        knegative = knegative + 1;
    end
end

Average = Sum/(k-knegative);
Average_Plot = [0 0 0];
for k = 1 : 1: s(1)
    if Psa_total(k) == 0
        Average_Plot(k) = 0;
    elseif Psa_total(k) >= 0
        Average_Plot(k) = Average;
    end
end

OBC = .35;
FineSunSensor = 0.35;
Gyro = 0.04;
GPS = 0.8;
EPS = 0.2; %always on
Transceiver = 0;
Transceiver_Time = 0; %seconds on
Thruster = 2;
PPTS = 0.5;
Magnetometer = 0.01;
Average_Consumption = [0 0 0];

for k = 1:1:s(1)

    if Psa_total(k) > 0
        Transceiver = 9;
        Transceiver_Time = Transceiver_Time + 1;
        if Transceiver_Time > 60
            Transceiver = 0;
        end
    elseif Psa_total(k) == 0
        Transceiver = 0;
        Transceiver_Time = 0;
    end

    Average_Consumption(k) = OBC + FineSunSensor + Gyro + GPS + EPS + Magnetometer +↙
Transceiver + Thruster;
end

    PSA = sum(Psa_total);
```

```matlab
Battery = [144000 0 0];
Power = [0 0 0];

%Battery_Total = [144000 0 0];
for k = 1:1:s(1)
   Power(k) = Psa_total(k) - Average_Consumption(k);
   if k == 1
    Battery(k) = Battery(1) + Power(k);
   else
    Battery(k) = Battery(k-1) + Power(k);
   end
   if Battery(k) > 144000
       Battery(k) = 144000;
   end

end

%Ploting Battery Capacity
plot(t, Battery/3600, 'LineWidth', 1.5);
title('Battery');
xlabel('Time [s]');
ylabel('Power [WattHours]');
grid on
grid minor


%Ploting Solar Panel Generation
figure
plot(t, Psa_total, t, Average_Consumption, 'LineWidth', 1.5);
title('Power Production vs. Time');
xlabel('Time [s]');
ylabel('Power [Watts]');
legend('Actual Solar Power', 'Power Consumption');
grid on
grid minor
```

Appendix E: Rendezvous Power Code

Table of Contents

CubeSat Power Subsystem Operation Rendezvous Mission

By Lucas Mancinelli, WPI 2018 Updated 2018/01/29

```
% The goal of the following code is to generate reports and run
% simulations of a nanosat in flight. This code models
% a 12 unit, 16 unit, and 20 unit CubeSat, with the potential to model
 any
% size CubeSat. This code focuses on the power
% generation and consumption aspects during detumble and routine
 flight.
% This code models the operational states of each component, the
 amount of
% power the solar arrays can generate, the amount of power consumed by
 each
% component, and the drain/recharge of the battery. The flight mission
 is
% generated from STK and allows the user to change the flight plan and
% still utilize this code.

% The components analyzed are the On-Board Computer (OBC), Electrical
 Power
% Subsystem (EPS), Solar Panels, Gyroscope, Magnetometers,
% Fine Sun Sensor, GPS, Radio/Transceiver, and PPT's.

% This program allows users to alter the states of components, as well
 as
% modify the code to fit any CubeSat specifications, following the
 format,
% as written.
```

Initializing

Clean work space to begin work

```
clc; clear variables; close all;
```

Power Code

Change the value of inclination in the load function to run the reports for different inclinations

```
load ('Sun_Intensity_Rendezvous_45_Inclination.mat')
load ('Sun_Vectors_Rendezvous_BodyFixed_45_Inclination.mat')
Gs = 1370; %Watts/m^2
eta = 0.3; % Solar Array Efficiency
RSE = 1.4831e+08; % [km]

s = size(TimeUTCG);
time_detumble = 1500; % Detumble Time
time_routine = 16200; % Time to run analysis in routine (use this to
 select number of orbits)
x = time_detumble + time_routine; % restricting parameter to select
 number of orbits
t = 1 : x; % [s]
```

STK Coordinate System -> Mechanical Design Coordinate System

This is used to translate the STK coordinate system to the coordinate system defined by the mechanical/structural design team.

```
sx = -STKy(1:x,:);
sy = -STKz(1:x,:);
sz = STKx(1:x,:);
```

Solar Panel Power

```
gamma(t, :) = [sx sy sz]; %[unitless]
Psa = [1 1 1 1 1 1]; % Power Solar Face array
Psa_total = [0 0 0 ]; % Define Result Array
Psa_positive = [1 1 1 1 1 1]; % Define Positive Value array
Psa_face_sum = [0 0 0 ]; % Define Face sum array

An_u = [0 0 1; 0 1 0; 1 0 0; 0 -1 0; -1 0 0 ; 0 0 -1];

% Note: In the below selection of CubeSat size, only one can be
 selected at
% a time. This can be modified for any size CubeSat. The 6 inital area
% definitions portray the coverage size of the solar arrays on each
 face of
% the CubeSat
```

```matlab
% 12U Solar Panel Coverage, Uncomment this to run a 12U report
%{
A_1s_12 = (3/4) * 400;
A_2s_12 = (3/6) * 600;
A_3s_12 = (3/6) * 600;
A_4s_12 = (3/6) * 600;
A_5s_12 = (3/6) * 600;
A_6s_12 = (3/4) * 400;
A = [A_1s_12 A_2s_12 A_3s_12 A_4s_12 A_5s_12 A_6s_12]'./10000;
%}

% 16U Solar Panel Coverage, Uncomment this to run a 16U report
%{
A_1s_16 = (3/4) * 400;
A_2s_16 = (5/8) * 800;
A_3s_16 = (5/8) * 800;
A_4s_16 = (5/8) * 800;
A_5s_16 = (5/8) * 800;
A_6s_16 = (5/8) * 400;
A = [A_1s_16 A_2s_16 A_3s_16 A_4s_16 A_5s_16 A_6s_16]'./10000;
%}

% 20U Solar Panel Coverage, Uncomment this to run a 20U report
%
A_1s_20 = (3/4) * 400;
A_2s_20 = (7/10) * 1000;
A_3s_20 = (7/10) * 1000;
A_4s_20 = (7/10) * 1000;
A_5s_20 = (7/10) * 1000;
A_6s_20 = (3/4) * 400;
A = [A_1s_20 A_2s_20 A_3s_20 A_4s_20 A_5s_20 A_6s_20]'./10000;
%}

An = An_u .* A;

for k = time_detumble : 1: x

    for face = 1 : 6
        Psa(face) = eta*Gs*dot(gamma(k,:), An(face,:));

        if Psa(face) > 0
            Psa_positive(face) = Psa(face);

        else
            Psa_positive(face) = 0;
        end

    end

    Psa_face_sum(k) = sum(Psa_positive);


    Psa_total(k) = Psa_face_sum(k) * Intensity(k, :)/100;
```

```
    end

PSA = sum(Psa_total);
```

Average Consumption Values

```
Avg_Consumption_In_Sun = mean(nonzeros(Psa_total));
Avg_Consumption_Total = mean(Psa_total);

Avg_Cons(time_detumble:x,1) = Avg_Consumption_Total;
Avg_Sun(time_detumble:x,1) = Avg_Consumption_In_Sun;
```

Definitions

```
numPoints = x;
tspan = 0:1:x;
total_time = x; % s
```

State & Power Initialization

Initializing Subsystem State Vectors

```
OBC_state = zeros(1,numPoints);
EPS_state = zeros(1,numPoints);
Radio_state = zeros(1,numPoints);

% Initializing Sensor State Vectors
Gyro_state = zeros(1,numPoints);
Magnetometer_state = zeros(1,numPoints);
FineSS_state = zeros(1,numPoints);
GPS_state = zeros(1,numPoints);

% Initializing Propulsion Vectors
Thruster_state = zeros(1,numPoints);
PPT_state = zeros(1,numPoints);

% Initializing Power Vectors
OBC_pwr_accum = zeros(1,numPoints);
EPS_pwr_accum = zeros(1,numPoints);
SolarPanel_pwr_accum = zeros(1,numPoints);
Gyro_pwr_accum = zeros(1,numPoints);
Magnetometer_pwr_accum = zeros(1,numPoints);
GPS_pwr_accum = zeros(1,numPoints);
FineSS_pwr_accum = zeros(1,numPoints);
Radio_pwr_accum = zeros(1,numPoints);
Thruster_pwr_accum = zeros(1,numPoints);
PPT_pwr_accum = zeros(1,numPoints);
```

System Operations

Create vectors which represent the ON/OFF state of a system, where entries are 0 when OFF and 1 when ON.

```matlab
%
% Radio State
% 45 Degree Orbit
Radio_state(5520:6070) = 1;
Radio_state(6840:7355) = 1;
Radio_state(11220:11740) = 1;
Radio_state(12520:13035) = 1;


% OBC State
% Turns on at Deployment, stays on until Deactivation
OBC_state(1:x) = 1;

% EPS State
% Turns on at Deployment, stays on until Deactivation
EPS_state(1:x) = 1;

% Gyro State
% On for Detumble and Routine
Gyro_state(1:x) = 1;


% Main Thruster
% Assumed constantly on during Routine
Thruster_state(time_detumble:x) = 1;

% PPT
% Two Slew Maneuvers per orbit, 5 minutes

% Detumble with PPT
PPT_state(1:time_detumble) = 1;

% Routine
PPT_state(4200:4500) = 1;
PPT_state(5000:5300) = 1;
PPT_state(9500:9800) = 1;
PPT_state(10500:10800) = 1;
PPT_state(16500:16800) = 1;


% Fine Sun Sensor State
% On for Sun Acquisition, only on for Routine when in Sun, on for
 Detumble
for m = 1:x
    if (Intensity(m) > 0)
        FineSS_state(m) = 1;
    else
        FineSS_state(m) = 0;
    end
end

% Magnetometer State
% On for Detumble, Sun Acquisition, and Routine, on for detumble
for m = 1:x
```

```matlab
    if (Intensity(m) > 0)
        Magnetometer_state(m) = 1;
    else
        Magnetometer_state(m) = 0;
    end
end


% GPS State
% On for Sun Acquisition and Routine
for m = time_detumble:x
    if (Intensity(m) > 0)
        GPS_state(m) = 1;
    else
        GPS_state(m) = 0;
    end
end

states_Mtx = [OBC_state; EPS_state; Radio_state; Thruster_state;
              PPT_state; Gyro_state; Magnetometer_state;
              GPS_state; FineSS_state];
```

Constant Power

Create vectors for power and current draw at each time interval in W and A

```matlab
% OBC Power
current = 150; % milliAmps
OBC_curr = current*OBC_state;
size = 1; % Watts
OBC_pwr = size*OBC_state;

% EPS Power
current = 24; % milliAmps
EPS_curr = current*EPS_state;
size = 0.202; % Watts
EPS_pwr = size*EPS_state;

% Radio Power
current = 600; % milliAmps
Radio_curr = current*Radio_state;
size = 4.848; % Watts
Radio_pwr = size*Radio_state;

% Solar Panel Power
SolarPanel_pwr = Psa_total;

% Gyro Power
current = 8; % milliAmps
Gyro_curr = current*Gyro_state;
size = 0.043; % Watts
Gyro_pwr = size*Gyro_state;
```

```matlab
% Magnetometer Power
size = 0.00033;% Watts
Magnetometer_pwr = size*Magnetometer_state;

% GPS Power
current = 160; % milliAmps
GPS_curr = current*GPS_state;
size = 0.860;
GPS_pwr = size*GPS_state;

% FineSS Power
current = 10; % milliAmps
FineSS_curr = current*FineSS_state;
size = 0.054;
FineSS_pwr = size*FineSS_state;

% Thruster Power
size = 13.6; % Watts
Thruster_pwr = size*Thruster_state;

% PPT Power
size = 5.25; % Watts
PPT_pwr = size*PPT_state;

% Maximum Power
Const_max = 20*ones(1,numPoints);

% Constant Subtotal

Const_pwr_Sum =  OBC_pwr + EPS_pwr + Radio_pwr + Thruster_pwr +...
                 PPT_pwr + Gyro_pwr + Magnetometer_pwr +...
                 GPS_pwr + FineSS_pwr;

Const_pwr_Mtx = [OBC_pwr; EPS_pwr; Radio_pwr; Thruster_pwr;...
                 PPT_pwr; Gyro_pwr; Magnetometer_pwr;...
                 GPS_pwr; FineSS_pwr];
```

Battery Characteristics

```matlab
Batt_cap = 40; % Watt-hours
DoD = 0.2; % Depth of Discharge (percent)
Batt_discharge_max = Batt_cap * DoD;
Batt_min_charge = Batt_cap - Batt_discharge_max;
Curr_max = 2400; % MilliAmps

% Track battery level over time, not exceeding the total battery
 capacity
Batt_charge = zeros(1, numPoints);
Batt_charge(1) = Batt_cap;
time_read = 1; % seconds b/w "readings"
N = 1;
for i = 2:N:numPoints
    consumption = Const_pwr_Sum(i)*N./3600;
```

```matlab
        Batt_charge(i:i+N) = Batt_charge(i-1) - consumption;

        % generation = Psa_total(i)/3600

        if Batt_charge(i) + Psa_total(i)/3600 >= Batt_cap
            Batt_charge(i:i+N) = Batt_cap;
        else
            Batt_charge(i:i+N) = Batt_charge(i) + Psa_total(i)/3600;
        end
    end
Batt_charge = Batt_charge(1:numPoints);
```

Accumulating Power

Create vectors for total power consumption

```matlab
% Tracks total power usage of each component (W-hr)
% Solar panel production tracked as "negative" power consumption

N = 1;
% OBC Power
for i = 2:1:numPoints
    size = OBC_pwr(i)*N./3600; % power consumed at each time step
    OBC_pwr_accum(i:i+N) = OBC_pwr_accum(i-1) + size;
end
OBC_pwr_accum = OBC_pwr_accum(1:numPoints);

% EPS Power
for i = 2:1:numPoints
    size = EPS_pwr(i)*N./3600; % power consumed at each time step
    EPS_pwr_accum(i:i+N) = EPS_pwr_accum(i-1) + size;
end
EPS_pwr_accum = EPS_pwr_accum(1:numPoints);

% Radio Power
for i = 2:1:numPoints
    size = Radio_pwr(i)*N./3600; % power consumed at each time step
    Radio_pwr_accum(i:i+N) = Radio_pwr_accum(i-1) + size;
end
Radio_pwr_accum = Radio_pwr_accum(1:numPoints);

% Gyro Power
for i = 2:1:numPoints
    size = Gyro_pwr(i)*N./3600; % power consumed at each time step
    Gyro_pwr_accum(i:i+N) = Gyro_pwr_accum(i-1) + size;
end
Gyro_pwr_accum = Gyro_pwr_accum(1:numPoints);

% Magnetometer Power
for i = 2:1:numPoints
    size = Magnetometer_pwr(i)*N./3600; % power consumed at each time
 step
```

```matlab
        Magnetometer_pwr_accum(i:i+N) = Magnetometer_pwr_accum(i-1) +
 size;
end
Magnetometer_pwr_accum = Magnetometer_pwr_accum(1:numPoints);

% GPS Power
for i = 2:1:numPoints
    size = GPS_pwr(i)*N./3600; % power consumed at each time step
    GPS_pwr_accum(i:i+N) = GPS_pwr_accum(i-1) + size;
end
GPS_pwr_accum = GPS_pwr_accum(1:numPoints);

% Fine Sun Sensor Power
for i = 2:1:numPoints
    size = FineSS_pwr(i)*N./3600; % power consumed at each time step
    FineSS_pwr_accum(i:i+N) = FineSS_pwr_accum(i-1) + size;
end
FineSS_pwr_accum = FineSS_pwr_accum(1:numPoints);

% Thruster Power
for i = 2:1:numPoints
    size = Thruster_pwr(i)*N./3600; % power consumed at each time step
    Thruster_pwr_accum(i:i+N) = Thruster_pwr_accum(i-1) + size;
end
Thruster_pwr_accum = Thruster_pwr_accum(1:numPoints);

% PPT Power
for i = 2:1:numPoints
    size = PPT_pwr(i)*N./3600; % power consumed at each time step
    PPT_pwr_accum(i:i+N) = PPT_pwr_accum(i-1) + size;
end
PPT_pwr_accum = PPT_pwr_accum(1:numPoints);

% Solar Panel Power
for i = 2:1:numPoints
    size = Psa_total(i)*N./3600; % power produced at each time step
    SolarPanel_pwr_accum(i:i+N) = SolarPanel_pwr_accum(i-1) + size;
end
SolarPanel_pwr_accum = SolarPanel_pwr_accum(1:numPoints);


% Maximum Available
Accum_max = Batt_discharge_max*ones(1,numPoints);

Batt_charge_max = Batt_cap*ones(1,numPoints);

Batt_charge_min = Batt_min_charge*ones(1,numPoints);

% Accumulating Subtotal
Accum_pwr_Sum = OBC_pwr_accum + EPS_pwr_accum + Radio_pwr_accum +
 Thruster_pwr_accum +...
                PPT_pwr_accum + Gyro_pwr_accum +
 Magnetometer_pwr_accum +...
                GPS_pwr_accum + FineSS_pwr_accum;
```

```
Accum_pwr_Mtx = [OBC_pwr_accum; EPS_pwr_accum; Radio_pwr_accum;
 Thruster_pwr_accum;...
                 PPT_pwr_accum; Gyro_pwr_accum;
 Magnetometer_pwr_accum;...
                 GPS_pwr_accum; FineSS_pwr_accum];
```

Plot

```
% Subsystem & Sensor States: Live Plot
%{
figure
set(gcf, 'Position', get(0,'Screensize'));
speed = 400;
% If you add/delete subsystems change these numbers to change the
 amount
% of subplots.
rows = 3;
columns = 3;

% ** Remember these names must be in the same order as the Subsystems
 are
%    listed in the corresponding Matrix for results to be significant!
names = {'OBC State';'EPS State';'Radio State';'Thruster State';
    'PPT State';'Gyro State';'Magnetometer State';'GPS State';
    'Fine Sun Sensor State'};

for u = linspace(1,numPoints/speed-1,numPoints/speed-1)
    for i = linspace(1,rows*columns,rows*columns)
        % Plot
        thisplot = states_Mtx(i,:);
        subplot(rows,columns,i)
        plot(tspan(1:floor(speed*u)),thisplot(1:floor(speed*u)),
 'LineWidth', 2)

        % Timeline Delineators
        if u*speed >= 0
            line([0 0], [-1 2],'Color','r')
            text(0,-0.4,' \rightarrow Detumble')
        end
        if u*speed >= time_detumble
            line([time_detumble time_detumble], [-1 2],'Color','r')
            text(time_detumble,-0.8,' \rightarrow Routine')
        end

        % Label
        axis([0,total_time,-1,2])
        xlabel('Time (s)')
        ylabel('State')
        words = {'OFF'; ' ON'};
        set(gca,'YTick',0:1,'YTickLabel',words)
        title(names(i))
        grid on
```

```matlab
        end

        % Make a GIF
        frame = getframe(1);
        im = frame2im(frame);
        [imind,cm] = rgb2ind(im,256);
        outfile = 'results_states_live.gif';
        if u==1
            imwrite(imind,cm,outfile,'gif','DelayTime',0,'loopcount',inf);
        else

  imwrite(imind,cm,outfile,'gif','DelayTime',0,'writemode','append');
        end

        % Delay
        %{
        pause(.5E-100)
        %}

    end
%}

% Subsystem & Sensor States: Instant Plot
%{
figure
set(gcf, 'Position', get(0,'Screensize'));
speed = 400;
% If you add/delete subsystems change these numbers to change the
 amount
% of subplots.
rows = 3;
columns = 3;

% ** Remember these names must be in the same order as the Subsystems
 are
%    listed in the corresponding Matrix for results to be significant!
names = {'OBC State';'EPS State'; 'Radio State';'Thruster State';
    'PPT State'; 'Gyro State'; 'Magnetometer State';'GPS State';
    'Fine Sun Sensor State'};


for i = linspace(1,rows*columns,rows*columns)
    % Plot
    thisplot = states_Mtx(i,:);
    subplot(rows,columns,i)
    plot(tspan(1:x),thisplot, 'LineWidth', 2)

    % Timeline Delineators
    text(0,-0.2,' \rightarrow Detumble')

    line([time_detumble time_detumble], [-1 2],'Color','r')
    text(time_detumble,-0.4,' \rightarrow Routine')

    % Label
```

```
        axis([0,total_time,-1,2])
        xlabel('Time (s)')
        ylabel('State')
        words = {'OFF'; ' ON'};
        set(gca,'YTick',0:1,'YTickLabel',words)
        title(names(i))
        grid on

    end

    % Save Image
    hgexport(gcf,'results_states_inst.png',hgexport('factorystyle'),'Format','png');

    %}
```

Power Plots

```
    % Constant/Individual/Live Plot
    %{
    figure
    set(gcf, 'Position', get(0,'Screensize'));
    speed = 400;
    % If you add/delete subsystems change these numbers to change the
     amount
    % of subplots.
    rows = 3;
    columns = 3;

    % ** Remember these names must be in the same order as the Subsystems
     are
    %     listed in the corresponding Matrix for results to be significant!
    names = {'OBC Power';'EPS Power';'Radio Power';'Thruster Power';'PPT
     Power';'Gyro Power';'Magnetometer Power';'GPS Power';'Fine Sun Sensor
     Power'};

    for u = linspace(1,numPoints/speed-1,numPoints/speed-1)
        top = max(max(Const_pwr_Mtx));
        bottom = min(min(Const_pwr_Mtx));
        for i = linspace(1,rows*columns,rows*columns)
            % Plot
            thisplot = Const_pwr_Mtx(i,:);
            subplot(rows,columns,i)
            plot(tspan(1:floor(speed*u)),thisplot(1:floor(speed*u)),
     'LineWidth', 2)

            % Timeline Delineators
            text(0,0.9*top,' \rightarrow Detumble')
            if u*speed >= 0
                line([time_detumble time_detumble], [1.1*bottom
     1.1*top],'Color','r')
                text(time_detumble,0.75*top,' \rightarrow Routine')
            end
```

```matlab
        % Label
        axis([0,total_time,1.1*bottom,1.1*top])
        xlabel('Time (s)')
        ylabel('Power (Watts)')
        title(names(i));
        grid on
    end

    % Make a GIF
    frame = getframe(1);
    im = frame2im(frame);
    [imind,cm] = rgb2ind(im,256);
    outfile = 'results_const_indiv_live.gif';
    if u==1
        imwrite(imind,cm,outfile,'gif','DelayTime',0,'loopcount',inf);
    else

  imwrite(imind,cm,outfile,'gif','DelayTime',0,'writemode','append');
    end

    % Delay
    %{
    pause(.5E-100)
    %}

end
%}

% Constant/Individual/Instant Plot
%{
figure
set(gcf, 'Position', get(0,'Screensize'));
speed = 400;
% If you add/delete subsystems change these numbers to change the
 amount
% of subplots.
rows = 3;
columns = 3;

% ** Remember these names must be in the same order as the Subsystems
 are
%    listed in the corresponding Matrix for results to be significant!
names = {'OBC Power';'EPS Power';'Radio Power';'Thruster Power';
        'PPT Power';'Gyro Power';'Magnetometer Power';'GPS Power';
        'Fine Sun Sensor Power'};

for i = linspace(1,rows*columns,rows*columns)
    % Plot
    thisplot = Const_pwr_Mtx(i,:);
    top = max(thisplot);
    bottom = 0;
    subplot(rows,columns,i)
    plot(tspan(1:x),thisplot, 'LineWidth', 2)
```

```matlab
    % Timeline Delineators
    text(0,0.9*top,' \rightarrow Detumble')

    line([time_detumble time_detumble], [1.1*bottom
 1.1*top],'Color','r')
    text(time_detumble,0.75*top,' \rightarrow Routine')

    % Label
    axis([0,total_time,1.1*bottom,1.1*top])
    xlabel('Time (s)')
    ylabel('Power (W)')
    title(names(i));
    grid on
end

% Save Image
hgexport(gcf,'results_const_indiv_inst.png',hgexport('factorystyle'),'Format','png

%}

% Constant/Sum/Live Plot
%{
figure
set(gcf, 'Position', get(0,'Screensize'));
speed = 400;

for u = linspace(1,numPoints/speed-1,numPoints/speed-1)
    % Plot Sum of Constant Power and Max Available

 plot(tspan(1:floor(speed*u)),Const_pwr_Sum(1:floor(speed*u)),tspan(1:x),SolarPane
k','LineWidth', 2)

    % Time Delineators
    top = max([SolarPanel_pwr,Const_pwr_Sum]);
    bottom = min([SolarPanel_pwr,Const_pwr_Sum]);

    text(0,0.9*top,' \rightarrow Detumble')
    if u*speed >= time_detumble
        line([time_detumble time_detumble], [1.1*bottom
 1.1*top],'Color','r')
        text(time_detumble,0.75*top,' \rightarrow Routine')
    end

    % Label
    axis([0,total_time,1.1*bottom,1.1*top])
    xlabel('Time (s)')
    ylabel('Power (Watts)')
    title('Sum of Constant Power')
    legend('Sum of Constant Power', 'Maximum Available Constant
 Power')
    grid on

    % Make a GIF
    frame = getframe(1);
```

```matlab
        im = frame2im(frame);
        [imind,cm] = rgb2ind(im,256);
        outfile = 'results_const_sum_live.gif';
        if u==1
            imwrite(imind,cm,outfile,'gif','DelayTime',0,'loopcount',inf);
        else

  imwrite(imind,cm,outfile,'gif','DelayTime',0,'writemode','append');
        end

        % Delay
        %{
        pause(.5E-100)
        %}

    end

    %}

    % Constant/Sum/Instant Plot
    %{
    figure
    set(gcf, 'Position', get(0,'Screensize'));
    speed = 400;

    % Plot Sum of Constant Power and Max Available
    plot(tspan(1:x),Const_pwr_Sum,tspan(1:x),SolarPanel_pwr,'k--','LineWidth',
     2)
    title('Sum of Constant Power')

    % Add Timeline Delineators
    top = max(SolarPanel_pwr);
    bottom = 0;

    text(0,0.9*top,' \rightarrow Detumble')

    line([time_detumble time_detumble], [1.1*bottom 1.1*top],'Color','r')
    text(time_detumble,0.75*top,' \rightarrow Routine')

    % Label
    axis([0,total_time,1.1*bottom,1.1*top])
    xlabel('Time (s)')
    ylabel('Power (W)')
    legend('Sum of Instantaneous Power Consumption','Solar Panel Power
     Production')
    grid on

    % Save Image
    hgexport(gcf,'results_const_sum_inst.png',hgexport('factorystyle'),'Format','png')

    %}

    % Accumulating/Individual/Live Plot
    %{
```

```matlab
figure
set(gcf, 'Position', get(0,'Screensize'));
speed = 400;
% If you add/delete subsystems change these numbers to change the
 amount
% of subplots.
rows = 3;
columns = 3;

% ** Remember these names must be in the same order as the Subsystems
 are
%     listed in the corresponding Matrix for results to be significant!
names = {'OBC Power';'EPS Power';'Radio Power';'Thruster Power';'PPT
 Power';...
         'Gyro Power';'Magnetometer Power';'GPS Power';'Fine Sun Sensor
 Power'};

for u = linspace(1,numPoints/speed-1,numPoints/speed-1)
    top = max(max(Accum_pwr_Mtx));
    bottom = min(min(Accum_pwr_Mtx));
    for i = linspace(1,rows*columns,rows*columns)
        % Plot
        thisplot = Accum_pwr_Mtx(i,:);
        subplot(rows,columns,i)
        plot(tspan(1:floor(speed*u)),thisplot(1:floor(speed*u)),
 'LineWidth', 2)

        % Time Delineators
        text(0,0.9*top,' \rightarrow Detumble')
        if u*speed >= time_detumble
            line([time_detumble time_detumble], [1.1*bottom
1.1*top],'Color','r')
            text(time_detumble,0.75*top,' \rightarrow Routine')
        end

        % Label
        axis([0,total_time,1.1*bottom,1.1*top])
        xlabel('Time (s)')
        ylabel('Power (W-hr)')
        title(names(i));
        grid on
    end

    % Make a GIF
    frame = getframe(1);
    im = frame2im(frame);
    [imind,cm] = rgb2ind(im,256);
    outfile = 'results_accum_indiv_live.gif';
    if u==1
        imwrite(imind,cm,outfile,'gif','DelayTime',0,'loopcount',inf);
    else

 imwrite(imind,cm,outfile,'gif','DelayTime',0,'writemode','append');
    end
```

```matlab
    % Delay
    %{
    pause(.5E-100)
    %}

end
%}

% Accumulating/Individual/Instant Plot
%{
figure
set(gcf, 'Position', get(0,'Screensize'));
speed = 400;
% If you add/delete subsystems change these numbers to change the
 amount
% of subplots.
rows = 3;
columns = 3;

% ** Remember these names must be in the same order as the Subsystems
 are
%    listed in the corresponding Matrix for results to be significant!
names = {'OBC Total Power';'EPS Total Power';'Radio Total
 Power';'Thruster Total Power';...
        'PPT Total Power';'Gyro Total Power';'Magnetometer Total
 Power';...
        'GPS Total Power';'Fine Sun Sensor Total Power'};


for i = linspace(1,rows*columns,rows*columns)
    % Plot
    thisplot = Accum_pwr_Mtx(i,:);
    top = max(max(thisplot));
    bottom = 0;
    subplot(rows,columns,i)
    plot(tspan(1:x),thisplot, 'LineWidth', 2)

    % Timeline Delineators

    text(0,0.9*top,' \rightarrow Detumble')

    line([time_detumble time_detumble], [1.1*bottom
 1.1*top],'Color','r')
    text(time_detumble,0.75*top,' \rightarrow Routine')

    % Label
    axis([0,total_time,1.1*bottom,1.1*top])
    xlabel('Time (s)')
    ylabel('Power (W-hr)')
    title(names(i));
    grid on
end
```

```matlab
% Save Image
hgexport(gcf,'results_accum_indiv_inst.png',hgexport('factorystyle'),'Format','png

%}

% Accumulating/Sum/Live Plot
%{
figure
set(gcf, 'Position', get(0,'Screensize'));
speed = 400;

for u = linspace(1,numPoints/speed-1,numPoints/speed-1)
    % Plot Sum of Accumulating Power and Max Available

 plot(tspan(1:floor(speed*u)),Accum_pwr_Sum(1:floor(speed*u)),tspan(1:x),Accum_max
k','LineWidth', 2)

    top = max(Accum_pwr_Sum);
    bottom = min(Accum_pwr_Sum);

    % Add Timeline Delineators
    if u*speed >= 0
        line([0 0], [1.1*bottom 1.1*top],'Color','r')
        text(0,0.75*top,' \rightarrow Detumble')
    end
    if u*speed >= time_detumble
        line([time_detumble time_detumble], [1.1*bottom
 1.1*top],'Color','r')
        text(time_detumble,0.60*top,' \rightarrow Routine')
    end

    % Label
    axis([0,total_time,1.1*bottom,1.1*top])
    xlabel('Time (s)')
    ylabel('Power (W-hr)')
    title('Sum of Accumulating Power')
    legend('Sum of Accumulating Power', 'Maximum Available
 Accumulating Power')
    grid on

    % Make a GIF
    frame = getframe(1);
    im = frame2im(frame);
    [imind,cm] = rgb2ind(im,256);
    outfile = 'results_accum_sum_live.gif';
    if u==1
        imwrite(imind,cm,outfile,'gif','DelayTime',0,'loopcount',inf);
    else

 imwrite(imind,cm,outfile,'gif','DelayTime',0,'writemode','append');
    end

    % Delay
    %{
```

```
        pause(.5E-100)
        %}

    end

%}

% Accumulating/Sum/Instant Plot
%{
figure
set(gcf, 'Position', get(0,'Screensize'));
speed = 400;

% Plot Sum of Accumulating Power and Max Available
plot(tspan(1:x),Accum_pwr_Sum,'LineWidth', 2)

% Timeline Delineators
top = max(max([Accum_pwr_Sum; Accum_max]));
bottom = 0;

text(0,0.9*top,' \rightarrow Detumble')

line([time_detumble time_detumble], [1.1*bottom 1.1*top],'Color','r')
text(time_detumble,0.75*top,' \rightarrow Routine')

% Label
axis([0,total_time,1.1*bottom,1.1*top])
xlabel('Time (s)')
ylabel('Power (W-hr)')
grid on
legend('Sum of Total Power Usage')
title('Sum of Total Power Usage')

% Save Image
hgexport(gcf,'results_accum_sum_inst.png',hgexport('factorystyle'),'Format','png')

%}

% Solar Panel Output
%{
figure
set(gcf, 'Position', get(0,'Screensize'));
speed = 400;

% Plot Sum of Accumulating Power and Max Available
plot(tspan(1:x),SolarPanel_pwr,'LineWidth', 2)

% Timeline Delineators
top = max(SolarPanel_pwr);
%bottom = min(min([Batt_charge]));
bottom = 0;

% Timeline Delineators
text(0,0.9*top,' \rightarrow Detumble')
```

```matlab
line([time_detumble time_detumble], [1.1*bottom 1.1*top],'Color','r')
text(time_detumble,0.75*top,' \rightarrow Routine')

% Label
axis([0,total_time,1.1*bottom,1.1*top])
xlabel('Time (s)')
ylabel('Total Power (W-hr)')
grid on
title('Solar Power Production')

% Save Image
hgexport(gcf,'results_accum_solar_inst.png',hgexport('factorystyle'),'Format','png

%}

% Battery Charge Plot
%{
figure
set(gcf, 'Position', get(0,'Screensize'));
speed = 400;

% Plot Sum of Accumulating Power and Max Available
plot(tspan(1:x),Batt_charge,tspan(1:x),Batt_charge_max,'--
k',tspan(1:x),Batt_charge_min,'--r','LineWidth', 2)

% Timeline Delineators
top = max(max([Batt_charge; Batt_charge_max]));
%bottom = min(min([Batt_charge]));
bottom = 25;

% Timeline Delineators
text(0,0.9*top,' \rightarrow Detumble')

line([time_detumble time_detumble], [1.1*bottom 1.1*top],'Color','r')
text(time_detumble,0.75*top,' \rightarrow Routine')

% Label
axis([0,total_time,1.1*bottom,1.1*top])
xlabel('Time (s)')
ylabel('Battery Charge (W-hr)')
grid on
legend('Total Battery Charge', 'Maximum Battery Capacity', 'Minimum
 Allowable Discharge Level')
title('Battery Charge')

% Save Image
hgexport(gcf,'results_batt_charge_inst.png',hgexport('factorystyle'),'Format','png

%}
```

Published with MATLAB® R2016b

Appendix F: eLEO Propulsion Code

```matlab
clc; close all; clear all;
%% Maneuver Calculations
mu = 3.986*10^14;  %m^3/s^2
M = 4.56437; %kg
Fs = 1367; %W/m^2
Md = 7.96*10^15; %T*m^3
l  = 0.4; %m
w  = 0.1; %m
d  = 0.1; %m
Ix = (1/12)*M*(l^2 + w^2); %kg*m^2
Iy = (1/12)*M*(l^2+ d^2); %kg*m^2
Iz = (1/12)*M*(w^2 + d^2); %kg*m^2
qr = 1; %unitless
As = 0.09; %m^2
i = 0; %rad
Ac = 0.0001; %A*m^2/kg
D = Ac*M; %A*m^2
rho = 2.3*10^-10; %kg/m^3
h = 210000; %m
r = 6.371*10^6 + h; %m
c = 2.997*10^8; %m/s
beta = 30*pi/180; %rad
% Ibit = 0.56*10^-6; %N*s
s = 0.2; %m
n = 1; %unitless
dtheta = 180*pi/180; %rad

%% Disturbance Torque Calculations ~~
%%%%% Variables %%%%%
A = 0.0120747; %m^2
Cd = 3; %unitless
cp_cg = 0.010292; %m

%%%%% Equations %%%%%
% Velocity
v = sqrt(mu/r); %m/s
% Aerodynamic Drag Torque
T_D = 1/2*rho*A*Cd*v^2*cp_cg;
% Gravity Gradient Torque
T_G = 3*mu/(2*r^3)*abs(Iz-Iy)*sin(2*beta);
% Solar Radiation
T_SR = Fs/c*As*cos(i)*(1+qr)*cp_cg;
% Magnetic Field Torque
T_M = D*2*Md/r^3;
% Total Torque on CubeSat
Ttot = T_D;
% Max Moment of Inertia
I = max([Ix Iy Iz]); %kg*m^2
% Duration of Maneuver in Seconds
deltat = (0:0.1:1500).*60;
deltat_RWA = linspace(0,16,10201); %slew maneuver max allowable time is 16.24secs
```

F-2

```matlab
% Duration of Maneuver in Minutes
T = deltat/60;
T_RWA = deltat_RWA; %in secs
T_RWA2 = linspace(0,31,15001); %for 0% idle 16 secs
T_RWA2c = linspace(0,31,15001); %for 90% idle

%% Slew Maneuvers and Detumble for uPPT
% Slew: 0% Idle
Hdot_slew_0 = 4*I*dtheta./((1+0^2).*deltat.^2);
% Slew: 90% Idle
Hdot_slew_90 = 4*I*dtheta./((1+0.9^2).*deltat.^2);
% Detumble at omega=5
Hdot_st_5 = I*5./deltat*pi/180;
% Detumble at omega=10
Hdot_st_10 = I*10./deltat*pi/180;
% Detumble at omega=20
Hdot_st_20 = I*20./deltat*pi/180;

%% Slew Maneuvers and Detumble for RWA
M_RWA = 4.50932; %kg
Ix_RWA = 1/12*M*(l^2 + w^2); %kg*m^2
Iy_RWA = 1/12*M*(l^2+ d^2); %kg*m^2
Iz_RWA = 1/12*M*(w^2 + d^2); %kg*m^2
% Max Moment of Inertia
I_RWA = max([Ix_RWA Iy_RWA Iz_RWA]); %kg*m^2

% Slew: 0% Idle
Hdot_slew_0_RWA = 4*I_RWA*dtheta./((1+0^2).*T_RWA2.^2);
% Slew: 90% Idle
Hdot_slew_90_RWA = 4*I_RWA*dtheta./((1+0.9^2).*T_RWA2.^2);
% Detumble at omega=5
Hdot_st_5_RWA = I_RWA*5./T_RWA2*pi/180;
% Detumble at omega=10
Hdot_st_10_RWA = I_RWA*10./T_RWA2*pi/180;
% Detumble at omega=20
Hdot_st_20_RWA = I_RWA*20./T_RWA2*pi/180;

% RWA Power
h_RWA = 0.015; %Nms Instantaneous Angular Momentum of Blue Canyon RWP015
RWA_slew_power_0      = (1000*Hdot_slew_0_RWA) + (4.51*(h_RWA^0.47));
RWA_slew_power_90     = (1000*Hdot_slew_90_RWA) + (4.51*(h_RWA^0.47));

RWA_detumble_power_5  = (1000*Hdot_st_5_RWA) + (4.51*(h_RWA^0.47));
RWA_detumble_power_10 = (1000*Hdot_st_10_RWA) + (4.51*(h_RWA^0.47));
RWA_detumble_power_20 = (1000*Hdot_st_20_RWA) + (4.51*(h_RWA^0.47));

%% Sizing
% Freq
fp = 0.01:0.01:1; % was 1-12, now 0.01-1
% Discharge
Ed = 2;
```

F-3

```matlab
% Min Impulse Bit
Ibit = 70; %For Dawgstar PPT microNewtons
% Impulse Bit Sizing
Ibit_S = (0:0.1:200)*10^-6;
% Power
P0 = Ed*fp;
% Pulse Freq
fp_10 = 10*10^-6./(Ibit_S.*n*s);
fp_20 = 20*10^-6./(Ibit_S.*n*s);
fp_30 = 30*10^-6./(Ibit_S.*n*s);
fp_40 = 40*10^-6./(Ibit_S.*n*s);
fp_50 = 50*10^-6./(Ibit_S.*n*s);

% Mission time in Seconds
duration = 31*24*3600;
% Period of the orbit
T_orbit = 2*pi*sqrt((6.678*10^6)^3/(3.986*10^14));
% number of orbit
n_orbits = duration/T_orbit;
% Total impulse
Impulse_total = Ttot/s*duration + 2*n_orbits*4*dtheta*I/s/(7*60) + 9*10^-6/s*7*60 % N*s

%% Reaction Wheels and Magnetorquers
% RWP015 reaction wheel
% ISIS iMTQ Magnetorquer Board

%%%% Variables %%%%
% Magnetic Field of Earth
B_Earth = 2.5*10^-5; % kg/A*s^2
% Magnetic Dipole
mu_torquers = 0.2; % A*m^2
% RWP-015 Momentum Capability
momentum = 0.015; %Nms
%Using the Blue Canyon RWP015 MicroWheel

RW_power = linspace(0,5.5,15001);

RW_torque = (.004/5.5).*RW_power; %%0.004 Nm max torque

%%%% Equations %%%%
% Magnetorquer Torque
T_mag = B_Earth*mu_torquers;
% # of Desaturations Required for Mission
Desat_number = (Ttot*duration)/momentum;
% Desaturation Time
Desat_time = duration/(Desat_number*3600*24); % days

%% Figures
figure(1)
plot(T,Hdot_slew_0*10^6,'b-'); hold on
plot(T,Hdot_slew_90*10^6,'r-');
```

```matlab
hold off
grid on
title('Angular Momentum Rate Versus Duration for Slew Maneuvers')
legend('Slew, 90% Idle','Slew, 0% Idle')
xlabel('delta t (mins)')
ylabel('Angular Momentum Rate (uN m s/s)')
axis([0 25 0 20]);

figure(2)
plot(T,Hdot_st_5*10^6,'r--'); hold on
plot(T,Hdot_st_10*10^6,'b--')
plot(T,Hdot_st_20*10^6,'g--')
hold off
grid on
grid minor
title('Angular Momentum Rate Versus Duration for Despin Maneuvers')
xlabel('delta t (mins)')
ylabel('Angular Momentum Rate (uN  m s/s)')
axis([0 95 0 150]);
legend('Despin, omega = 5 deg/s','Despin, omega = 10 deg/s','Despin, omega = 20 deg/s')

figure(3)
plot(T,Ttot.*ones(size(T))*10^6,'k-.')
legend('Total Disturbance Torques')
title('Angular Momentum Rate Versus Duration for Disturbance torques')
xlabel('delta t (mins)')
ylabel('Angular Momentum Rate (uN m s/s)')
grid on
axis([0 25 0 3]);

figure(4)
semilogy(Ibit_S*10^6,fp_10,'k-'); hold on
semilogy(Ibit_S*10^6,fp_20,'k--')
semilogy(Ibit_S*10^6,fp_30,'k-.')
semilogy(Ibit_S*10^6,fp_40,'k:')
semilogy(Ibit_S*10^6,fp_50,'k-')
hold off
grid on
% legend('Total Disturbance Torques')
title('Pulse Frequency vs. Impulse Bit')
ylabel('Pulse Frequency (Hz)')
xlabel('Impulse Bit (uN s)')
axis([0 200 0 10]);
legend('10 uN m s/s','20 uN m s/s','30 uN m s/s','40 uN m s/s','50 uN m s/s')

% Energy per Discharge
e_bit = 5; % J

figure(5)
plot(Ibit_S*10^6,fp_10*e_bit,'k-'); hold on
plot(Ibit_S*10^6,fp_20*e_bit,'k--')
```

```matlab
plot(Ibit_S*10^6,fp_30*e_bit,'k-.')
plot(Ibit_S*10^6,fp_40*e_bit,'k:')
plot(Ibit_S*10^6,fp_50*e_bit,'k-')
hold off
grid on
title('Power Draw vs. Impulse Bit')
ylabel('Power (Watts)')
xlabel('Impulse Bit (uN s)')
axis([0 100 1 100]);
legend('10 uN m s/s','20 uN m s/s','30 uN m s/s','40 uN m s/s','50 uN m s/s')

%% uPPT Dawgstar Power DATA
H_dot                = 0:1:300;
Ibit_PPT             = 70; %uPPT
f_p                  = H_dot./(Ibit_PPT.*s);
fp_slew_0            = Hdot_slew_0./(Ibit_PPT*10^-6*s);
fp_slew_90           = Hdot_slew_90./(Ibit_PPT*10^-6*s);
PPT_slew_power_0     = fp_slew_0.*Ed;
PPT_slew_power_90    = fp_slew_90.*Ed;
fp_st_5              = Hdot_st_5./(Ibit_PPT*10^-6*s);
fp_st_10             = Hdot_st_10./(Ibit_PPT*10^-6*s);
fp_st_20             = Hdot_st_20./(Ibit_PPT*10^-6*s);
PPT_detumble_power_5  = fp_st_5.*Ed;
PPT_detumble_power_10 = fp_st_10.*Ed;
PPT_detumble_power_20 = fp_st_20.*Ed;

% RWA Power Data
%%%%% Figure %%%%%
figure(7)
plot3(T,Hdot_slew_0*10^6,PPT_slew_power_0,'-hb')
xlabel('time (min)')
ylabel('H dot N m s/s')
zlabel('Power (watts)')
axis([0 25 0 20 0 10])
grid on
grid minor
title('Power for a Slew Maneuver for a Given Time or Torque, uPPT')

%%Combined Power vs Time and Torque slew maneuver for uPPT
figure(8)
yyaxis left
plot(PPT_slew_power_0,T,'-'); hold on
plot(PPT_slew_power_90,T,'--')
hold off
grid on
grid minor
title('\mu PPT Power for a slew maneuver for a Given Time or Torque')
xlabel('Power [W]')
ylabel('Time [min]') %% Change this to seconds
axis([0 12.5 0 25]);
r = Hdot_slew_0;
```

```matlab
yyaxis right
plot(PPT_slew_power_90,r)
ylabel('Torque [Nm]')
legend('90% Idle','0% Idle','Torque')

% RWA Slew maneuver
figure(9)
yyaxis left
plot(RWA_slew_power_0,T_RWA2,'-'); hold on
plot(RWA_slew_power_90,T_RWA2c,'--')
grid on
grid minor
title('Power for a slew maneuver for a Given Time or Torque RWA')
xlabel('Power [W]')
ylabel('Time [s]')
axis([0 5.5 0 31]);
yyaxis right
%plot(RWA_slew_power_90,Hdot_slew_0_RWA*10^6)
plot(RW_power,RW_torque)
ylabel('Torque [Nm]')
legend('90% Idle','0% Idle','Torque')
%axis([0 5.5 0 0.01]);

figure(10)
plot3(T,Hdot_st_20*10^6,PPT_detumble_power_20,'-pr')
xlabel('time (min)')
ylabel('H dot N m s/s')
zlabel('Power (watts)')
axis([90 190 0 25 0 5])
grid on
grid minor
title('Power for a Despin Stabilization for a Given Time or Torque, uPPT')

%%New combined graph Despin Power vs Time & H dot for uPPT
figure(11)
yyaxis left
plot(PPT_detumble_power_5,T,'-'); hold on
plot(PPT_detumble_power_10,T,'--')
plot(PPT_detumble_power_20,T,':')
grid on
grid minor
hold off
title('\mu PPT Power for a Despin Stabilization for a Given Time or Torque')
xlabel('Power [W]')
ylabel('Time [min]')
axis([0 5 0 190]);
yyaxis right
plot(PPT_detumble_power_5,Hdot_st_5*10^6);
ylabel('Torque [Nm]')
legend('\omega = 5 deg/s','\omega = 10 deg/s','\omega = 20 deg/s','Torque')
```

```matlab
% RWA Despin Maneuver
figure(12)
yyaxis left
plot(RWA_detumble_power_5,T_RWA2,'-'); hold on
plot(RWA_detumble_power_10,T_RWA2,'--')
plot(RWA_detumble_power_20,T_RWA2,':')
grid on
grid minor
title('RWA Power for a Despin Stabilization for a Given Time or Torque')
xlabel('Power [W]')
ylabel('Time [s]')
axis([0 5.5 0 30]);
yyaxis right
plot(RW_power,RW_torque);
ylabel('Torque [Nms/s]')
legend('\omega = 5 deg/s','\omega = 10 deg/s','\omega = 20 deg/s','Torque')
```

Appendix G: Rendezvous Propulsion Code

Contents

```
clc; close all;
```

Maneuver Calculations

```
mu     = 3.986*10^14;            %m^3/s^2
M      = 16;                     %kg
Fs     = 1367;                   %W/m^2
Md     = 7.96*10^15;             %T*m^3
l      = 0.4;                    %m
w      = 0.2;                    %m
d      = 0.2;                    %m
Ix     = 1/12*M*(l^2 + w^2);     %kg*m^2
Iy     = 1/12*M*(l^2+ d^2);      %kg*m^2
Iz     = 1/12*M*(w^2 + d^2);     %kg*m^2
qr     = 1;                      %unitless
As     = 0.16;                   %m^2
i      = 0;                      %rad
Ac     = 0.001;                  %A*m^2/kg
D      = Ac*M;                   %A*m^2
rho    = 9.93*10^-13;            %kg/m^3, found from https://www.spaceacademy.net.au/watch/deb
ris/atmosmod.htm
h      = 500000;                 %m
r      = 6.371*10^6 + h;         %m
c      = 2.997*10^8;             %m/s
beta   = 30*pi/180;              %rad
s      = 0.2;                    %m
n      = 2;                      %unitless
dtheta = 180*pi/180;             %rad
```

Disturbance Torque Calculations ~~~~~~~~~~~~~~~~~~~~~~~~~~~~~~~~~~~~~

```
%%%%% Variables %%%%%
rho   = 9.93*10^-13;      %kg/m^3, found from https://www.spaceacademy.net.au/watch/debris/atmo
smod.htm
A     = 0.24;             %m^2
Cd    = 3;                %unitless
cp_cg = 0.05;             %m
```

G-2

```
%%%%% Equations %%%%%
% Velocity
v    = sqrt(mu/r); %m/s
% Aerodynamic Drag Torque
T_D  = 1/2*rho*A*Cd*v^2*cp_cg
% Gravity Gradient Torque
T_G  = 3*mu/(2*r^3)*abs(Iz-Iy)*sin(2*beta)
% Solar Radiation
T_SR = Fs/c*As*cos(i)*(1+qr)*cp_cg
% Magnetic Field Torque
T_M  = D*2*Md/r^3
% Total Torque on CubeSat
Ttot = T_D + T_G + T_SR + T_M
% Max Moment of Inertia
I    = max([Ix Iy Iz]); %kg*m^2
```

```
T_D =

   1.0369e-06


T_G =

    2.554e-07


T_SR =

    7.298e-08


T_M =

   7.8524e-07


Ttot =

   2.1505e-06
```

Slew Maneuvers and Detumble

Duration of Maneuver in Seconds

```
deltat       = (0:0.1:1500).*60;
% Duration of Maneuver in Minutes
T            = deltat/60;
% Slew: 0% Idle
Hdot_slew_0  = 4*I*dtheta./((1+0^2).*deltat.^2);
% Slew: 90% Idle
Hdot_slew_90 = 4*I*dtheta./((1+0.9^2).*deltat.^2);
% Detumble at omega=5
```

```
Hdot_st_5    = I*5./deltat*pi/180;
% Detumble at omega=10
Hdot_st_10   = I*10./deltat*pi/180;
% Detumble at omega=20
Hdot_st_20   = I*20./deltat*pi/180;
```

Sizing

```
% Freq
fp      = 0.01:0.0001:1.51000; % was 1-12, now 0.01-19
% Discharge
Ed      = 2;
% Min Impulse Bit
Ibit    = 40; %40 for PPTCUP
% Impulse Bit Sizing
Ibit_S = (0:0.1:200)*10^-6;
% Power
P0      = Ed*fp;
% Pulse Freq
fp_10   = 10*10^-6./(Ibit_S.*n*s);
fp_20   = 20*10^-6./(Ibit_S.*n*s);
fp_30   = 30*10^-6./(Ibit_S.*n*s);
fp_40   = 40*10^-6./(Ibit_S.*n*s);
fp_50   = 50*10^-6./(Ibit_S.*n*s);

% Mission time in Seconds
duration = 31*24*3600;
% Period of the orbit
T_orbit  = 2*pi*sqrt((6.678*10^6)^3/(3.986*10^14));
% number of orbit
n_orbits = duration/T_orbit;
% Total impulse
Impulse_total = Ttot/s*duration + 2*n_orbits*4*dtheta*I/s/(7*60) + 9*10^-6/s*7*60 % N*s
```

```
Impulse_total =

      68.167
```

Reaction Wheels and Magnetorquers

RWP100 reaction wheel ISIS iMTQ Magnetorquer Board

```
%%%%% Variables %%%%%
% Magnetic Field of Earth
B_Earth = 2.5*10^-5; % kg/A*s^2
% Magnetic Dipole
mu_torquers = 0.2; % A*m^2
% RWP-100 Momentum Capability
momentum = 0.1;

%%%%% Equations %%%%%
```

```matlab
% Magnetorquer Torque
T_mag = B_Earth*mu_torquers;
% # of Desaturations Required for Mission
Desat_number = Ttot*duration/momentum;
% Desaturation Time
Desat_time = duration/Desat_number/(3600*24); % days
```

Figures

```matlab
figure(1)
plot(T,Hdot_slew_0*10^6,'-'); hold on
plot(T,Hdot_slew_90*10^6,'--');
hold off
grid on
title('Angular Momentum Rate Versus Duration for Slew Maneuvers')
legend('Slew, 90% Idle','Slew, 0% Idle')
xlabel('delta t (Minutes)')
ylabel('Torque (uNms/s)')
axis([0 25 0 20]);

figure(2)
plot(T,Hdot_st_5*10^6,'-'); hold on
plot(T,Hdot_st_10*10^6,'--')
plot(T,Hdot_st_20*10^6,'-.')
hold off
grid on
grid minor
title('Angular Momentum Rate Versus Duration for Despin Maneuvers')
xlabel('delta t (minutes)')
ylabel('Torque (uNms/s)')
axis([0 95 0 150]);
legend('Despin, omega = 5 deg/s','Despin, omega = 10 deg/s','Despin, omega = 20 deg/s')

figure(3)
y = [T_SR 0 0 0; 0 T_G 0 0; 0 0 T_M 0; 0 0 0 T_D; T_SR T_G T_M T_D]*10^6
z = bar(y,'stacked')
ylabel('Torque uNms/s')
xlabel('Disturbance Torques')
title('Disturbance Torques')
grid on
legend('Solar Pressure Torque','Gravity Gradient Torque','Magnetic Torque','Atmospheric Drag
Torque','Total Disturbance Torques')
grid minor

figure(4)
semilogy(Ibit_S*10^6,fp_10,'k-'); hold on
semilogy(Ibit_S*10^6,fp_20,'k--')
semilogy(Ibit_S*10^6,fp_30,'k-.')
semilogy(Ibit_S*10^6,fp_40,'k:')
semilogy(Ibit_S*10^6,fp_50,'k-')
hold off
grid on
legend('Total Disturbance Torques')
title('Pulse Frequency vs. Impulse Bit')
ylabel('Pulse Frequency (Hz)')
xlabel('Impulse Bit (uN s)')
```

```matlab
axis([0 200 0 10]);
legend('10 uN m s/s','20 uN m s/s','30 uN m s/s','40 uN m s/s','50 uN m s/s')

% Energy per Discharge
e_bit = 5; % J

figure(5)
plot(Ibit_S*10^6,fp_10*e_bit,'k-'); hold on
plot(Ibit_S*10^6,fp_20*e_bit,'k--')
plot(Ibit_S*10^6,fp_30*e_bit,'k-.')
plot(Ibit_S*10^6,fp_40*e_bit,'k:')
plot(Ibit_S*10^6,fp_50*e_bit,'k-')
hold off
grid on
title('Power Draw vs. Impulse Bit')
ylabel('Power (Watts)')
xlabel('Impulse Bit (uN s)')
axis([0 100 1 100]);
legend('10 uN m s/s','20 uN m s/s','30 uN m s/s','40 uN m s/s','50 uN m s/s')

figure(6)
plot(fp,P0,'k-'); hold on
hold off
grid on
title('Power Draw vs. Frequency')
ylabel('Power (Watts)')
xlabel('Frequency (Hz)')
```

```
y =

     0.07298            0            0            0
           0       0.2554            0            0
           0            0      0.78524            0
           0            0            0       1.0369
     0.07298       0.2554      0.78524       1.0369


z =

  1×4 Bar array:

    Bar    Bar    Bar    Bar

Warning: Ignoring extra legend entries.
```
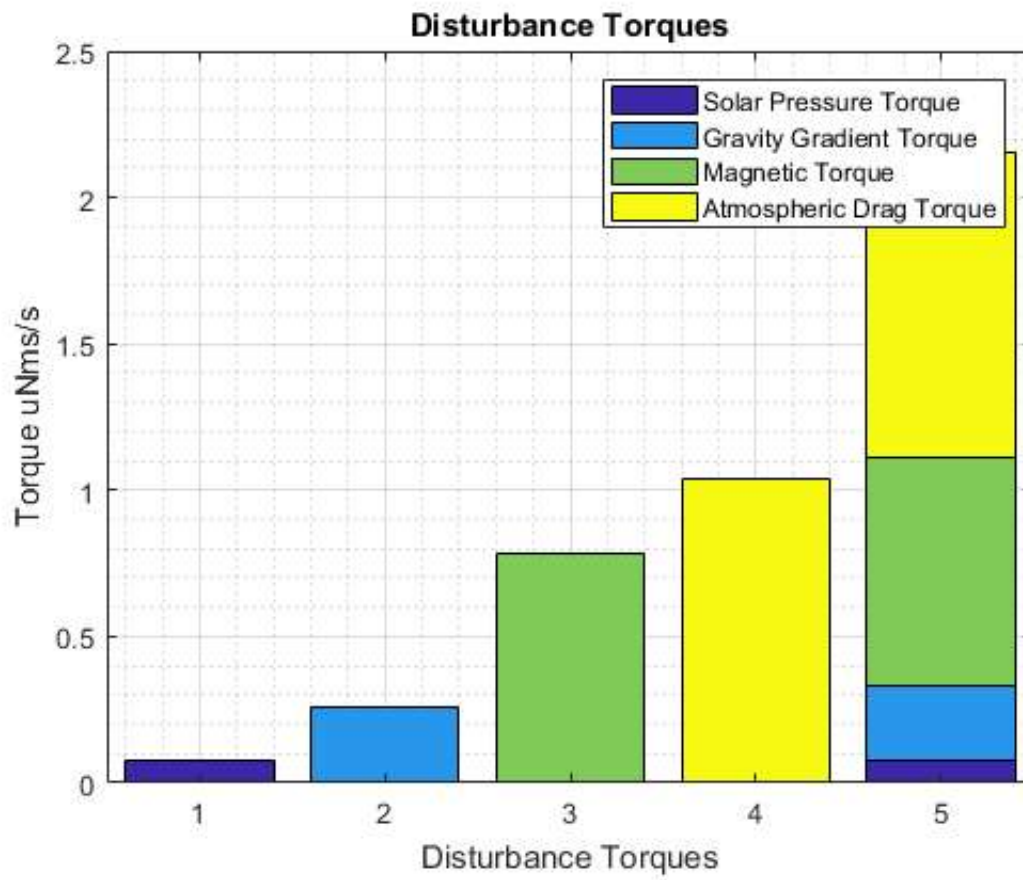
Angular Momentum Rate Versus Duration for Slew Maneuvers

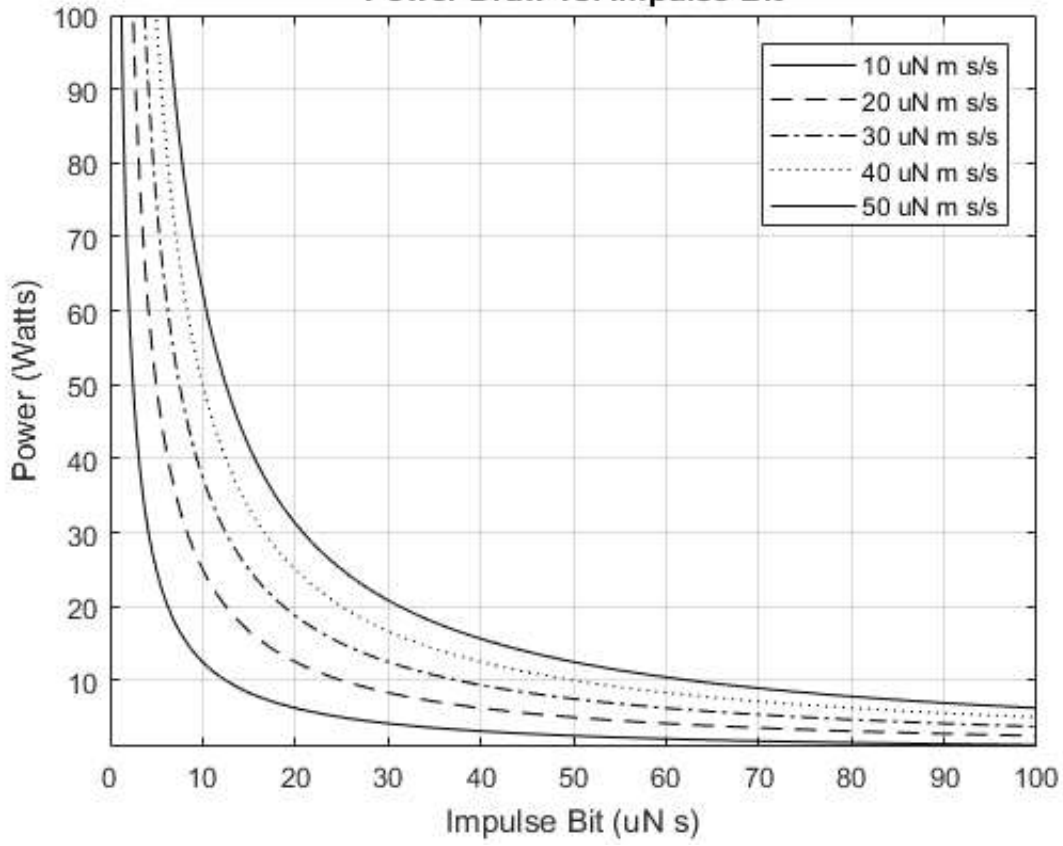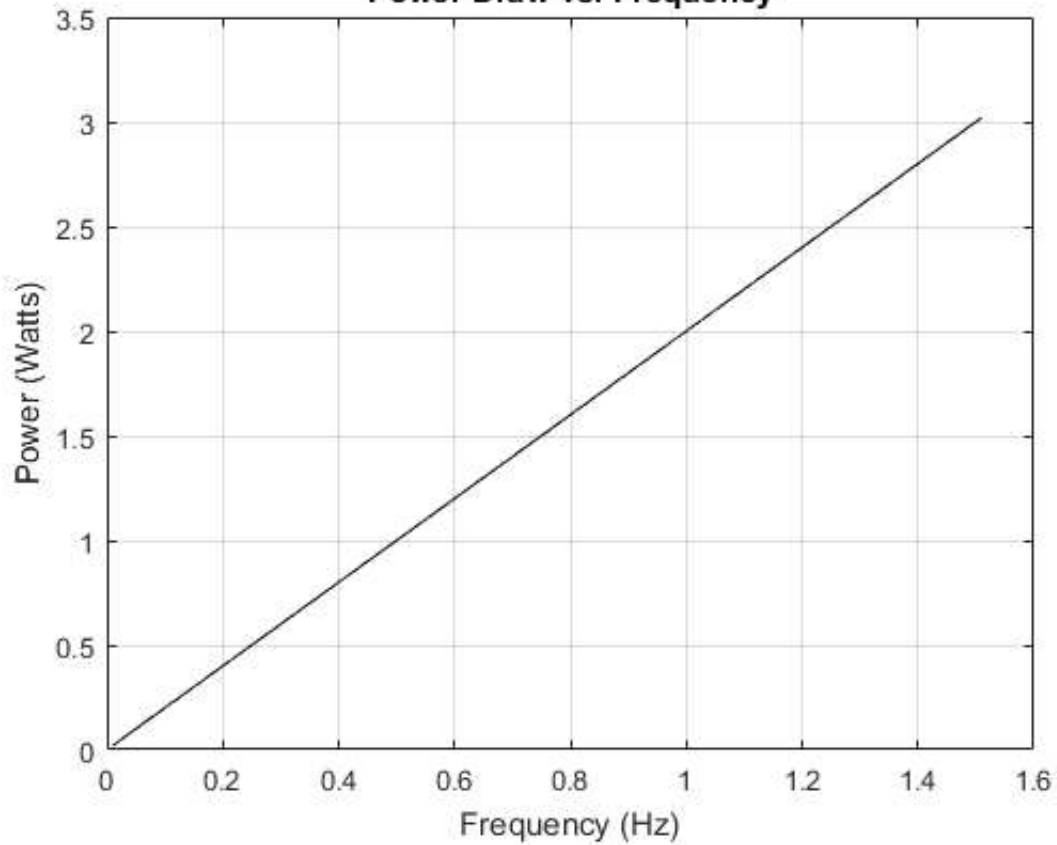Angular Momentum Rate Versus Duration for Despin Maneuvers

Disturbance Torques
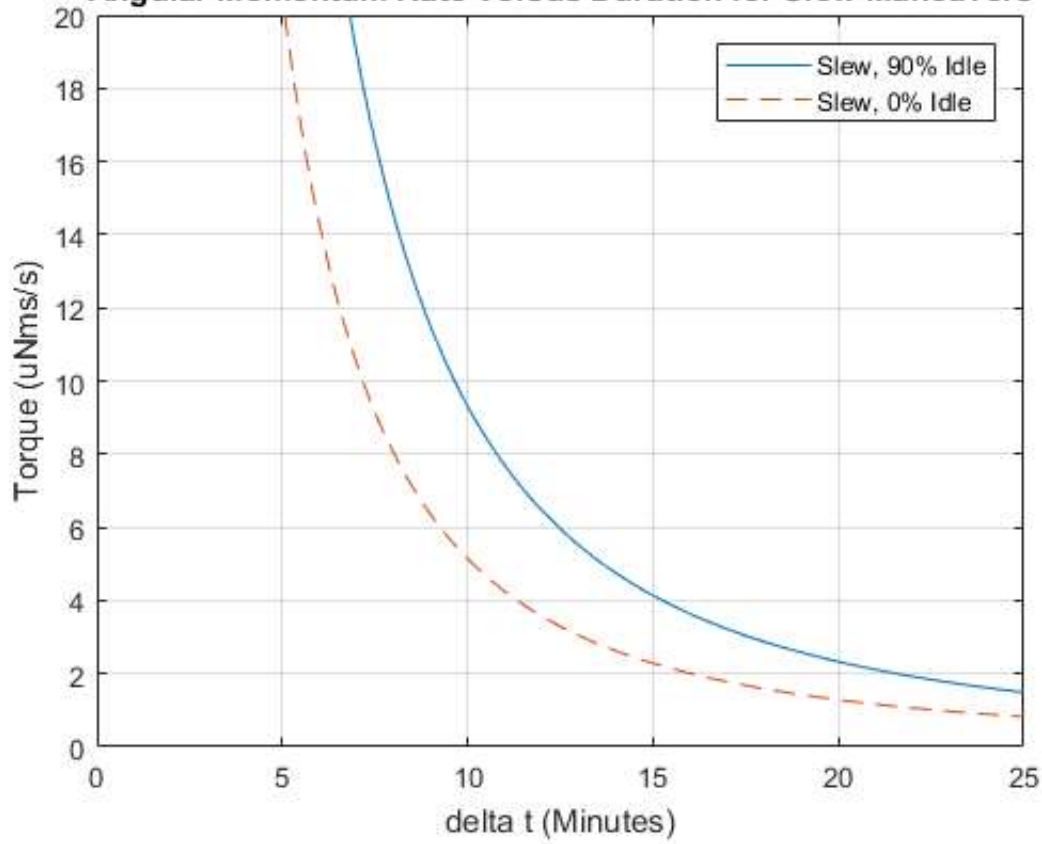
Pulse Frequency vs. Impulse Bit
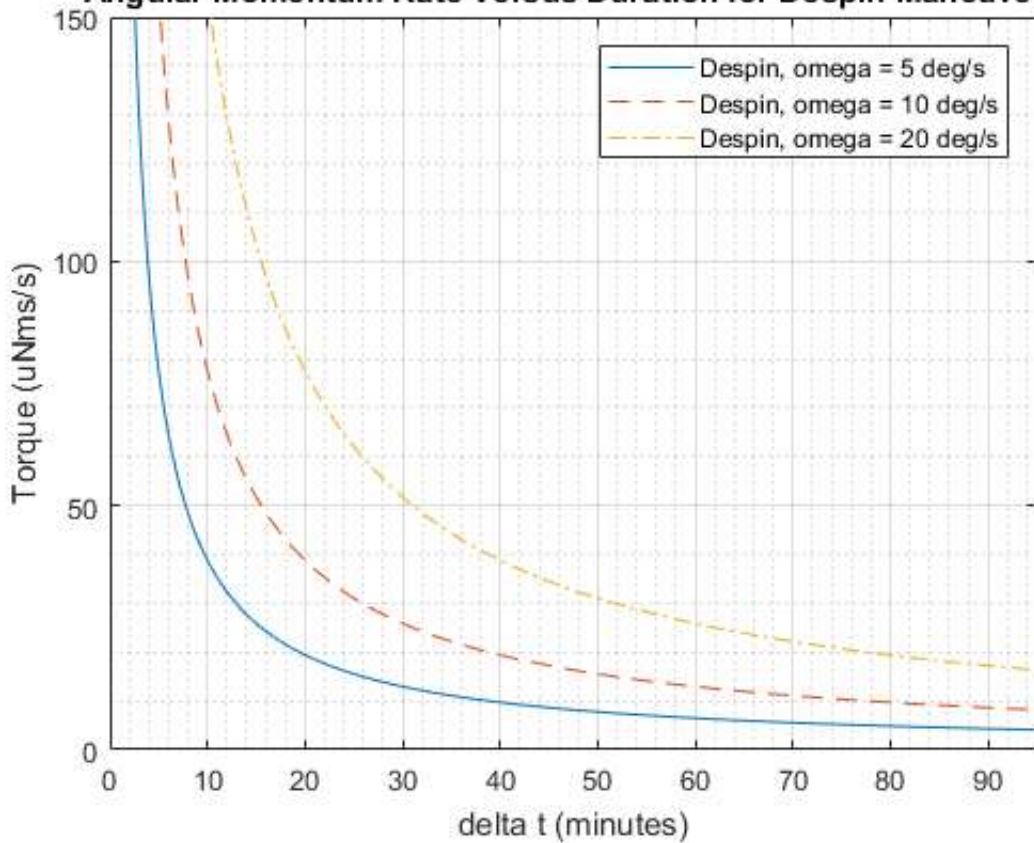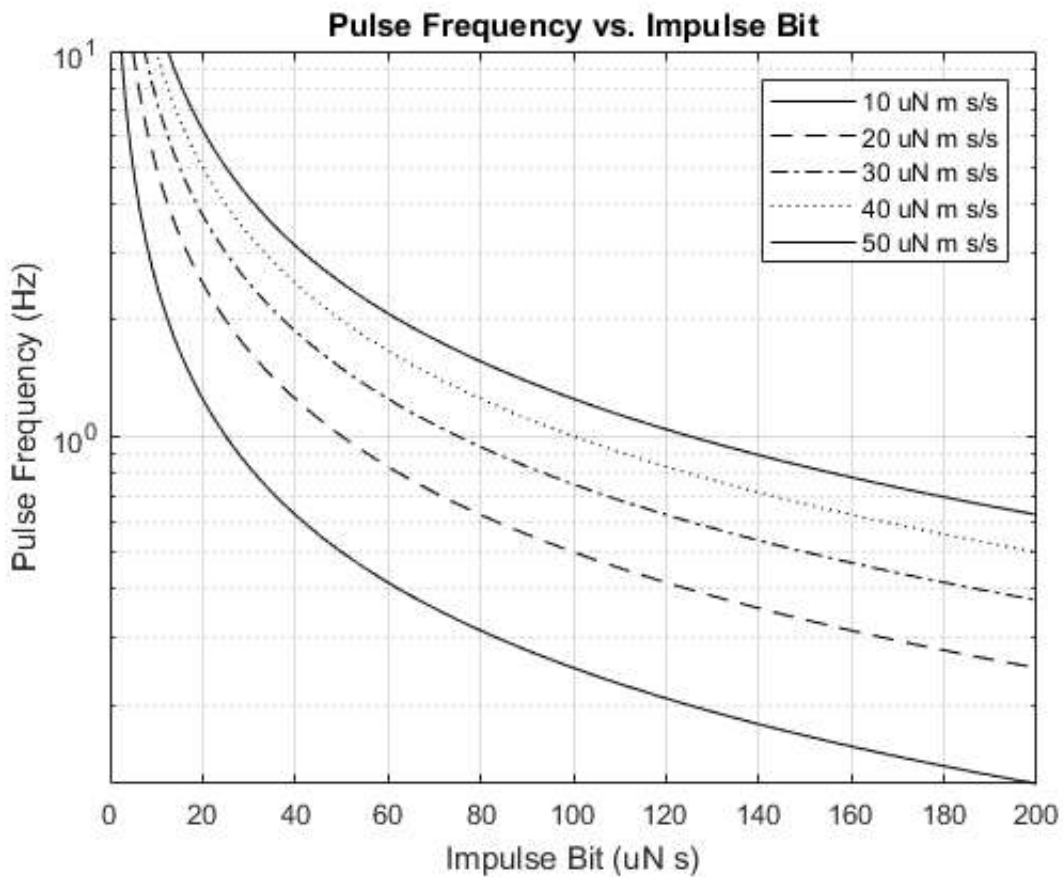
Power Draw vs. Impulse Bit

Power Draw vs. Frequency

PPT CUP DATA

```matlab
H_dot                   = 0:1:300;
Ibit_PPT                = 40; %PPTcup Ibit
f_p                     = H_dot./(Ibit_PPT.*s);
fp_slew_0               = Hdot_slew_0./(Ibit_PPT*10^-6*s);
fp_slew_90              = Hdot_slew_90./(Ibit_PPT*10^-6*s);
PPT_slew_power_0        = fp_slew_0.*Ed;
PPT_slew_power_90       = fp_slew_90.*Ed;
fp_st_5                 = Hdot_st_5./(Ibit_PPT*10^-6*s);
fp_st_10                = Hdot_st_10./(Ibit_PPT*10^-6*s);
fp_st_20                = Hdot_st_20./(Ibit_PPT*10^-6*s);
PPT_detumble_power_5  = fp_st_5.*Ed;
PPT_detumble_power_10 = fp_st_10.*Ed;
PPT_detumble_power_20 = fp_st_20.*Ed;


%%%%% Figure %%%%%
figure(7)
yyaxis left
plot(PPT_slew_power_0,T); hold on
plot(PPT_slew_power_90,T)
hold off
xlabel('Power (Watts)')
ylabel('Time (Minutes)')
axis([0 10 0 25])
grid on
grid minor
title('PPTCUP: 180-Degree Slew')
yyaxis right
plot(PPT_slew_power_0,Hdot_slew_0*10^6,'-.')
ylabel('Torque (Nms/s)')
axis([0 10 0 40])
legend('0% Idle Time','90% Idle Time','Torque')

figure(8)
yyaxis left
plot(PPT_detumble_power_5,T,'-'); hold on
plot(PPT_detumble_power_10,T,'--')
plot(PPT_detumble_power_20,T,':')
hold off
xlabel('Power (Watts)')
ylabel('Time (Minutes)')
axis([0 4 0 1500])
grid on
grid minor
title('PPTCUP: Detumble')
yyaxis right
plot(PPT_detumble_power_20,Hdot_st_20*10^6,'-.');
ylabel('Torque Nms/s')
axis([0 4 0 16])
legend('\omega = 5 degrees','\omega = 10 degrees','\omega = 20 degrees','Torque')

figure(9)
yyaxis left
plot(PPT_slew_power_0,T); hold on
plot(PPT_slew_power_90,T)
hold off
xlabel('Power (Watts)')
```
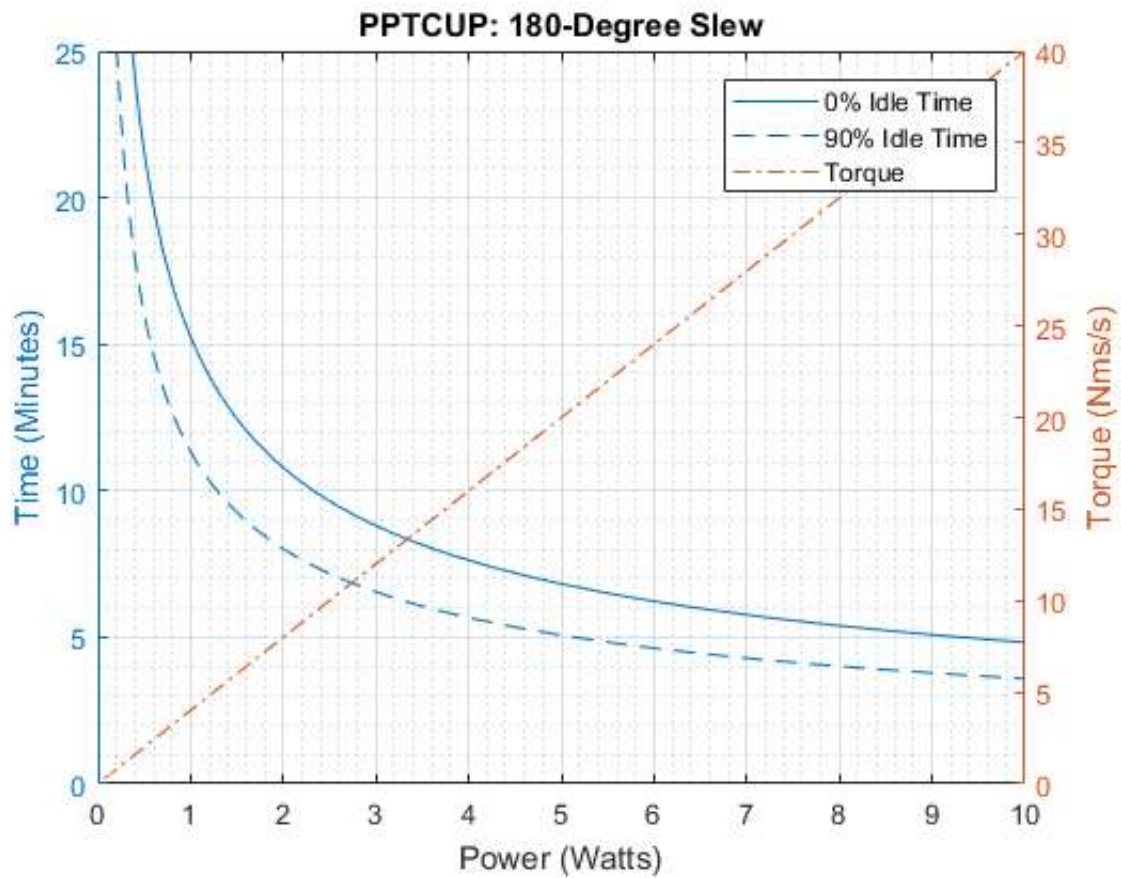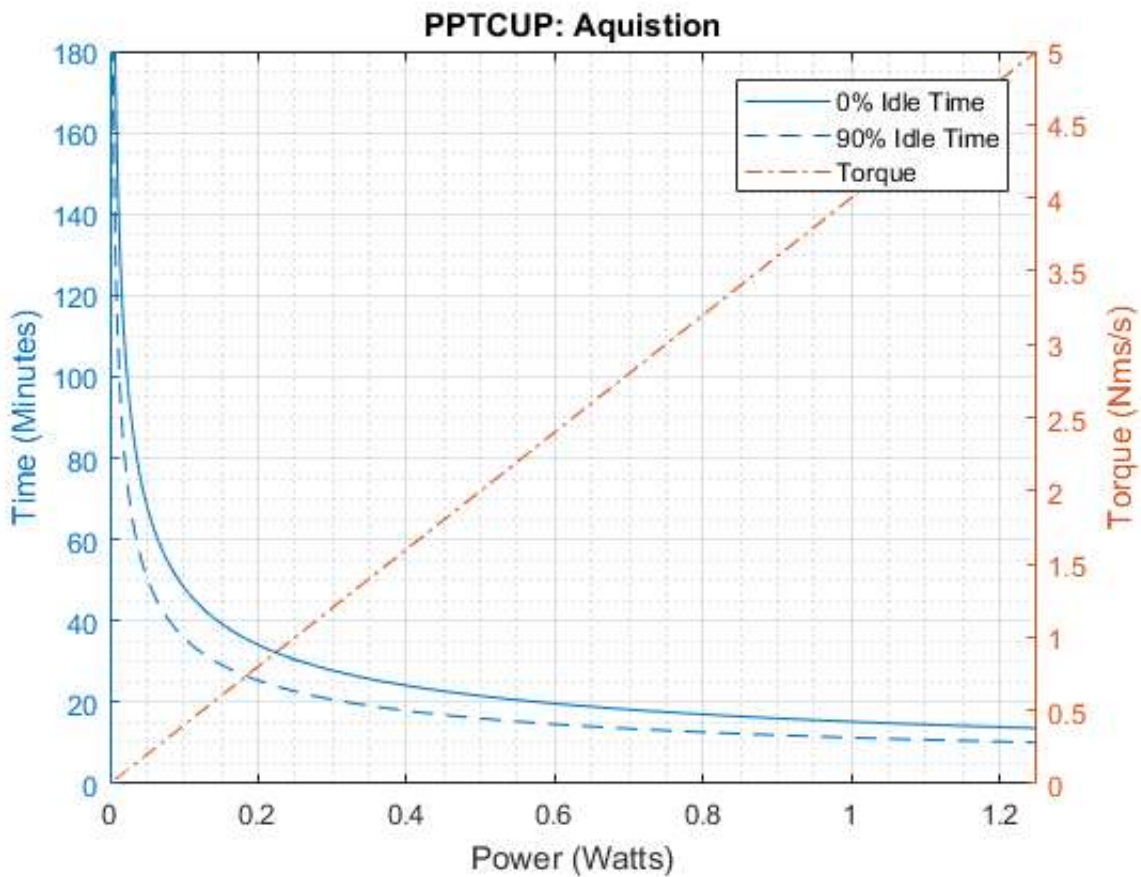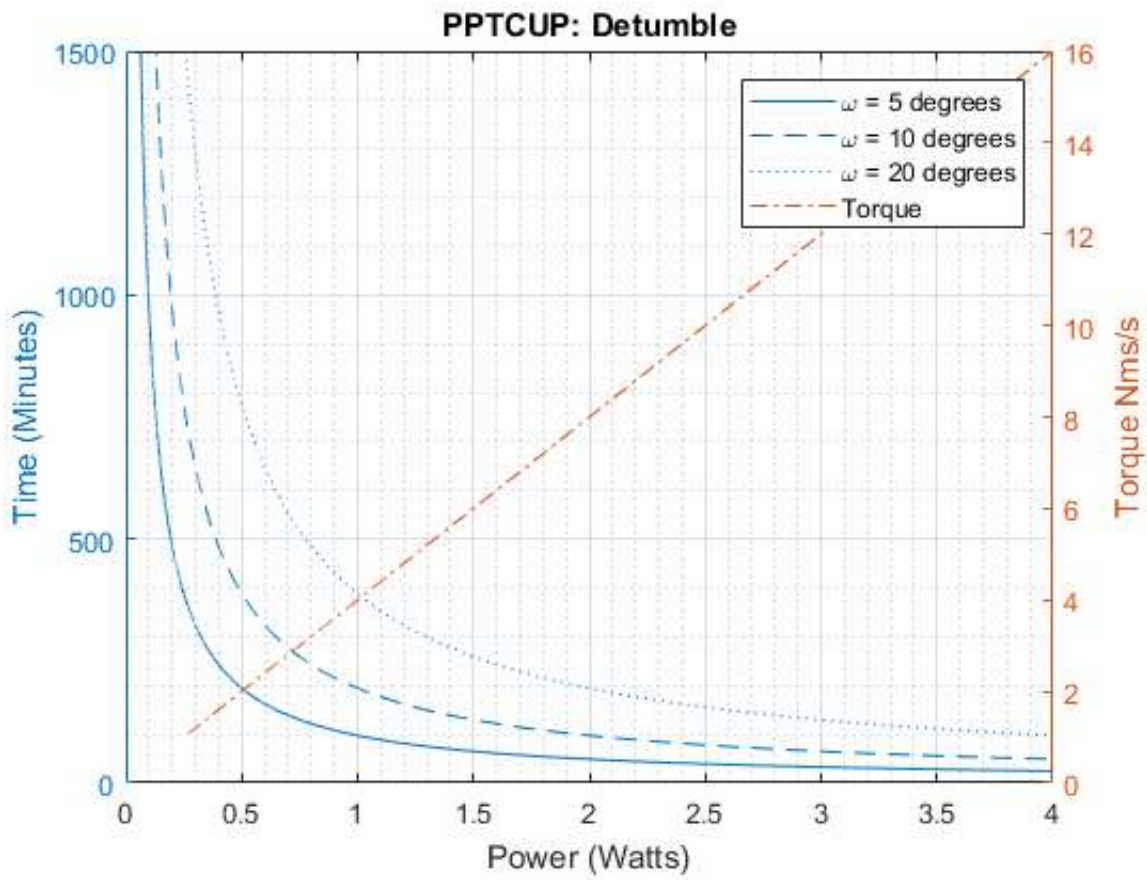
```
ylabel('Time (Minutes)')
axis([0 1.25 0 180])
grid on
grid minor
title('PPTCUP: Aquistion')
yyaxis right
plot(PPT_slew_power_0,Hdot_slew_0*10^6,'-.')
ylabel('Torque (Nms/s)')
axis([0 1.25 0 5])
legend('0% Idle Time','90% Idle Time','Torque')
```

PPTCUP: Detumble

PPTCUP: Aquistion

Hybrid ADN/RCS Calculations

1. of Thrusters firing

```matlab
n       = 2;
% Moment arm
s       = .15;
% Hybrid Ibit
Ibit   = 0.0001;
% Max Torque
T_max = 0.01*s*n;
% Power Required for the Slew Maneuver
ADN_slew_power_0 = Hdot_slew_0./T_max*15;
ADN_slew_power_90 = Hdot_slew_90./T_max*15;
% Power Required for the Detumble
ADN_detumble_power_0 = Hdot_st_5./T_max*15;
ADN_detumble_power_10 = Hdot_st_10./T_max*15;
ADN_detumble_power_20 = Hdot_st_20./T_max*15;


figure(10)
yyaxis left
plot(ADN_slew_power_0,T);hold on
plot(ADN_slew_power_90,T)
hold off
xlabel('Power (Watts)')
ylabel('Time (Minutes)')
axis([0 1 0 25])
grid on
grid minor
title('Hybrid Thruster: 180-Degree Slew')
yyaxis right
plot(ADN_slew_power_0,Hdot_slew_0*10^6,'-.')
ylabel('Torque (Nms/s)')
axis([0 1 0 200])
legend('0% Idle Time','90% Idle Time','Torque')

figure(11)
yyaxis left
plot(ADN_detumble_power_0,T,'-'); hold on
plot(ADN_detumble_power_10,T,'--')
plot(ADN_detumble_power_20,T,':')
hold off
xlabel('Power (Watts)')
ylabel('Time (Minutes)')
axis([0 .5 0 300])
grid on
grid minor
title('Hybrid Thruster: Detumble')
yyaxis right
plot(ADN_detumble_power_20,Hdot_st_20*10^6,'-.')
ylabel('Torque (Nms/s)')
axis([0 .5 0 100])
legend('\omega = 5 degrees','\omega = 10 degrees','\omega = 20 degrees','Torque')

figure(12)
yyaxis left
plot(ADN_slew_power_0,T);hold on
```
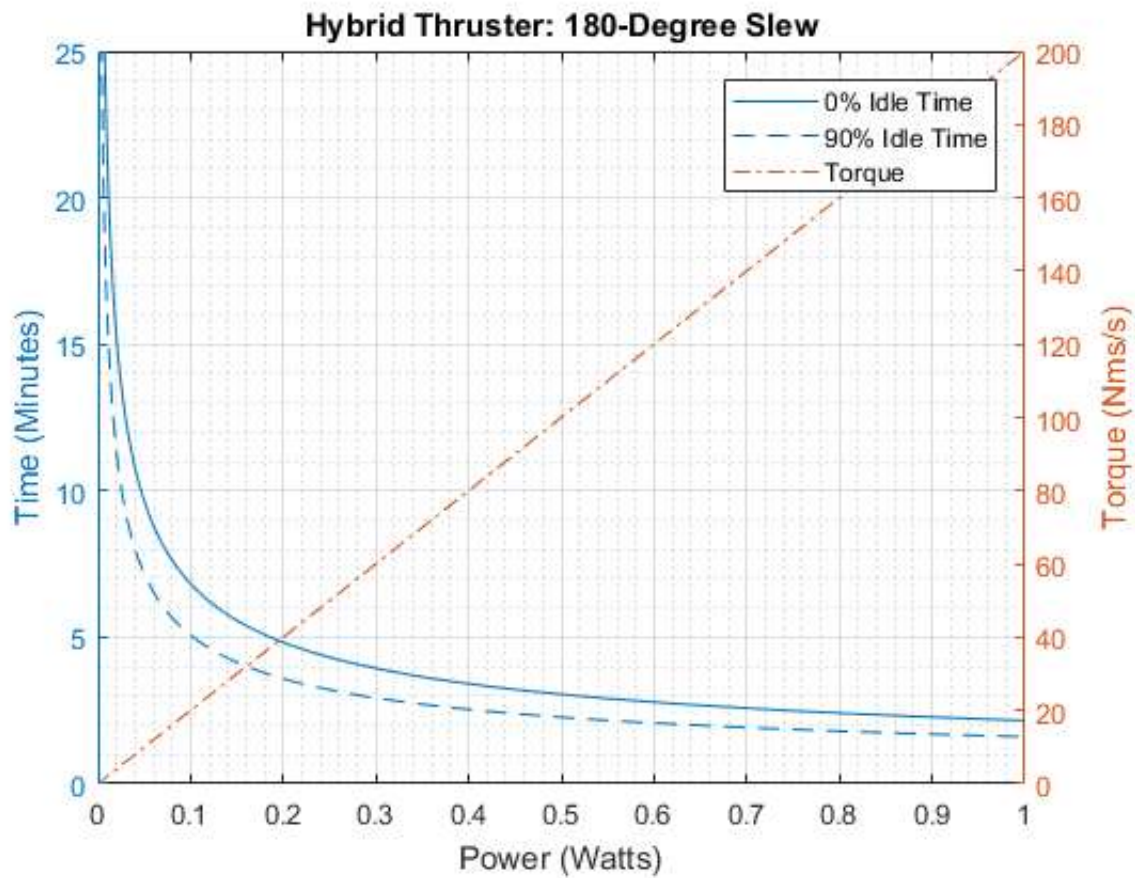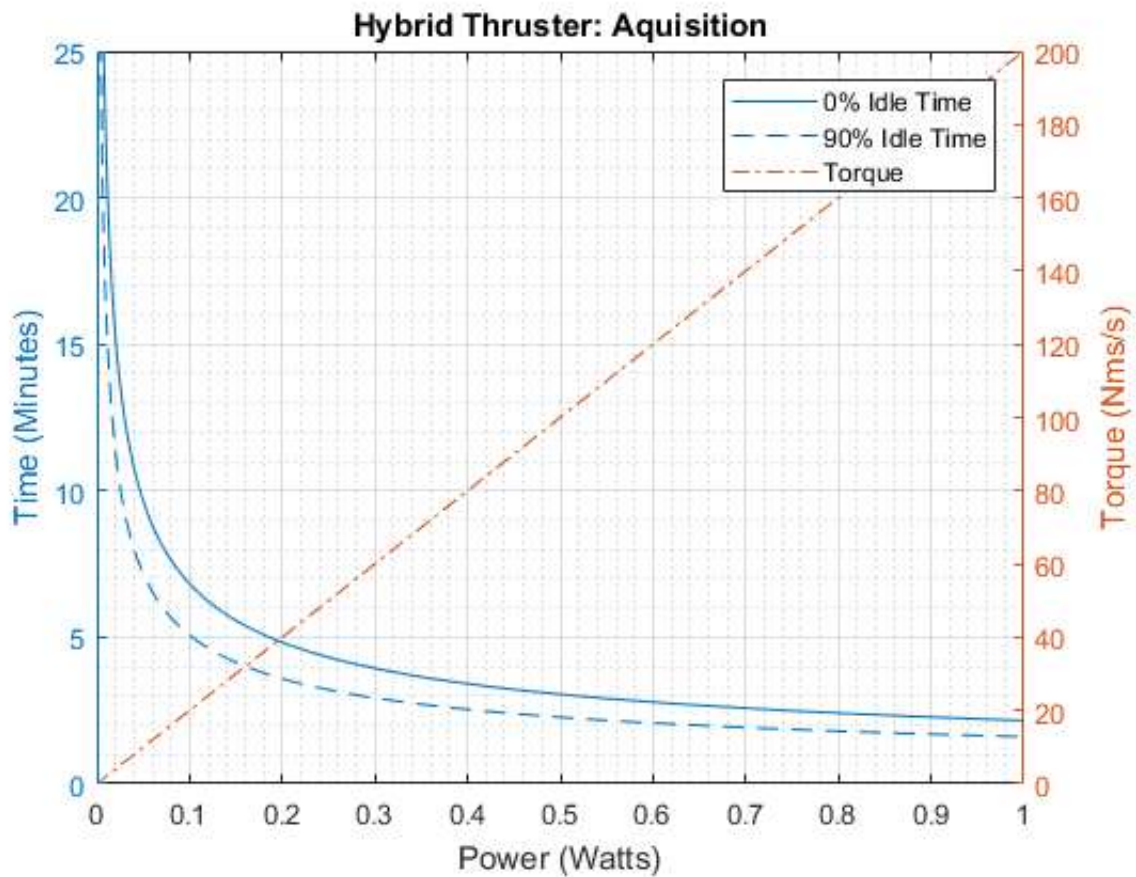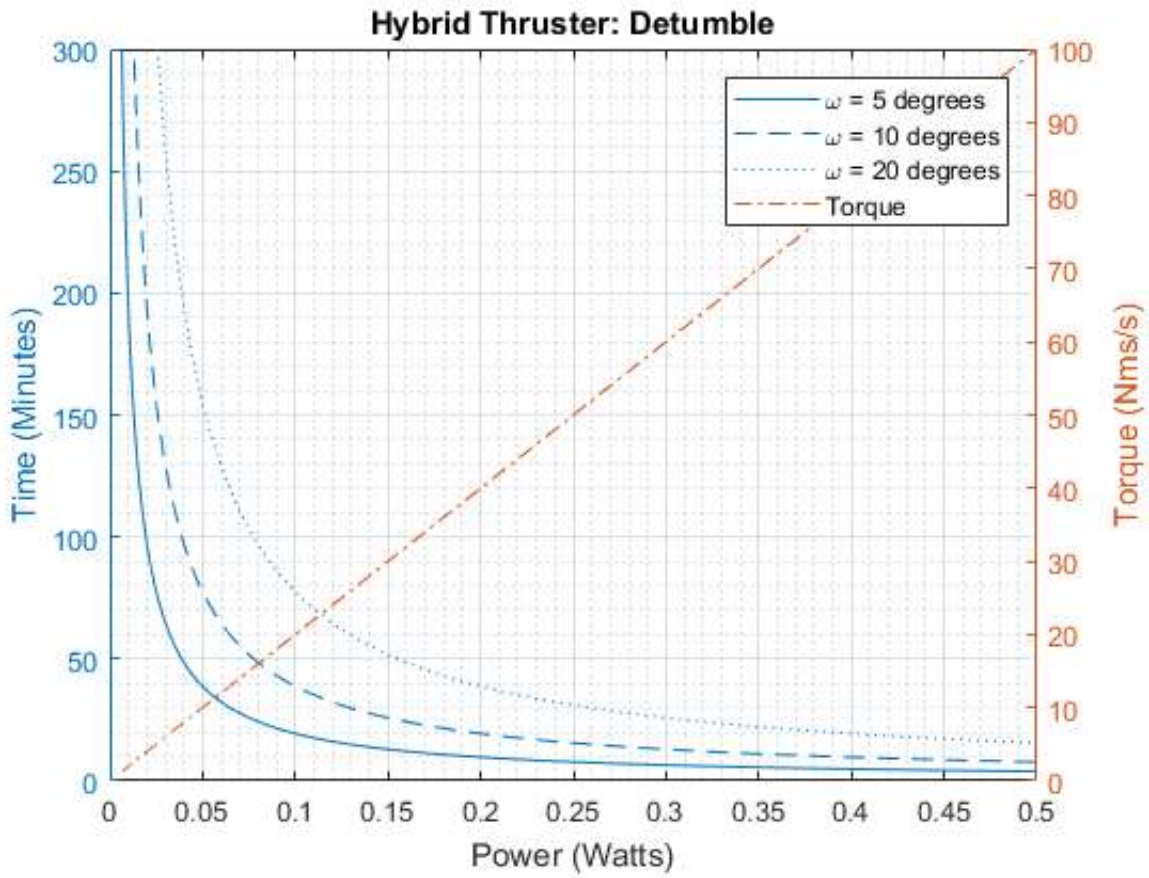
```
plot(ADN_slew_power_90,T)
hold off
xlabel('Power (Watts)')
ylabel('Time (Minutes)')
axis([0 1 0 25])
grid on
grid minor
title('Hybrid Thruster: Aquisition')
yyaxis right
plot(ADN_slew_power_0,Hdot_slew_0*10^6,'-.')
ylabel('Torque (Nms/s)')
axis([0 1 0 200])
legend('0% Idle Time','90% Idle Time','Torque')
```

Hybrid Thruster: Detumble

Hybrid Thruster: Aquisition

Reaction Wheels

```matlab
%Momentum
Momentum     = 0.10; %Nms
%Power
RW_Max_Power = 9;
RW_Power     = [0:9/15000:9];
%Torque
Torque_RW    = .007;
torque_RW    = (Torque_RW.*RW_Power)./RW_Max_Power;

%Slews
RW_slew_time_0  = 2*sqrt((pi.*I)./((Torque_RW.*RW_Power)./RW_Max_Power));
RW_slew_time_90 = sqrt((4.*pi.*I)./((1+.9).*(1-.9).*torque_RW));
%OMEGA
omega_5      = 5*(pi/180);
omega_10     = 10*(pi/180);
omega_20     = 20*(pi/180);
RW_omega_5  = ((I*omega_5)./torque_RW);
RW_omega_10 = ((I*omega_10)./torque_RW);
RW_omega_20 = ((I*omega_20)./torque_RW);

figure(13)
yyaxis left
plot(RW_Power,RW_slew_time_0); hold on
plot(RW_Power,RW_slew_time_90)
hold off
xlabel('Power (Watts)')
ylabel('Time (Seconds)')
axis([0 5 0 1000])
grid on
grid minor
title('Reaction Wheels: 180-Degree Slew')
yyaxis right
plot(RW_Power,torque_RW,'-.')
axis([0 5 0 4e-3])
legend('0% Idle Time','90% Idle Time','Torque')
ylabel('Torque Nms/s')

figure(14)
yyaxis left
plot(RW_Power,RW_omega_5); hold on
plot(RW_Power,RW_omega_10)
plot(RW_Power,RW_omega_20)
hold off
xlabel('Power (Watts)')
ylabel('Time (Seconds)')
axis([0 1 0 1000])
grid on
grid minor
title('Reaction Wheels: Detumble')
yyaxis right
plot(RW_Power,torque_RW,'-.')
legend('\omega = 5 degrees','\omega = 10 degrees','\omega = 20 degrees','Torque')
axis([0 1 0 1e-3])
ylabel('Torque (Nms/s)')

figure(15)
yyaxis left
```

```
plot(RW_Power,RW_slew_time_0); hold on
plot(RW_Power,RW_slew_time_90)
hold off
xlabel('Power (Watts)')
ylabel('Time (Seconds)')
axis([0 5 0 1000])
grid on
grid minor
title('Reaction Wheels: Aquisition')
yyaxis right
plot(RW_Power,torque_RW,'-.')
axis([0 5 0 4e-3])
legend('0% Idle Time','90% Idle Time','Torque')
ylabel('Torque (Nms/s)')
```

Reaction Wheels: Detumble

Reaction Wheels: Aquisition